Norwegian University
of Life Sciences

**Master's Thesis 2020 60 ECTS**

Faculty of Chemistry, Biotechnology and Food Sciences (KBM)

# Vibrational Spectroscopy for Qualitative and Quantitative Analysis of Fatty Acids in Edible Fats and Oils

Nina Marit Øyunn Knobel

Organic analytical chemistry

# Acknowledgments

I want to thank my supervisor Nils Kristian Afseth at Nofima for giving me the opportunity to work with an interesting project in organic analytical chemistry, for patiently answering my countless questions and never losing his optimism and good spirit. Thanks also to Ulrike Böcker at Nofima for helping me with both the instruments in the lab and Unscrambler.

At NMBU I want to thank my supervisor Dag Ekeberg for taking me on as a master student and letting me work in his laboratory, for answering questions and giving med feedback on my work. I also want to thank Hanne Devle for showing me how everything works in the lab, and for giving me advice and feedback.

Thank you also to Orivo for supplying samples of marine oils that I got to use in my thesis!

Thanks to my family for always being there for me and supporting me, and my flatmates for making my home in Ås truly feel like home. Thank you, Camilla and Siri, for walking this path with me, for always listening when I have something to say, giving me advice and for all the great laughter we have shared. Last but not least, I want to thank my dear Rappkjefta Ryper for sharing so many amazing moments over the last five years; my time at NMBU would not have been the same without you.

Norwegian University of Life Sciences (NMBU)
Ås, June 2020

Nina Knobel

# Abstract

Fats and oils are an important part of the diet for many organisms, and fatty acids (FA) are important structural components within organisms. Vibrational spectroscopy are rapid and non-destructive analytical tools, and in this study FTIR and Raman spectroscopy were applied for qualitative and quantitative analysis of fats and oils. Gas chromatography mass spectrometry (GC-MS) served as reference method. The goal was to develop calibration models that enable the prediction of FA content of single FAs, by creating a sample design with low correlation between the FAs. Multivariate methods were used to make the calibration models.

The first step concerned the classification of marine oils based on analysis with FTIR and Raman spectroscopy. Principal component analysis was used to differentiate oils based on their chemical composition. Next, the FA profiles of a set of reference oils was determined with GC-MS, by transforming the samples to fatty acid methyl esters prior to analysis. Based on these FA profiles a sample design with low correlation between the FAs was made, which gave rise to 80 calibration samples. The calibration set was analysed with FTIR and Raman spectroscopy. The obtained spectral data were used in combination with the reference analyses and partial least squares regression to establish calibration models. Lastly, the obtained calibration models were validated through analysis of independent oil samples.

Classification of marine oils showed that FTIR was a suitable method for differentiating various types of oils, while Raman spectroscopy could not be used for this purpose due to a strong fluorescence background. The calibration set was shown to have little correlation between the main FAs, and calibration models were achieved for the FAs C14:0, C16:0, C18:0, C18:1n-9, C18:2n-6, C18:3n-3, C20:5n-3 and C22:6n-3. All models had an $R^2 \geq 0.93$, some as high as 0.99. The models based on FTIR spectroscopy had lower RMSECV values than the models for Raman spectroscopy, and generally seemed to be more accurate and robust. Validation of the calibration models showed that both FTIR and Raman spectroscopy gave good predictions of FA content that clearly reflected the FA profiles in the analysed samples. In conclusion, both FTIR and Raman spectroscopy were shown to be promising methods for qualitative and quantitative FA determination in samples of edible oils.

# Sammendrag

Fett og oljer er en viktig bestanddel av kostholdet til mange organismer, og både fett og fettsyrer har viktige funksjoner i organismer. Vibrasjonsspektroskopiske metoder brukes til rask og ikke-destruktive analyser, og i denne studien ble FTIR og Ramanspektroskopi anvendt til kvalitativ og kvantitativ analyse av oljer. Gasskromatografi massespektrometri (GC-MS) ble brukt som referansemetode. Målet med denne studien var å lage modeller for å bestemme innholdet av enkeltfettsyrer i fett og oljer. Dette skulle gjøres ved å lage et kalibreringssett med prøver basert på et prøvedesign med lav korrelasjon mellom de ulike fettsyrene. Analyse av kalibreringssettet i kombinasjon med multivariate metoder skulle gi kalibreringsmodeller for fettsyreprediksjon i fett og oljer.

Det første steget var å bruke FTIR og Ramanspektroskopi til klassifisering av marine oljer. Prinsipal komponent analyse ble anvendt for å skille oljene basert på kjemiske ulikheter. Neste steg var å bestemme fettsyreprofilene til et sett med referanseoljer, hvilket ble gjort ved å omestre oljene til fettsyremetylestere før analyse med GC-MS. På bakgrunn av disse fettsyreprofilene ble det laget et prøvedesign med lav korrelasjon mellom de ulike fettsyrene. Prøvedesignet ble brukt for å lage et kalibreringssett, som så ble analysert med FTIR og Ramanspektroskopi. PLS regresjon basert på spektrale data fra analysene og referansedata ble brukt for å lage modeller for fettsyreprediksjon. Det siste steget var å validere modellene som ble laget ved å analysere uavhengige oljeprøver.

Klassifiseringen av marine oljer viste at FTIR var en egnet metode for å skille mellom ulike typer olje. Raman spektroskopi var derimot lite egnet til analyse av marine oljer, da signalet i for stor grad ble påvirket av fluorescens. Kalibreringssettet hadde lav korrelasjon mellom hovedfettsyrene, og kalibreringsmodeller ble opprettet for fettsyrene C14:0, C16:0, C18:0, C18:1n-9, C18:2n-6, C18:3n-3, C20:5n-3 og C22:6n-3. Alle modellene hadde $R^2 \geq 0.93$, for noen modeller var $R^2 = 0.99$. Modellene basert på FTIR spektroskopi hadde generelt lavere RMSECV verdier enn modellene for Raman spektroskopi, og de så også ut til å være mer nøyaktige og robuste. Validering av modellene viste at både FTIR og Raman spektroskopi ga gode verdier for fettsyreinnhold som gjenspeilet den faktiske fettsyreprofilen i de analyserte oljene. Det kan altså konkluderes med at både FTIR og Ramanspektroskopi er lovende metoder for kvalitative og kvantitative analyser av fettsyrer i oljeprøver.

## Abbreviations

| | |
|---|---|
| ALA | Alpha-linolenic acid |
| ATR | Attenuated total reflectance |
| DHA | Docosahexaenoic acid |
| EMSC | Extended multiplicative signal correction |
| EPA | Eicosapentaenoic acid |
| ES | External standard |
| FA | Fatty acids |
| FAME | Fatty acid methyl ester |
| FT | Fourier transform |
| FTIR | Fourier transform infrared spectroscopy |
| GC | Gas chromatography |
| IR | Infrared |
| IS | Internal standard |
| LA | Linoleic acid |
| MF | Match factor |
| MIR | Mid-infrared |
| MP | Mobile phase |
| MS | Mass spectrometer |
| MUFA | Monounsaturated fatty acid |
| NIR | Near-infrared spectroscopy |
| PC | Principal component |
| PCA | Principal component analysis |
| PLS-DA | Partial least squares discriminant analysis |
| PLSR | Partial least squares regression |
| PUFA | Polyunsaturated fatty acid |
| RMSECV | Root mean square error of cross validation |
| RRF | Relative response factor |
| RT | Retention time |
| SFA | Saturated fatty acid |
| SIMCA | Soft independent modelling of class analogies |
| SP | Stationary phase |
| TAG | Triacylglycerol |

| | |
|---|---|
| UI | Unsaturation index |

# Contents

# 1. Introduction

## 1.1 Background

### 1.1.1 Human consumption of fats and oils in relation to health

Fats and oils are an important part of the nutrition for many animals, including humans. Compared to carbohydrates and proteins, fats are the macronutrients with the highest energy content, and certain fatty acids (FA) are essential for life and must be provided through the diet. However, the type of FAs as well as the consumed amounts do impact human health in different ways. According to the World Health Organization (WHO) dietary fats should not contribute more than 30% of the daily energy intake, and the energy uptake from saturated fatty acids (SFA) should ideally be less than 10%. Trans FAs are generally considered to be unhealthy, and less than 1% of the energy uptake should be from trans FAs (WHO, 2020).

High consumption of SFA has been associated with adverse health effects such as cardiovascular diseases (Nettleton et al., 2018; Sacks et al., 2017), and a diet low in SFAs is often recommended. The topic of SFA-consumption in relation to human health is however quite complex, and there are arguments for and against this recommendation (Krauss & Kris-Etherton, 2020b; Kris-Etherton & Krauss, 2020). Further research is clearly needed to better understand the chronic effects of SFA-consumption (Krauss & Kris-Etherton, 2020a). On the other hand, monounsaturated FAs (MUFA) and especially polyunsaturated FAs (PUFA) are considered healthy in certain amounts. Among the unsaturated FAs the n-3 FAs have shown many positive health benefits. The n-3 FAs alpha-linolenic acid (ALA), eicosapentaenoic acid (EPA) and docosahexaenoic acid (DHA) have been found to reduce the risk of coronary heart disease, and EPA and DHA also have other positive health benefits such as lowering blood pressure (Wijendran & Hayes, 2004). For healthy adults the daily recommended intake of EPA and DHA is in the range of 250 – 1000 mg per day, while the daily intake of DHA should be somewhat higher for pregnant and lactating women (Hamilton et al., 2020).

There are two FAs which are characterized as essential fatty acids (EFA) because they cannot be synthesised by the human body and therefore must be included in the diet (Punia et al., 2019). These two fatty acids are linoleic acid (LA); C18:2n-6, and ALA; C18:3n-3. ALA can further be converted to EPA and DHA; all three are n-3 FAs with important biological activities in the human body (Punia et al., 2019). The ratio between essential n-6 and n-3 FAs is considered to be important for maintaining good health and to evade chronic diseases, with an optimal ratio of 1:1 – 2:1 (Saini & Keum, 2018). A high ratio of dietary n-6/n-3 fatty acids

is often considered to be problematic because n-6 FAs are precursors for pro-inflammatory signalling molecules in the body called eicosanoids, while n-3 FAs are precursors for anti-inflammatory eicosanoids (Balić et al., 2020). Nevertheless, the absolute mass of consumed fats might be more important than the ratio of n-6/n-3 (Wijendran & Hayes, 2004).

### 1.1.2 Quality control of fats and oils

Quality control of fats and oils is important for different reasons, one of them being human health. As mentioned above, the total amount of daily consumed fat as well as the type of FAs that are consumed have an impact on our physical wellbeing. Thus, it is essential to know the fat content of foods and the FA composition of edible fats and oils.

Today, FA composition is often determined using GC; a time-consuming and laborious method, which is not suitable for continuous monitoring of quality parameters directly in the food and supplement production line (Tao & Ngadi, 2018). Controlling the quality and safety of fats and oils is, however, very important. The quality is affected by factors throughout the production process, such as raw material, processing method, refining, bottling and storage (Pereira et al., 2008). The quality is controlled by measuring different parameters such as iodine value, saponification value, peroxide value, acidity and colour (Pereira et al., 2008). The largest safety-concern for oils is oxidation, as toxic compounds are formed in this process, leading to rancidity (Guillén & Goicoechea, 2007; Li et al., 2018). Very often the peroxide value is the parameter monitored to assess the oxidation state (Li et al., 2018). Quality control of fats and oils is also important to ensure the authenticity of a product and to detect any adulteration. This is first and foremost done by monitoring the FA composition (Didham et al., 2020; Rohman & Irnawati, 2020).

### 1.1.3 Previous research

In the last decades, research has been conducted on the use of vibrational spectroscopy in food analysis, both for the determination of fat content and FA composition in foods and fish oil supplements. Mid-infrared spectroscopy (MIR) became interesting as an analytical method after the introduction of Fourier-transform IR (FTIR) spectrometers (Li-Chan et al., 2006), and instrumental improvements made Raman spectroscopy a suitable detection technique (Tao & Ngadi, 2018). Both methods are frequently used in combination with chemometrics and multivariate data analysis.

In a study from 1997, edible oils and lard were characterized by FTIR, and relationships between the composition of the fats and oils and specific bands in the fingerprint region were

studied (Guillén & Cabo, 1997). In a different publication, FTIR was applied to determine the relative amounts of n-3 and n-6 PUFAs in vegetable oils (Yoshida & Yoshida, 2003). Vibrational spectroscopic methods, including both FTIR and Raman, have been applied for the determination of n-3 FAs in fish oil supplements. The results showed that these methods in combination with PLSR could be applied for the quantification of EPA, DHA and sum of total n-3 FAs (Bekhit et al., 2014). In 2020 Rohman and Irnawati published a study concerning the determination of three oils in ternary mixtures by using FTIR and multivariate data analysis. The conclusion of this study was that certain wavenumbers can be used for accurate determination of the different oils in the mixtures (Rohman & Irnawati, 2020). Today, a commercial analysis service called QTA (Quality Trait Analysis) is provided by Eurofins. QTA is based on FTIR technology and can for instance provide information on FA contents in edible oil samples (Eurofins, 2020).

Raman spectroscopy has been used for the classification of fats and oils, where the results showed that intensities at different Raman shift values were highly correlated with the FA profile of the analysed fats and oils (Baeten et al., 1998). In another study Raman spectroscopy was applied to a complex food model system with the goal of quantifying the fat fraction of the samples. Raman gave promising results for the prediction of total unsaturation in the samples, and different FA classes could also be predicted quantitatively, with good correlations and low estimation errors (Afseth et al., 2005). Raman spectroscopy has also been applied to salmon samples: on intact salmon muscle, ground muscle and fat extracts, with the goal of characterizing the fatty acid unsaturation. Here it was found that the oil extracts gave the best results (Afseth et al., 2006).

Despite the high number of publications related to vibrational spectroscopy and quantification of FA features, there is still a lack of knowledge related to how suitable these techniques are for quantification of single FAs. The possibility for rapid analysis of FA features comes with a “cost”, and there are several limitations in using vibrational spectroscopy for this purpose. The limitations include:

1. FTIR and Raman have far lower chemical resolution than GC. Whereas the latter technique can provide individual signals from most FA features in an oil, the peaks in Raman and FTIR spectra will always be the sum of multiple FA features.
2. Quantification of FAs can only be done after multivariate calibration of FTIR or Raman spectra. For calibration, larger samples sets are needed. In samples sets, unfortunately, one will always find higher or lower correlation patterns between

different FAs (Eskildsen et al., 2014). If two FAs are highly correlated in a sample set, the sample set cannot be used for predicting these two FAs independently in new samples.

## 1.2 Aims of thesis

The main objective of this thesis was to study and develop a rapid and robust method for the determination of the FA composition in fats and oils using vibrational spectroscopy. The objective was divided into three sub-objectives:

1. Study the use of FTIR and Raman spectroscopy for the classification of closely related marine oils.
2. Develop a FA calibration system based on an experimental design of fat and oil mixtures containing uncorrelated FA features. All measurements included FTIR and Raman spectroscopy, with GC-MS as the reference method.
3. Validate the obtained FTIR and Raman calibrations using marine oils from objective 1 and independent oil samples.

# 2. Theory

## 2.1 Fatty acids

FAs are hydrocarbon chains with a methyl-group in one end and a carboxyl-group in the other end. Naturally occurring FAs are usually unbranched with an even number of carbon atoms, ranging from four to 28 carbon atoms per FA (Moss et al., 1995). However, branched FAs and FAs with odd numbered carbon chains do exist (Christie, 1997; Hart, 2012). Figure 1 shows the general structure of a straight chain SFA.

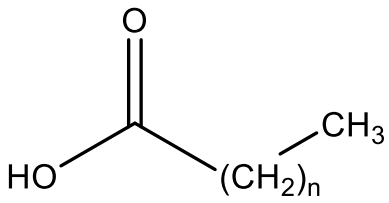


*Figure 1 – General structure of a SFA, where n can be any number from 2 to 26.*

The hydrocarbon chain of a FA can contain one or more double bonds, most commonly in *cis* configuration. The opposite configuration of *cis* is called *trans* (Hart, 2012). The melting point of a FA is partly dependent on the number of double bonds in the FA, called the degree of unsaturation, because double bonds in *cis* configuration make the FAs bend at an angle. This leads to less interaction with other FAs through van der Waals forces, thus giving rise to a lower melting point (Hart, 2012). Increased chain length will increase the melting point.

### 2.1.1 Nomenclature

FAs are named after the number of carbon atoms in the carbon chain and the number of double bonds present in the chain. All FAs have a systematic name, and the common ones also have trivial names. For example, oleic acid is a common FA in olive oil, with 18 carbon atoms and one double bond in the carbon chain. The systematic name is (Z)-octadec-9-enoic acid, and the shortened form is C18:1n-9 (U.S. National Library of Medicine). The first number in the shorthand notation indicates the number of carbon atoms in a FA, the second number states the number of double bonds present, and the number after *n* states the position of the first double bond counted from the methyl terminal carbon. The abbreviated form used here is called the *n-x* notation, which is equivalent to the omega notation. The *n* indicates that the position of a double bond is counted from the methyl terminal carbon and *x* indicates the

position of the first double (or triple) bond (Davidson & Cantrill, 1985). The table in appendix A lists all the FAs relevant in this thesis.

Classification of FAs is based on the position of the first double bond counted from the methyl terminal carbon, and the total number of double bonds in the hydrocarbon chain. FAs with the first double bond in n-3 position are called n-3 FAs, n-6 FAs are one group and so on. If there is no double bond present, the FA is classified as a SFA. MUFAs contain one double bond, PUFAs contain two or more double bonds (Orsavova et al., 2015).

If a double bond is in *cis*- configuration, this is indicated with a Z in the name of the FA. For a *trans*-double bond, the letter E is used in the name. The shorthand notation used here will include *trans* if it is a *trans*-FA, and if nothing is indicated the FA is a *cis*-FA.

### 2.1.2 Triacylglycerol

FAs in the free form are rarely found in large amounts in nature. They are usually part of more complex lipids, one example being triacylglycerol (TAG), more commonly called a triglyceride. TAGs consist of three FAs that are esterified to one molecule of glycerol, which is a trivalent alcohol. The three FAs bound to glycerol can be identical, this is called a simple TAG. In contrast, mixed TAGs contain two or three different FAs, which can be placed in any of the three possible positions (Hart, 2012). Mixed TAGs are much more common than simple TAGs. The three carbon atoms in the glycerol backbone allow for stereochemically different FA bond positions. These positions are called sn-1, sn-2 and sn-3 (Lichtenstein, 2013). Both the type of FAs and the position they occupy determines the physical properties of a TAG.

Figure 2 shows the general structure of a TAG, where $R_1$, $R_2$ and $R_3$ are the hydrocarbon chains of identical or different FAs (Matthews et al., 2013).

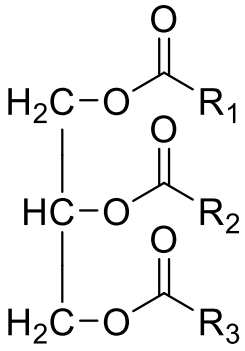


*Figure 1 - General structure of a triacylglycerol, where R1, R2 and R3 are the hydrocarbon chains of identical or diverse FAs. The three fatty acids can be identical or different.*

### 2.1.3 Unsaturation index

For oils of a known FA composition, a value for the total degree of unsaturation can be calculated. This is called the unsaturation index (UI), and it is presented in equation 1 (Suutari, 1995). A value of one in the unsaturation index indicates that the average number of unsaturations is one for each FA in an oil.

Eq. 1: $$Unsaturation\ index = \frac{(\Sigma(\%\ monoene + 2\times\%\ diene + 3\times\%triene + \cdots)}{100}$$

## 2.2 Sources of edible fats and oils

TAGs are the preferred form of energy storage in most organisms (Matthews et al., 2013), and thus TAGs can be extracted from both animal and plant sources. Depending on the FA composition in the TAGs, the extracted fat will be more solid or liquid at room temperature. Animal fats from mammals tend to be solid at room temperature; examples are butter, tallow and lard, while fats from plants are often liquid; such as olive oil and sunflower oil. Fish oil is often rich in PUFAs and is thus liquid at room temperature. There also exist plant oils with a higher melting point such as coconut oil and shea butter.

## 2.3 Analytical methods

### 2.3.1 Transesterification of fatty acids

GC is a method used to analyse volatile substances; however, edible oils are not volatile enough for this analysis. Thus, the TAGs in oils and fats must be derivatized into volatile fatty

acid methyl esters (FAME) prior to analysis. This process is called transesterification; where an ester is transformed into a different ester by exchange of the alkoxy moiety (Schuchardt et al., 1998). Typically, the TAGs will react with methanol in the presence of a catalyst, which can be either a base or an acid. Sodium methoxide is a common base catalyst that gives high yields of FAMEs in short reaction times (Schuchardt et al., 1998). Equation 2 shows the net reaction for the formation of sodium methoxide.

Eq. 2: $$2Na + 2CH_3OH \rightarrow 2CH_3ONa + H_2$$

Equation 3 displays the net reaction for one mole of a TAG (an ester) that is transesterified into FAMEs (Schuchardt et al., 1998). A catalyst is added to speed up the reaction, and once all three esters of a TAG have reacted, the final products are FAMEs and glycerol. The FAMEs are extracted into a non-polar organic solvent, and can then be analysed using GC-MS.

Eq. 3:

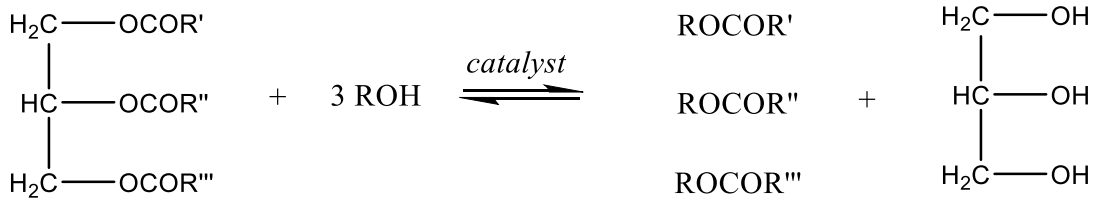


### 2.3.2 GC-MS

The conventional way of quantifying FAs is using gas chromatography (GC) (Coltro et al., 2005; Tao & Ngadi, 2018). This is a proven method for the separation of different components in a sample, and GC can perform highly accurate quantitative and qualitative analyses when the instrument is equipped with a suitable detector, such as a mass spectrometer (MS) (Miller, 2005). Chromatography uses two different phases for the separation of different components in a sample, where one phase is held stationary on a GC column, while the other phase is passed over it. The different components in the sample that is introduced to the GC system will ideally equilibrate or differently partition between the stationary phase (SP) on the column and the mobile phase (MP), here a carrier gas (Miller,

2005). Depending on the strength of the interaction with either the SP or the MP, the different components in the mixture will be separated from each other. In GC the MP is an inert gas such as nitrogen, helium or hydrogen. Thus, there is no chemical interaction between the analyte and the MP, and it is the interaction between the SP and the analyte which is of interest (Miller, 2005). Open tubular columns are often used with GC-MS instruments. These columns have a small diameter, and a thin layer of SP is coated on the inside of the column (Miller, 2005).

A variety of detectors can be used with a GC, here the detector was a MS. This detector first ionizes and/or fragments the incoming molecules from the GC, before they are separated by a mass filter. The MS instrument used in this research was equipped with a single quadrupole as mass filter, which separates the incoming ions based on their mass-to-charge ratio. These fragments are then detected, and a mass spectrum is produced. This spectrum is characteristic for the original analyte and can be used for structural identification. Nowadays it is quite common to use a database such as the mass spectral library by the National Institute of Standards and Technology (NIST), where obtained mass spectra are compared to spectra in the database for identification of the original analyte (Miller, 2005).

### 2.3.3 Qualitative and quantitative analysis

Qualitative analysis based solely on chromatography is not ideal. Different retention parameters can be used for qualitative analysis, such as retention time (RT), when compared to the RT of standards. This can give a first indication on what compounds a sample consists of. However, spectral measurements are required for positive identification of the analytes in a sample (Miller, 2005). Thus, GC systems are often coupled to a MS when the goal is to perform qualitative analysis (Miller, 2005). A MS will enable identification of a compound based on its unique mass spectrum, and often a database such as NIST 2017 is used as reference. With GC-MS it is thus possible to identify analytes in a sample based on their mass spectra followed by comparison of their RTs to the RTs of standards that have been analysed with the same GC-MS instrument.

In order to quantify analytes in a sample, one can use an external standard (ES) or internal standard (IS) (Wang et al., 2017). An ES is usually identical to the analyte of interest, and a pure form of it is used to establish a calibration curve. Nevertheless, it is essential to maintain identical experimental conditions when analysing both the sample and the standard, which cannot be guaranteed when applying an ES (Wang et al., 2017). Thus, an IS is often the more accurate choice. The IS should ideally be a compound which is not naturally present in the

sample, but with similar chemical characteristics as the analyte of interest. It should be added to the sample as early as possible during sample preparation, and due to simultaneous analysis of the analyte and IS, any variations in preparation and/or experimental conditions will be compensated for (Wang et al., 2017).

After analysis of a sample containing FAMEs and IS with GC-MS, followed by identification of the peaks in the chromatogram, the amount of a FA in the sample can be determined using equation 3. In this equation the mass of a FA in the sample is determined by comparing the peak area of a chosen FAME with the peak area of the IS in the same chromatogram. The amount of IS is known, and by dividing with a relative response factor (RRF) it is possible to correct for the mass differences between the IS and the chosen FA. Lastly, multiplication with the molecular mass of the chosen FA will result in the total mass of the FA in the sample. In equation 3 $A_{Fame}$ denotes the area of the chosen FAME in a chromatogram, $A_{IS}$ is the area of the IS in the same chromatogram, $n_{IS}$ is the number of moles IS added to the sample and RRF is the relative response factor for the chosen FAME.

Eq. 3: $$Mass_{FA} = \frac{A_{FAME} \cdot n_{IS}}{A_{IS} \cdot RRF} \cdot Molecular\ mass_{FA}$$

### 2.3.4 Vibrational spectroscopic methods

Over the course of the last few decades, vibrational spectroscopic methods have increased in popularity (Berghian-Grosan & Magdas, 2020; Li-Chan, 2010; Matsakidou et al., 2020). These methods include Raman spectroscopy and infrared (IR) spectroscopy; both mid-IR (MIR) and near-IR (NIR). In contrast to the classical method for analysis of FAs, which is GC, IR and Raman spectroscopy are optical-based methods which rarely require any sample preparation. They are quick and easy to apply, require no use of hazardous solvents, and are ideal for application directly at the production line. Spectra obtained with vibrational spectroscopy give structural information and can be used for quantitative analysis when combined with regression models (Li et al., 2018).

### 2.3.5 FTIR

IR spectroscopy is an analytical method used to obtain an absorption or emission spectrum of a sample by irradiation with light in the IR region (Hart, 2012). In FTIR spectroscopy, high resolution spectra are collected over a wide spectral range simultaneously as opposed to the

way of measuring with dispersive IR instruments in the early days of IR spectroscopy. Nowadays most IR instruments are Fourier transform (FT) instruments, which require a conversion by applying a FT to the raw data in order to obtain transmission or absorbance spectra.

In a MIR instrument such as the one used in this study, the IR region includes the frequencies from 4000 $cm^{-1}$ to 400 $cm^{-1}$ (Li et al., 2018). The different chemical bonds present in the analyte will emit or absorb different wavelengths of light based on changes in dipole moment (Tao & Ngadi, 2018). This means that polar groups such as C=O, O-H and N-H give a strong signal in IR spectroscopy (Li-Chan, 2010; Tao & Ngadi, 2018).

The FTIR instrument utilized here was an instrument of attenuated total reflectance (ATR). This method is based on the total reflection of an IR-beam through a refractive crystal, and in this case the ATR sampling unit is equipped with a diamond. As the light is reflected internally in the crystal, an evanescent wave is formed which extends beyond the surface of the crystal, and into the sample that is applied directly on top of the crystal. The evanescent wave will then be attenuated in the infrared regions where the sample absorbs the light (PerkinElmer, 2005). The light that has passed through the sample is detected, and based on the observed changes in frequencies, the system will generate an IR spectrum for the analysed sample (PerkinElmer, 2005).

### 2.3.6 Interpretation of FTIR spectra

The presence of certain functional groups give characteristic absorption bands at specific frequencies in an IR spectrum. These localised vibrations of individual bonds can mostly be found in the higher-frequency area from 4000 $cm^{-1}$ to 1500 $cm^{-1}$ in a MIR instrument. Two factors that influence the vibrational frequency of a given bond are the bond strength and the mass of the atoms involved. Strong bonds will vibrate at a higher frequency, meaning that C≡C > C=C > C-C, and if all else is equal, C – H stretching vibrations will be higher than those of C – C, which in turn are higher than the frequency of C – Halogen (Williams & Fleming, 2008). The area below 1500 $cm^{-1}$ is often called the fingerprint region because the absorptions in this area are characteristic for each compound (Williams & Fleming, 2008).

When working with analysis of oils, the functional groups of interest are those that can be found in the TAG structure. The most prominent peak in the IR spectrum of oils can often be found around 1743 $cm^{-1}$ and is caused by the carbonyl group (C=O) in the ester linkage of the TAG. Any peak around 3007 $cm^{-1}$ is due to the =C–H stretch in *cis* configuration, and

absorptions in the area of 2980 – 2800 $cm^{-1}$ are from the asymmetric stretching of C–H in -$CH(CH_3)$ and -$CH(CH_2)$-, and the symmetric stretch of -$CH(CH_3)$. The stretch of an alkene group, –C=C–, can be found around 1654 $cm^{-1}$ in TAGs with unsaturated FAs, but this signal is usually quite weak. A strong signal at 1460 $cm^{-1}$ and a medium signal at 1376 $cm^{-1}$ are due to the scissoring vibrations of –$CH_2$– and –$CH_3$. Stretching vibrations from the hydrocarbon skeletal can be found at approximately 1237 $cm^{-1}$, and a band caused by –C–O stretching vibration will be in the area from 1159 $cm^{-1}$ to 1096 $cm^{-1}$. Presence of a weak peak at 970 $cm^{-1}$ can indicate trans-FAs because of the =C–H *trans* stretching vibrations (Guillén & Cabo, 1997; Li-Chan et al., 2006; Li et al., 2018; Rohman & Irnawati, 2020). Table 1 shows a summary of the relevant absorption bands for analysis of edible fats and oil.

*Table 1 – Frequencies of absorption bands (b) and shoulders (sh) of different chemical vibrations, for MIR spectrum of soybean oil. The table is adapted from Guillen & Cabo, 1997, and assignments are based on various articles (Guillén & Cabo, 1997; Li-Chan et al., 2006; Li et al., 2018; Rohman & Irnawati, 2020).*

| Frequency ($cm^{-1}$) | Functional group | Mode of vibration | Intensity* |
|---|---|---|---|
| 3008 (b) | =C–H (*cis*) | Stretching | w |
| 2953 (sh) | –C–H ($CH_3$) | Stretching (asym) | vw |
| 2922 (b) | –C–H ($CH_2$) | Stretching (asym) | vs |
| 2853 (b) | –C–H ($CH_3$) | Stretching (sym) | vs |
| 1743 (b) | –C=O (ester) | Stretching | vs |
| 1655 (b) | –C=C– (*cis*) | Stretching | vw |
| 1461 (b) | –C–H ($CH_2$, $CH_3$) | Bending (scissoring) | m |
| 1377 (b) | –C–H ($CH_3$) | Bending (sym) | w |
| 1239 (b) | –C–O, –$CH_2$– | Stretching, bending | w |
| 1161 (b) | –C–O, –$CH_2$– | Stretching, bending | s |
| 1120 (b) | –C–O | Stretching | vw |
| 1098 (b) | –C–O | Stretching | w |
| 1037 (s) | –C–O | Stretching | vw |
| 966 (b) | –HC=CH– (trans) | Bending out of plane | vw |
| 909 (b) | –HC=CH– (cis) | Bending out of plane | vw |
| 722 (b) | –$(CH_2)_n$–. –HC=CH– | Bending (rocking) | m |

* vw, very weak; w, very weak; m, medium; vs, very strong; s, strong

Figure 3 provides the FTIR absorbance spectra of three replicates of soybean oil with marked frequencies for each band/shoulder. The peak of medium intensity at 3008 $cm^{-1}$ is attributed to a *cis* =C–H stretching vibration while the shoulder at 2953 $cm^{-1}$ and the intense peaks at 2922 and 2853 $cm^{-1}$ come from the asymmetrical stretching of –C–H in $CH_3$ and $CH_2$ and the symmetrical stretching of –C–H in $CH_2$. At 1743 $cm^{-1}$ the most intense peak can be observed, it arises from the ester groups (C=O) in the TAGs. The very weak peak at 1655 $cm^{-1}$ is caused

by the *cis* –C=C– stretching vibration, and the remaining peaks are part of the fingerprint region. The –C–H bending vibration of $CH_2$ and $CH_3$ give rise to the peak at 1461 $cm^{-1}$ and symmetrical bending vibrations of –C–H in $CH_3$ cause the medium peak at 1377 $cm^{-1}$. The peak at 1239 $cm^{-1}$ is caused by the –C–O and $–CH_2–$ stretching and bending vibrations of the hydrocarbon skeleton, and the strong peak at 1161 $cm^{-1}$ arises from the same vibrations. At 1120, 1098 and 1037 $cm^{-1}$ one can find peaks due to the –C–O stretching vibration in the TAGs, while the peaks at 966 and 909 $cm^{-1}$ are associated with the *trans* and *cis* out of plane bending of –HC=CH–, respectively. The last peak that can be assigned to any vibrations in TAGs is the peak at 722 $cm^{-1}$, which can be associated with the bending vibrations of *cis* –HC=CH– and $–(CH_2)_n–$ (Guillén & Cabo, 1997; Li-Chan et al., 2006; Li et al., 2018; Rohman & Irnawati, 2020). A summary of the mentioned bands and shoulders can be found in table 1.

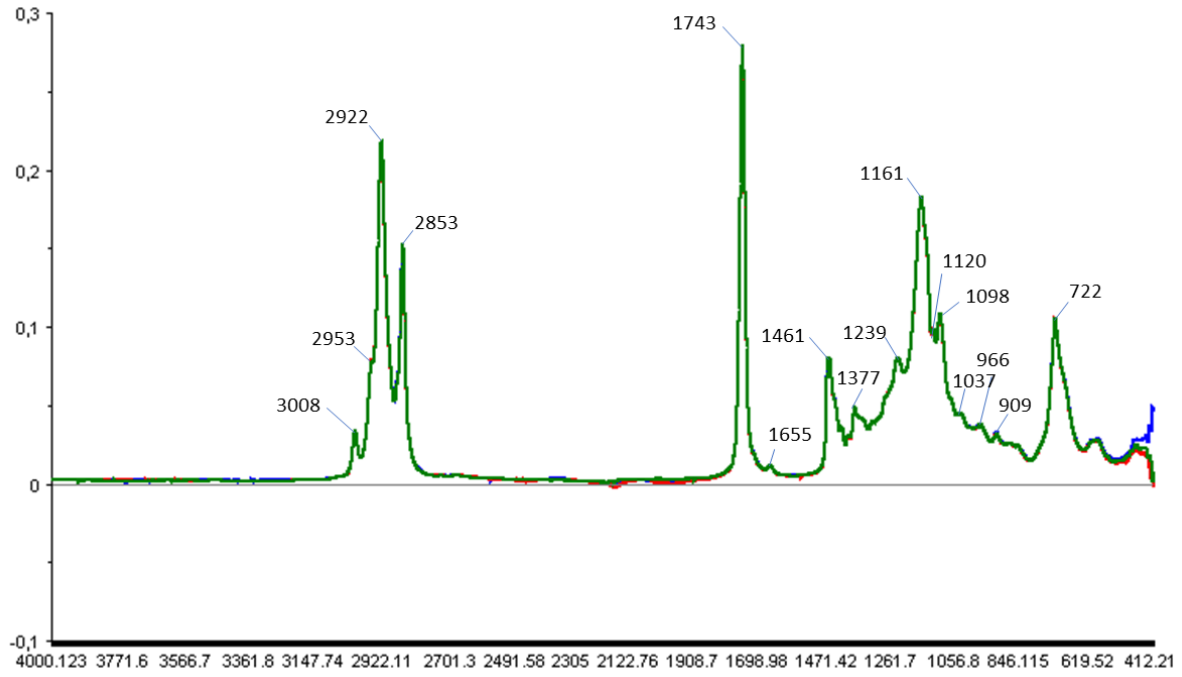


*Figure 3 – FTIR spectrum for three replicates of soybean oil in the MIR region, including the wavenumbers 4000-400 $cm^{-1}$. The numbers above the peaks indicate the wavenumbers in $cm^{-1}$.*

### 2.3.7 Raman spectroscopy

While FTIR measures elastic scattering of photons, called Rayleigh scattering, Raman spectroscopy is based on inelastic scattering of light, named Raman scattering. In other words: FTIR deals with the photons of the same energy as the incident light, while Raman measures the photons with a shifted frequency (Tao & Ngadi, 2018). A source of monochromatic light

is used to excite the molecules in the sample, and a small fraction of this light will be Raman scattering (Li-Chan, 2010). These photons are detected and give information about the change in polarizability of the molecule. A Raman spectrum will thus show intense bands for nonpolar groups such as C=C, C–C and S–S (Li-Chan, 2010; Tao & Ngadi, 2018). FTIR and Raman spectroscopy are complementary methods, because they give intense bands for polar and nonpolar groups, respectively. In recent years instrumental improvements have made Raman spectroscopy more accessible than before. Instrumental improvements regarding sensitivity, stability and sampling technique have been introduced, as well as better filters and lasers (Tao & Ngadi, 2018).

### 2.3.8 Interpretation of Raman spectra

Raman spectra provide structural information about the sample in the same way as FTIR spectra do, but these results are based on Raman scattering. Stretching and deformation of chemical bonds in the sample give rise to distinct spectral bands. However, the intensity of Raman spectra may vary a lot. Factors such as laser intensity and wavelength, acquisition time, physical properties of the chosen matrix and in this case also the set-up of the ball-probe can impact the intensity of the spectra (Afseth et al., 2006). Fluorescence in the samples can result in large variations in the spectral offset between different measurements (Afseth et al., 2005) and the biological matrix will influence the peak intensities. Nonpolar groups generally result in high intensity stretching vibrations and stretching vibrations result in more intense bands than deformation vibrations. Symmetrical vibrations result in scattering bands with higher intensities than asymmetric vibrations, and multiple bonds such as a C=C can give intense bands (Baeten et al., 1998). It is essential to use the right type of preprocessing methods to correct for these differences in baseline and spectral intensities prior to interpretation of the spectra. The chapters 2.4 and 2.4.1 will deal with the topic of data preprocessing.

Raman spectra are based on Raman shift values ($cm^{-1}$), and the important bands can be found in the same region as in IR spectra. The specific values for the bands have been reported with some variations. The asymmetric stretch of *cis* =C–H will give a band at approximately 3012 $cm^{-1}$, while for –C–H the symmetric and asymmetric stretches are found at 2930 $cm^{-1}$ and 2900 $cm^{-1}$, respectively. The symmetric stretch of –C–H gives a signal at 2855 $cm^{-1}$. A carbonyl stretch can be seen around 1745 $cm^{-1}$ and the very strong peak of the C=C stretch is positioned around 1656 $cm^{-1}$. For $CH_2$ the scissoring and twisting vibrations can be found at 1445 $cm^{-1}$ and 1300 $cm^{-1}$, and 1263 $cm^{-1}$ shows the =C–H symmetric rocking (Afseth et al.,

2005). The bands below 1200 $cm^{-1}$ are in the fingerprint region of the Raman spectrum. MUFAs and PUFAs in *cis*-configuration will have a band in the area 1670 – 1680 $cm^{-1}$, while the band for the *trans*-configuration will be around 1650 – 1665 $cm^{-1}$ (Afseth et al., 2005; Baeten et al., 1998; Li-Chan et al., 2006; Tao & Ngadi, 2018). Table 2 shows a summary of the most relevant values for Raman bands in TG analysis.

*Table 2 – Raman shift values for absorption bands of different chemical vibrations, based on Raman spectrum of soybean oil. The table is adapted from Guillen & Cabo, 1997, and assignments are based on various articles (Afseth et al., 2005; Baeten et al., 1998; Li-Chan et al., 2006; Tao & Ngadi, 2018).*

| Raman shift ($cm^{-1}$) | Functional group | Mode of vibration | Intensity* |
|---|---|---|---|
| 3012[a] | =C –H | Stretching (asym) | |
| 2930[a] | C–H | Stretching (asym) | |
| 2900[a] | C–H | Stretching (sym) | |
| 2855[a] | –C–H | Stretching | |
| 1747 | C=O (ester) | Stretching | m |
| 1658 | –C=C– (*cis*) | Stretching | s |
| 1440 | $CH_2$ | Scissoring | s |
| 1302 | $CH_2$ | Twisting | s |
| 1265 | =C–H | Bending (rocking, sym) | s |
| 1079 | –C–C–, –C–O– | Stretching | m |
| 1066 | –C–C–, –C–O– | Stretching | vw |
| 972 | –C–C–, –C–O– /=C–H | Stretching/ out of plane deformation | w |
| 870 | –C–C–, –C–O– | Stretching | w |
| 843 | –C–C–, –C–O– | Stretching | w |

[a] = Values outside the spectral area recorded by the Raman instrument used in this study. The values are based on an article by Afseth *et al.* from 2006.

A typical Raman spectrum of soybean oil for the frequencies of 500 $cm^{-1}$ to 1890 $cm^{-1}$ is provided in figure 4. The peaks below 1200 $cm^{-1}$ are mostly caused by skeletal stretching vibrations such as C–C and C–O, while the peak at 1265 $cm^{-1}$ is caused by the symmetric rocking of =C–H. Twisting and rocking of $CH_2$ creates the band at 1302 $cm^{-1}$, while the intense peak at 1440 $cm^{-1}$ is caused by $CH_2$ scissoring vibrations. The peak at 1658 $cm^{-1}$ comes from *cis* –C=C– stretching vibrations, and the final peak at 1747 $cm^{-1}$ is caused by the –C=O stretch found in the ester linkage of the TAGs.

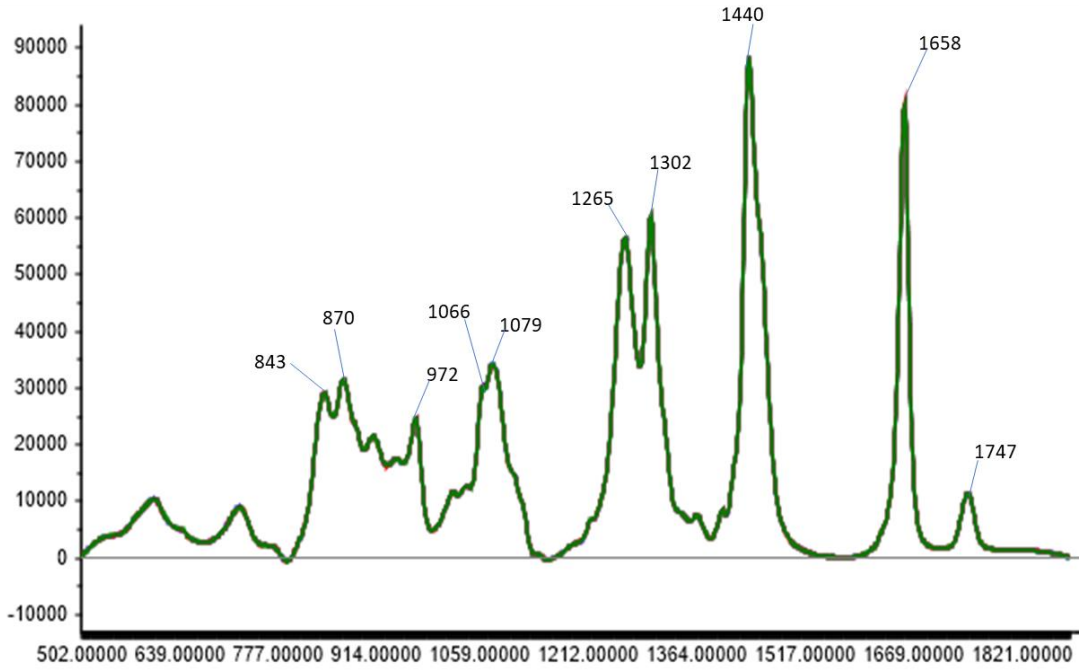


*Figure 4 – Raman spectrum for three replicates of soybean oil in the Raman shift region of 500-1890 $cm^{-1}$. The numbers above the peaks indicate the Raman shift values in $cm^{-1}$.*

## 2.4 Multivariate data analysis

Multivariate data analysis is a necessary tool whenever there are multiple variables measured per sample (Esbensen, 2002). Spectroscopic data is such a case. Usually an entire spectrum of wavelengths is measured for every sample that is analysed, which creates an extensive data set. Multivariate data analysis often seeks to determine a desired parameter based on indirect observations (Esbensen, 2002). In spectroscopy this would equal the prediction of one or more components present in a sample based on the absorption of light at specific wavelengths. However, multivariate observations will always consist of both relevant data and irrelevant information, called noise. This principle is illustrated in figure 5, which is adapted from Esbenesen (2002).

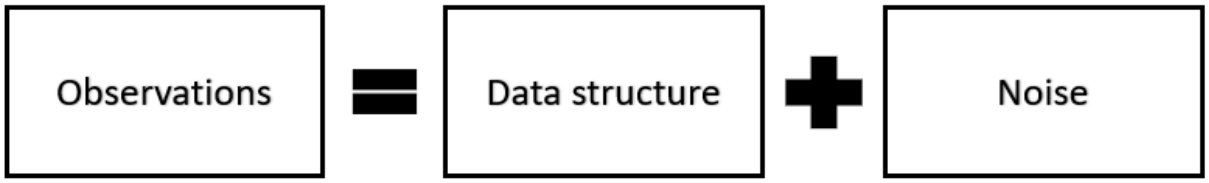


*Figure 5 – Illustration of the principle behind multivariate data analysis, which is to separate the data structure in the observations from the noise (Esbensen, 2002).*

Multivariate data analysis aims to extract the relevant information while reducing the irrelevant information (Reich, 2005). In this thesis principal component analysis (PCA) and partial least squares regression are the multivariate methods of interest, however the spectral data needs preprocessing prior to multivariate analysis.

### 2.4.1 Preprocessing of data

Preprocessing of data is important before applying any multivariate methods. This way many unwanted effects of physical nature such as light scattering, path length variations and random noise as well as instrumental effects can be removed, reduced or standardized (Reich, 2005). Thus, such effects will not impact further transformation or analysis of the data set. Preprocessing methods can be divided into filtering methods and model-based methods. Filtering methods only improve or "smooth" the data by removing some undesired types of variation (Afseth & Kohler, 2012), while model-based methods can be applied to quantify and separate different types of chemical and physical variations in the obtained spectra (Afseth & Kohler, 2012).

Derivation is a common filtering method, which is often used for baseline corrections, and can remove additive and multiplicative effects (Rinnan et al., 2009). The first derivative will only remove the baseline of a spectrum, while the second derivative removes the baseline and the linear trend in the data (Rinnan et al., 2009). Derivation can often amplify spectral noise, which is why a smoothing algorithm such as the Savitzky-Golay is applied prior to derivation (Reich, 2005).

One of the common model-based methods is the multiplicative scatter correction (MSC), which is a method used to correct for physical variability between samples due to scattering (Rinnan et al., 2009). The basic idea of MSC can be applied to signal processing in general and has been extended in what is called extended multiplicative signal correction (EMSC).

EMSC is more selective regarding scattering and other unwanted variation effects, and can correct for baseline effects, interference effects and multiplicative scaling effects (Afseth & Kohler, 2012). Transformation through EMSC requires a reference spectrum, and often the average spectrum of the calibration set is used (Rinnan et al., 2009). In many cases the main effect of EMSC is a normalisation of each spectrum of the data set. Once the baseline of the obtained spectra has been corrected and unwanted scattering effects have been removed, multivariate methods can be applied to the preprocessed data.

### 2.4.2 Principal component analysis

Principal component analysis (PCA) is a common multivariate method used to extract relevant information from large datasets (Jollife & Cadima, 2016). It can be used in an early step to check for outliers and sample variation, to detect trends or groupings in the data, and to find and evaluate relevant structures in the data set (Bekhit et al., 2014). The main principle of PCA is to reduce the dimensionality of the dataset while keeping as much as possible of the statistical information (Jollife & Cadima, 2016). When relating this to figure 5, the goal of PCA is to separate the data structure from the noise.

The starting point for PCA is a dataset consisting of *n* objects (samples) and *p* variables (measurements) (Esbensen, 2002). These points are plotted in a coordinate system with *p* dimensions, and the goal is to model the phenomena (data structure) which differentiates the data. This phenomenon is defined as the axis which maximizes the longitudinal variance and at the same time minimizes the squared projection distance (Esbensen, 2002). This axis is called the first principal component (PC) and explains the largest amount of variation. Per definition, PC-2 will be orthogonal to PC-1 and will be directed to model the second largest variation. PC-3 (and all following PC's) will be orthogonal to previous PC's while modelling the largest remaining variance (Esbensen, 2002). This method will generate many PC's; however, the first ones often contain the useful information while higher order PC's explain the noise part. The number of dimensions is thus reduced dramatically. A new coordinate system is formed by the PC's, and the variables in this new system do not co-vary. Figure 6 visualizes how PC-1 and PC-2 create a new coordinate system (Esbensen, 2002).

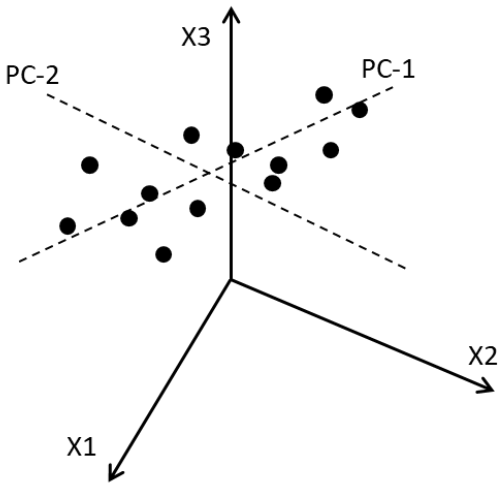


*Figure 6 – Illustration of observations (dots) in a coordinate system. PCA seeks to find the pattern in these observations and creates a new coordinate system by placing the different principal components orthogonal to each other. This illustration is adapted from Esbensen (2002).*

When using a data program to perform PCA on a data matrix, there are two plots which are of special interest. First there is the score plot, which visualizes the score vectors of two chosen PC's. This plot is useful for the detection of outliers, groupings and trends in the data by studying the pattern of the samples. Similar samples will be located close to each other. Secondly, the loading plot shows how the different variables contribute to each PC. These two plots are interesting because the score plot indicates *how* the objects of two PC's are related, while the complementary loading plot can be used for explaining *why* the objects are related (Esbensen, 2002).

In spectroscopy it is especially useful to always study the score plot and the associated 1-D loading plot. By studying the position of the individual samples in the score plot, one may get an idea of what the hidden phenomena is. The 1-D loading plot will supply information regarding which spectral bands vary the most, and this information can be used to determine which functional groups differentiate the samples.

### 2.4.3 Partial least squares regression

Partial least squares regression (PLSR) is a multivariate method used to make calibration models (Viscarra Rossel et al., 2006). It is an extension of PCA, however, instead of considering only the predictor variables *X* when reducing the information to a few important PC's, PLSR also takes a response variable *Y* into account (Boulesteix & Strimmer, 2006; Viscarra Rossel et al., 2006). These *Y* variables will guide the decomposition of the *X* matrix,

which is performed much the same way as for PCA (Esbensen, 2002). Here the spectral data will equal the predictor variables *X* and the different parameters which might explain the variation in *X* will be the response variables *Y*. PLSR searches for the model with maximum covariance between *X* and *Y*, and reduction of dimensions is performed simultaneously to regression (Boulesteix & Strimmer, 2006). A fitted model should ideally consist of a few factors that explain most of the variation in both the response and predictor variables (Viscarra Rossel et al., 2006). The result of PLSR will thus be an optimal regression for the prediction of the chosen parameter *Y* based on spectral information *X* (Esbensen, 2002).

The PLSR models are evaluated based on the number of factors that explain most of the variation, the root mean square error of cross validation (RMSECV) and the coefficient of determination ($R^2$). Cross-validation is used to determine the optimal number of PLSR factors (Afseth et al., 2010). RMSECV is calculated by comparing the actual chemical values to the ones predicted by the linear model, and the prediction error of this cross-validated calibration model is calculated by use of equation 4 (Afseth et al., 2010).

Eq. 4: $$RMSECV = \sqrt{\frac{1}{N}\sum_{i=1}^{N}(y_i - \hat{y}_i)^2}$$

Here *i* is the number of samples from 1 to *N*, $y_i$ is the observed value and $\hat{y}_i$ is the predicted value for *Y* (Afseth et al., 2010). The value of RMSECV is generally wanted to be as small as possible (Esbensen, 2002), and has the same unit as predictor variables. The coefficient of determination, $R^2$, does explain how much of the variation in the predictor variables is explained by the response variable. $R^2$ will always have a value between zero and one, where a value of zero would mean that no variation in the predictor variables is explained by the chosen response variable, and one would mean that all variation is explained (Ross, 2010).

## 2.5 Classification of oils

The goal in classification is to distinguish two groups based on collected data, or to assign a new sample to one of the groups (Esbensen, 2002; Olkin & Sampson, 2001). Classification can be performed based solely on the collected data without any *a priori* information about class membership; this is called unsupervised classification (Rajalahti & Kvalheim, 2011). A common method used for unsupervised classification is PCA. Other methods such as soft

independent modelling of class analogies (SIMCA) and partial least squares discriminant analysis (PLS-DA) are supervised methods that incorporate *a priori* information about class membership (Rajalahti & Kvalheim, 2011). Classification results based on supervised methods will generally be more optimistic regarding class affiliation than results from unsupervised methods. Before classification, it is important to preprocess the spectral data in order to remove any physical effects that may differentiate the samples. A classification method can then discriminate the samples based on the chemical differences.

## 2.6 Correlation coefficient

The correlation coefficient is a measurement for the relationship between two variables. It indicates both the strength and direction of this relationship. Pearson's correlation coefficient (r) is calculated as described in equation 5.

Eq. 5: $$r_{x,y} = \frac{\Sigma(\mathrm{x}-\bar{x})(y-\bar{y})}{\sqrt{\Sigma(\mathrm{x}-\bar{x})^2\Sigma(y-\bar{y})^2}}$$

Here $\bar{x}$ and $\bar{y}$ are the mean values for array 1 and array 2. The coefficient is always between 1 and -1, where 1 indicates a perfect correlation and -1 is a perfect inverse correlation. A value of 0 means there is no correlation between the chosen variables (Akoglu, 2018).

# 3. Experimental

## 3.1 Project description

As mentioned in the introduction, the main objective of this thesis was the classification and quantification of FAs in edible oils using vibrational spectroscopy. Figure 7 illustrates how the main objective is divided into three sub-objectives. The first sub-objective dealt with the classification, where 72 samples of marine oils from Orivo (table 6) were analysed with FTIR and Raman spectroscopy and the results were studied using PCA. In sub-objective two, the reference method was used to determine the FA composition in 18 reference oils (table 7) and based on these results a sample design with low correlation between the FAs was created. Based on the sample design a calibration set of 80 samples was made (appendix D). These calibration samples were analysed with FTIR and Raman, and the obtained information was used in the development of calibration models using PLSR. In sub-objective three the calibration models were validated by analysing independent oil samples.

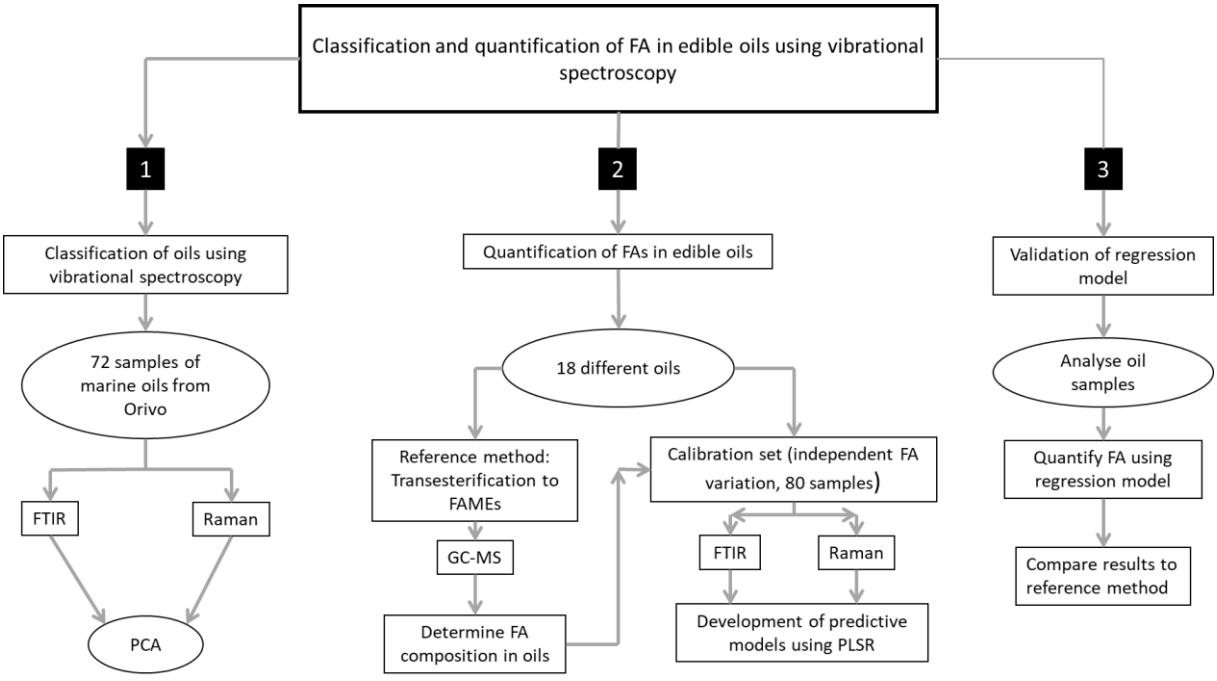


*Figure 7 – Illustration of the main objective of this research and how it is divided into three sub-objectives.*

## 3.2 Materials and chemicals

Table 3 presents all the chemicals used for this research, while table 4 lists the equipment and instrumentations. Applied software systems are provided in table 5 and all the oils that were analysed can be found in tables 6 and 7.

*Table 3 – All chemicals used in this research, with manufacturer, purity grade and CAS-number.*

| Product | Manufacturer | Purity [%] | CAS-nr. |
|---|---|---|---|
| n-Heptane | VWR Chemicals, Poland | ≥ 99 | 142-82-5 |
| Methanol | VWR Chemicals, Netherlands | ≥ 99.9 | 67-56-1 |
| Sodium | Merck, Germany | | |
| Chloroform | VWR Chemicals, France | 100 | 67-66-3 |
| Trinonadecanoin | Larodan AB, Sweden | | 26536-13-0 |
| Food industry fame mix (37 components) | RESTEK, USA | | |
| Isopropanol prima | Kemetyl Norge AS | | |

*Table 4 – Equipment and instruments used in this research with name, manufacturer and other specifications.*

| Instrumentation/ Equipment | Name | Manufacturer | Specifications |
|---|---|---|---|
| Centrifuge | EBA 20 | Hettich® | |
| Orbital shaker | PSU-10i | Biosan | |
| Vortex mixer | Yellowline TTS2 | IKA-Werke | |
| Heater | Dri-Block® | Techne® | |
| Mass spectrometer | ISQ™ QD | Thermo Scientific™ | Single quadrupole |
| Gas Chromatograph | Trace™ 1310 | Thermo Scientific™ | |
| GC column | Rtx-2330 | Restek | 60 m, 0,25 mm ID, 0,2 µm $d_f$ |
| Manual pipette | Acura 826 | Socorex | 10-100 µL |
| Manual pipette | M10 | BioHit | 0.5-10 µL |
| Evaporator | Reacti-Vap™ | Thermo Scientific™ | 27 ports |
| Micro balance | CP2P Sartorius | VWR International | |
| Culture tubes | Culture tubes with screw cap | Duran® | |
| Pasteur pipettes | Disposable glass Pasteur pipettes | VWR International | 150 mm |
| GC vials | Crimp neck vials | VWR International | 32 x 11,6 mm |
| Aluminium cap | Aluminium crimp seal | VWR International | |
| Aluminium micro weighing dishes | Oval Weighing dishes | VWR International | 0.04 mL |
| Plastic tubes with cap | Tube 25ml 90x25PP + Cap NAT | SARSTEDT | 25 mL |
| FTIR spectrometer | Nicolet™ iS™5 Spectrometer | Thermo Scientific™ | |
| ATR accessory for FTIR spectrometer | iD7 ATR | Thermo Scientific™ | With monolithic diamond ATR crystal |
| Laboratory drying oven | Series TS8000 | Termaks | Used at 40 °C |
| Raman spectrometer | RamanRxn2™ Hybrid | Kaiser Optical Systems, Inc. | Used with MR-probe |
| MR-probe | RamanRxn™Probe | Kaiser Optical Systems, Inc. | Connected to MultiRxn Probe – 785 |
| Polypropylene tube | CELLSTAR® | Greiner Bio-One International | 15 mL |
| Blue cap bottle | Duran® Laboratory glass bottle | SCHOTT DURAN® | 200 mL |

*Table 5 – Software used in this research, listed with name and manufacturer.*

| Software | Name | Manufacturer |
|---|---|---|
| Chromatography data system software | Chromeleon™ 7 | Thermo Scientific™ |
| Spectroscopy data system software | OMNIC™ Series Software | Thermo Scientific™ |
| Raman Software | iC Raman™Software | Kaiser Optical Systems, Inc. |
| Multivariate analysis software | The Unscrambler X 10.3 | Camo Analytics |
| Spreadsheet program | Excel | Microsoft |

## 3.3 Sample storage

All the oil samples were stored at -20 °C to prevent oxidation. Before analysis with spectroscopy they were put in a fridge at 4 °C over night, and an hour before analysis the samples were put in room temperature so they could be analysed at approximately the same temperature (22–23 °C). The samples were homogenised through manual shaking or use of a vortex mixer. Some of the samples from Orivo contained particles, which had to sediment as much as possible before the oils could be analysed. Some samples containing coconut oil were not fully melted at 23 °C and were heated to 38 °C in a laboratory drying oven for approximately 20 minutes. Once they were cooled down to room temperature again, they were analysed before any precipitation could form. This was the standard procedure for preparation of all samples before analysis with spectroscopy.

Prior to preparation of FAME samples for analysis with GC-MS, the oil samples were put in room temperature until fully melted. They were thoroughly shaken to ensure homogeneity. The fats were used in their solid state.

## 3.4 Part I – Classification of marine oils

The company Orivo supplied samples of seven different types of marine oils for the use in this research. The types of oil and number of different samples received for each type are listed in table 6.

*Table 6 – The seven types of marine oils from Orivo, listed with number of samples per type of oil.*

| Type of oil | Nr. of samples |
|---|---|
| Wild salmon | 10 |
| Farmed salmon | 12 |
| Krill | 10 |
| Anchovy | 10 |
| Sardine | 10 |
| Norwegian cod liver | 10 |
| Islandic cod liver | 10 |

### 3.4.1 Analysis of oils with FTIR spectroscopy

For the FTIR analyses the Thermo Scientific™ Nicolet™ iS™5 spectrometer with the iD7 ATR accessory was used. The instrument was equipped with a monolithic diamond. For the analyses the absorbance was measured, and the instrument was set to take 40 scans with a resolution of 4 $cm^{-1}$ for each measurement. First a background spectrum was obtained with the clean crystal, before a drop of sample was applied over the entire surface of the crystal with a disposable Pasteur pipette. A new spectrum was obtained and corrected relative to the background spectrum. The crystal was then cleaned using tissue paper and 70% isopropanol (Kemetyl Norge AS), before analysing the next sample. One sample was used as a reference and was measured once a day over the period of sample analysis in order to monitor changes in the instrument. Three replicates were taken for each sample. The software used with the instrument was the Thermo Scientific™ OMNIC™.

### 3.4.2 Analysis of oils with Raman spectroscopy

These analyses were conducted using the Raman spectrometer RamanRxn2™ Hybrid by Kaiser Optical Systems, Inc. A ball-probe was connected to the system and mounted every morning before analysis of the fish oil samples from Orivo. The laser was set to 400 mW. Once the system was ready, the samples were transferred into plastic tubes (SARSTEDT) that were wide enough for the ball-probe. The head of the probe was immersed in the oil sample until it was fully covered. All the lights in the room were turned off to avoid pollution of the measurement, and the sample was analysed with 6 scans of 5 seconds. Once the measurement was done, the probe was lightly swirled inside the sample, and the next replicate was measured. A total of three replicate measurements for each sample were recorded. Between the different samples the probe was cleaned using dish soap, water and tissue paper. The probe was dried thoroughly before analysing the next sample to avoid contamination by

water. A reference oil was analysed regularly to monitor any changes in the measurements which could be due to changes in the instrument or instrumental set up.

### 3.4.3 Multivariate data analysis

The software The Unscrambler X 10.3 (Camo Analytics) was used to determine whether the different fish oils from Orivo (table 6) could be classified based on analysis by vibrational spectroscopy. All spectra were plotted in Unscrambler to check if the overall picture looked normal, and PCA was performed on the raw data to check for any outliers.

Preprocessing of all spectra was performed prior to data analysis. The FTIR spectra were preprocessed by applying Savitzy Golay second derivatives (with second order polynomial and 27 smoothing points). Subsequently, EMSC was applied to the spectral area with information of interest, in this case the area of 4000 – 2700 $cm^{-1}$ and 1800 – 500 $cm^{-1}$. The last step was calculating the average of the three replicates for each sample. For the classification PCA was performed with random cross-validation, and only on the areas with relevant spectral information.

A custom-made routine (Matlab) for baseline correction was used in order to remove the fluctuating baselines of the Raman spectra. In the routine, a sixth-ordered polynomial was fitted and then subtracted from the Raman spectra (Lieber & Mahadevan-Jansen, 2003). Subsequently, normalization using EMSC was performed in the region of 500 – 1890 $cm^{-1}$. The last step was calculating the average of the three replicates for each sample.

## 3.5 Part II – Method development

### 3.5.1 Prepared solutions

**Sodium methoxide**

A sodium methoxide solution was prepared using 200 mL methanol (VWR Chemicals, Netherlands) which were transferred to a blue cap bottle (SCHOTT DURAN®). Approximately 1.0 gram of metallic sodium (Merck, Germany) was added to the methanol while the bottle was standing in a fume hood, to attain a concentration of 5 mg/mL of sodium methoxide in methanol. After ended reaction the bottle was closed, and the sodium methoxide was stored at room temperature until use.

**Internal standard – Trinonadecanoin**

It was decided to use one IS for the quantification of all FAs in the reference oils. Trinonadecanoin, a simple TAG with three C19:0 FAs, was chosen because this FA should not occur naturally in edible oils. A stock solution with a concentration of 10 mg/mL was prepared by dissolving 80 mg of trinonadecanoin (Larodan AB) in 8.0 mL chloroform (VWR Chemicals, France). The solution was prepared in a plastic tube (Greiner Bio-One International) and homogenized using a vortex mixer (IKA-Werke) before it was stored at 4 °C until use. The stock solution was vortexed again before it was added to any samples. In total two IS stock solutions had to be prepared, see appendix B for exact amounts.

### 3.5.2 Reference oils

For the reference analysis different edible oils were bought. 18 different oils were chosen, the types of oil and manufacturers are presented in table 7.

*Table 7 – 18 reference oils, listed with manufacturer.*

| Type of oil | Manufacturer |
|---|---|
| Rapeseed | Eldorado |
| Peanut | International collection |
| Sesame | Apotek 1 |
| Olive | Eldorado |
| Flaxseed | Helios |
| Soybean | Eldorado |
| Sunflower | Eldorado |
| Vita hjertego' OPTIMAL | Mills |
| Frying oil | Eldorado |
| Möller's tran | Peter Möller (Orkla) |
| Rice bran oil | Emmy's choice |
| Salmon | Nofima |
| Herring | Nofima |
| Coconut, extra virgin | Helios |
| 0370[a] | GC Rieber |
| 4030[a] | GC Rieber |
| 3040[a] | GC Rieber |
| Camelina oil | Nofima |

[a] = oils enriched in EPA and DHA

### 3.5.3 Transesterification of neutral lipids

The method applied here is based on the master thesis by Katarina Breivik Halvorsen (Halvorsen, 2019). Two series of FAMEs with different IS concentration were made from the reference oils in table 7, in order to be able to quantify both the major fatty acids as well as the ones present in smaller amounts. Series one had a low IS concentration, while series two had a high IS concentration. Three replicates of FAMEs were prepared for each oil in both series.

In the first series (low IS concentration), approximately 50 mg of each reference oil were weighed into separate culture tubes (Duran®). 100 µL of IS solution (trinonadecanoin, 10 mg/mL) was added to each culture tube. The samples were dried for approximately 30 minutes using low heat and a flow of $N_2$-gas. The triglycerides were then solvated in 2.0 mL of n-heptane (VWR Chemicals, Poland), before 1.5 mL of sodium methoxide solution (5 mg/ml methoxide in methanol) was added. For 30 minutes the samples were shaken at 385 g in room temperature and then centrifuged at 381 rcf for five minutes to properly separate the two phases in the samples. Approximately 1.5 mL of the heptane phase (upper phase) was transferred to GC-vials. These solutions were then diluted 1:5 with n-heptane in order to achieve a suitable concentration for the analysis with GC-MS. The samples were stored at -20 °C before and after analysis.

For the second series (high IS concentration), the steps above were repeated using approximately 5 mg of oil, which were weighed into small aluminium micro weighing dishes (VWR®). These FAME samples were not diluted before analysis with GC-MS.

### 3.5.4 Analysis using GC-MS

The FAME samples made from the oils of table 7 were analysed with GC-MS. A Trace™ 1310 gas chromatograph was coupled to an ISQ™ QD mass spectrometer, both were from Thermo Scientific™. The GC was run in split operating mode with a split ratio of 10. It was equipped with a 60 m fused silica column from Restek with an inner diameter of 0.250 mm and a film thickness of 0.20 µm. Figure 8 shows the temperature run of the GC oven. At sample injection, the oven temperature was at 50 °C and by the end of the run it had risen to 245 °C. The MS had a single quadrupole mass filter with a selected mass range of 50-700 amu. The software used with the GC-MS was Chromeleon 7 (Thermo Scientific™).

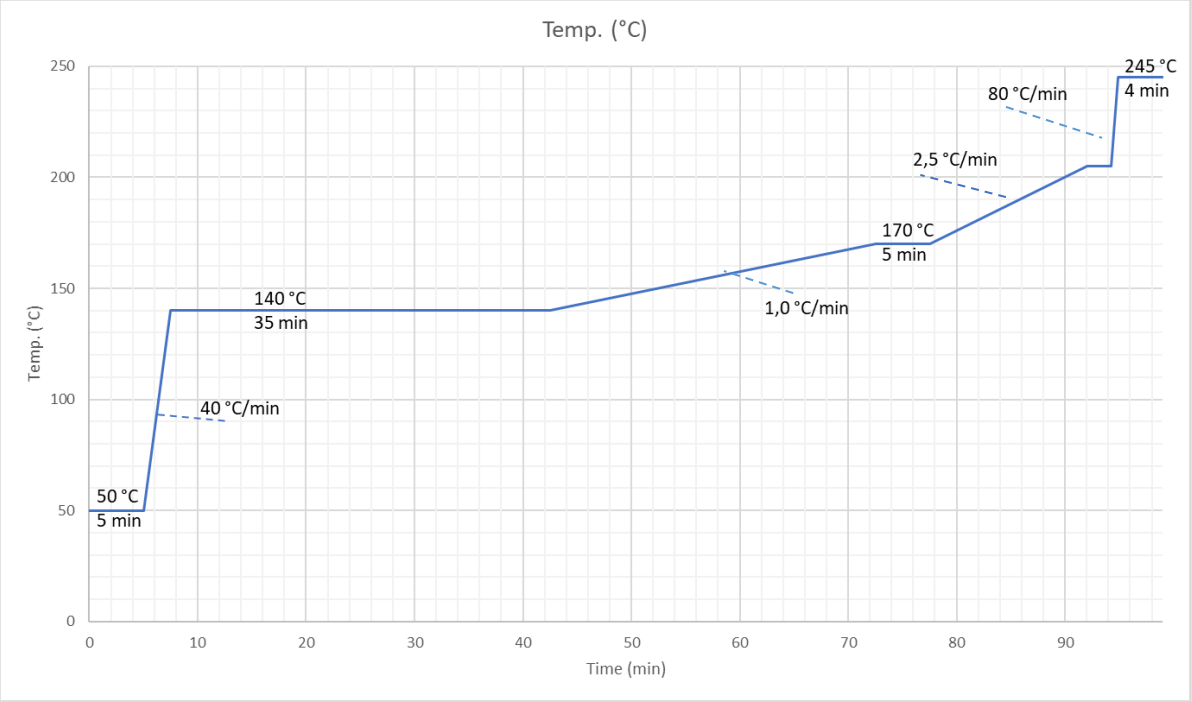


*Figure 8 – Temperature run of the GC oven. Total run-time was 99 minutes, with a starting temperature of 50 °C and a final temperature of 245 °C.*

### 3.5.5 Identification and quantification of FAs

The FAMEs were identified by comparing the RT of the peaks in the sample chromatograms to the peaks of the reference mix containing 38 different FAMEs (Food Industry FAME mix, Restek, with added 19:0). In addition, NIST 2017 database was used to identify the FAs based on the obtained mass spectra. Once the peaks were assigned to FAMEs from the reference mix, the masses of the different FAs were calculated based on equation 3, as described in section 2.3.3. The RRF-values (Molversmyr, 2020) and molecular masses for the various FAs can be found in appendix C.

The reference oils from marine sources contained FAs that could not be identified with a standard in the Food industry FAME mix (RESTEK). In order be able to quantify as many of the FAs present as possible, some of these FAs were identified only by spectral searches in a database (NIST 2017). The exact isomers were not determined. The table presented in appendix C lists all the unidentified isomers that were found, with RRF-values based on the values that were found for equivalent isomers in the Food industry FAME mix. Three of the unidentified isomers did not have an equivalent isomer in the Food industry FAME mix and thus were assigned RRF-values of one.

The series of FAME samples with a high IS concentration (series two) was used to quantify the largest peaks in the chromatograms, while the other series (series one) was used for the remaining peaks. The ratio of the peak areas of FA/IS were used to determine which series was best suited for the individual peaks, and the series with the smallest ratio of FA/IS was used.

### 3.5.6 Calibration set

Based on one replicate of each of the 18 oils with known FA composition, a sample design for the calibration models was made by a chemometrician at Nofima. Eight different FAs were chosen based on their concentration in the oils. All these FAs are important FAs commonly found in foods and biological samples. A mixture design was used to make "theoretical" mixtures of all the 18 reference oils. This included:

1. All Combinations of two oils in ratios 25 / 75 and 50 / 50
2. All combinations of three oils in the ratios 25 / 25 / 50 and 33 / 33 / 33
3. Pure oils

In total, this resulted in 3741 oil mixtures and candidates for our calibration design. Subsequently, the Kennard-Stone algorithm was used to choose the set of 80 mixtures that spanned the variation of all eight chosen FAs, and at the same time provided the lowest correlation between these FAs in the 80 samples (Daszykowski et al., 2002).

The samples were prepared by mixing the respective oils of a sample in 25 mL plastic tubes with cap (SARSTEDT) in the given ratios and homogenising them using a vortex mixer. A 100 % of a sample was chosen to equal 15 g, and the exact masses were recorded so that the actual mixing ratios of the samples could be calculated. This data was used together with the data for the FA content in the reference oils to calculate the theoretical amount of each FA in these 80 samples, as is demonstrated in equation 6.

Eq. 6: $$Mass_{FA1} = \left(\frac{w1}{tw} \cdot FA1_{ref1}\right) + \left(\frac{w2}{tw} \cdot FA1_{ref2}\right) + \left(\frac{w3}{tw} \cdot FA1_{ref3}\right)$$

FA1 denotes a chosen FA, w1, w2 and w3 are the recorded masses of the reference oils which were mixed in each sample. tw is the total weight of the sample, and $FA1_{ref1}$, $FA1_{ref2}$ and $FA1_{ref3}$ equal the FA content (% FA of total FA content) of the one, two or three reference oils in each sample. Lastly, ΣSFA, ΣMUFA, ΣPUFA and the UI for all calibration samples

was calculated based on the FA composition of the samples. UI was calculated as described in section 2.1.3.

### 3.5.7 Analysis of the calibration set

All the samples of the calibration set were analysed with FTIR and Raman as described in sections 3.4.1 and 3.4.2, with the same settings and three replicates per sample.

### 3.5.8 Calibration models based on FTIR

The obtained spectral data from the samples of the calibration set were preprocessed prior to performing PLSR, as described in section 3.4.3. The data was transformed using EMSC on the area containing important spectral information, which here was the area of 3100-2750 $cm^{-1}$ and 1800-500 $cm^{-1}$. PLSR (15 maximum components) with random cross-validation (20 segments, four samples per segment) was performed on the spectral area of 3100 – 2750 $cm^{-1}$ and 1700 – 500 $cm^{-1}$. The spectral data served as the predictor variables (X), and the calculated FA content in the calibration samples for the FAs 14:0, 16:0, 18:1(n-9), 18:2(n-6), 18:3(n-3), 20:5(n-3), 22:6(n-3) in addition to ΣSFA, ΣMUFA, ΣPUFA and the calculated UI were response variables.

### 3.5.9 Calibration models based on Raman

Again, the same preprocessing methods as in section 3.4.3 were applied to the obtained Raman spectral data prior to performing PLSR analysis. The average of the three replicates for each sample was calculated, and PLSR (15 maximum components) with random cross-validation (20 segments, four samples per segment) was performed on the spectral area of 500 $cm^{-1}$ to 1800 $cm^{-1}$. The spectral data from Raman analyses of the calibration samples served as predictor variables (X), and the FAs 14:0, 16:0, 18:1(n-9), 18:2(n-6), 18:3(n-3), 20:5(n-3), 22:6(n-3) in addition to ΣSFA, ΣMUFA, ΣPUFA and the calculated UI were response variables.

## 3.6 Part III – Model validation

### 3.6.7 Validation of calculated FA profiles in calibration set

Prior to validation of the calibration models, a validation was performed to check how accurate the calculated FA profiles of the calibration set were. The samples with numbers 32, 54, 58 and 77 were chosen randomly from the calibration set, and their FA profiles were

determined according to the procedure described in sections 3.5.3, 3.5.4 and 3.5.5. The results were compared to the previously calculated FA profiles of these samples.

### 3.6.8 Validation of calibration models

Validation of the established calibration models was done by comparing predicted FA content in independent oil samples with their reference values. For this step four new oils were purchased and analysed with GC-MS. These oils are listed in table 8. The FA profiles were determined as described in sections 3.5.3, 3.5.4 and 3.5.5.

*Table 8 – Oils for validation of the calibration models. Listed with manufacturer.*

| Type of oil: | Manufacturer: |
|---|---|
| Grapeseed oil | Pietro Coricelli |
| Frying oil | Helios /Alma Norge AS |
| Walnut oil | International collection |
| Cooking oil | Coop |

### 3.6.9 FTIR

The independent oils were analysed with FTIR as described in section 3.4.1. All spectral data (raw data) from FTIR analysis of the 80 samples of the calibration set, the 10 samples of norwegian cod liver oil (Orivo) and from the four validation samples were put into one Unscrambler file. The data was preprocessed as described in section 3.4.3. All the data was preprocessed in the same Unscrambler file because EMSC had to be performed on the data of all samples at the same time. This way all data sets were treated the same way, which was necessary in order to predict the FA content in the independent samples.

A PCA was run on the preprocessed data to check for deviations in spectral values of the validation samples compared to the calibration set. PLSR for the different response parameters was performed as described in section 3.5.8 and based on these models the FA content of the eight main FAs in the validation samples was predicted. The predicted values were compared to the reference values found with GC-MS.

### 3.6.10 Raman spectroscopy

Samples of the validation oils were analysed with Raman spectroscopy as described in section 3.4.2. All spectral data from Raman analysis of the 80 samples of the calibration set and the four validation samples were preprocessed as described in section 3.4.3. All spectral data was preprocessed in the same Unscrambler file. PCA was run on the preprocessed data, and PLSR

was performed for the response variables as described in section 3.5.9. Based on these models the FA content of the eight main FAs in the validation samples was predicted. The values were compared to the reference values found with GC-MS.

# 4. Results and discussion

## 4.1 Part I – Classification

Marine oil samples were analysed with FTIR and Raman spectroscopy, and PCA was the classification method used to check if the samples of different groups could be separated from each other. The marine oils (Orivo) that analysed were quite diverse in colour. Krill oil had a deep red colour, while anchovy and sardine had a brown to yellow tone. Samples from both types of salmon oil were orange with a tone of pink, and the two types of cod liver oil were transparent and colourless. Some of the samples from anchovy, sardine and krill oil also had particles in them, and the consistency of these three types of oil was quite thick. Figure 9 shows a photo of samples of farmed salmon oil, sardine oil and norwegian cod liver oil.

*Figure 9 – From left to right: one samples of farmed salmon oil, two samples of sardine oil and three samples of norwegian cod liver oil. The samples were from Orivo.*

### 4.1.1 Raman spectra of marine oils

The average Raman spectra of the three replicates for each marine oil are presented in figure 10. Quite a few of these samples showed a spectrum that was not possible to interpret due to a saturated signal. A reduction of the scanning time from five to one second gave no significant change in the recorded spectra. This saturation is most likely caused by fluorescence (Bekhit et al., 2014). A strong fluorenscence background is a common problem in Raman spectroscopy, because the probability for fluorescence is much higher than for Raman scattering (Kostamovaara et al., 2013). The samples with a saturated spectrum were all of the types krill, sardine and anchovies. Thus, these three types of marine oils could not be used for

classification. Although the remaining four types of marine oils were possible to analyse, it was decided not to pursue the classification of marine oils with Raman, since the remaining dataset was very limited. The classification was thus only based on the results from FTIR analysis.

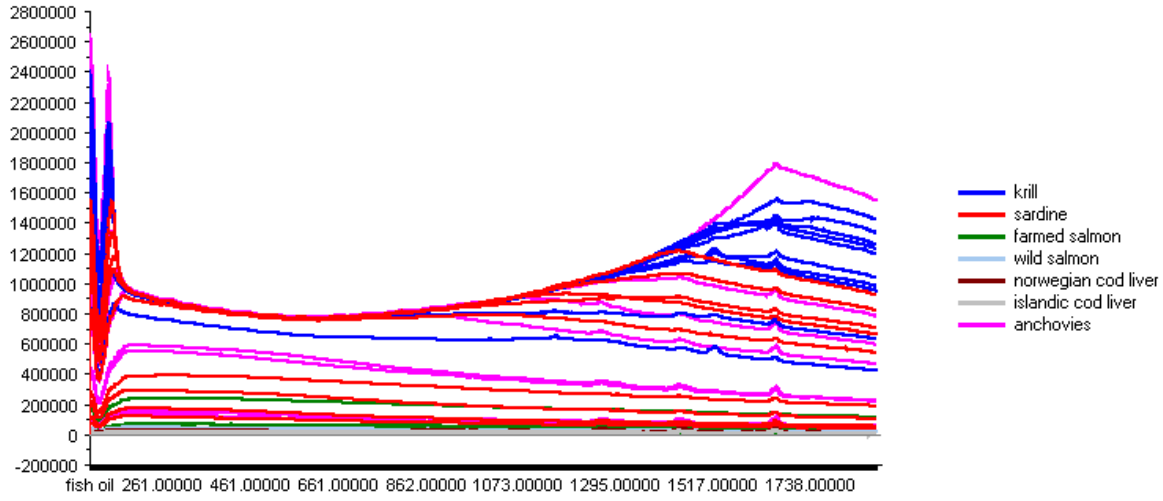


*Figure 10 – Average (n=3) Raman spectra for the 72 samples marine oils from Orivo. The spectra are colour-coded based on type of oil.*

### 4.1.2 FTIR spectra of marine oils

The average FTIR spectra for each sample of the marine oils are provided in figure 11.

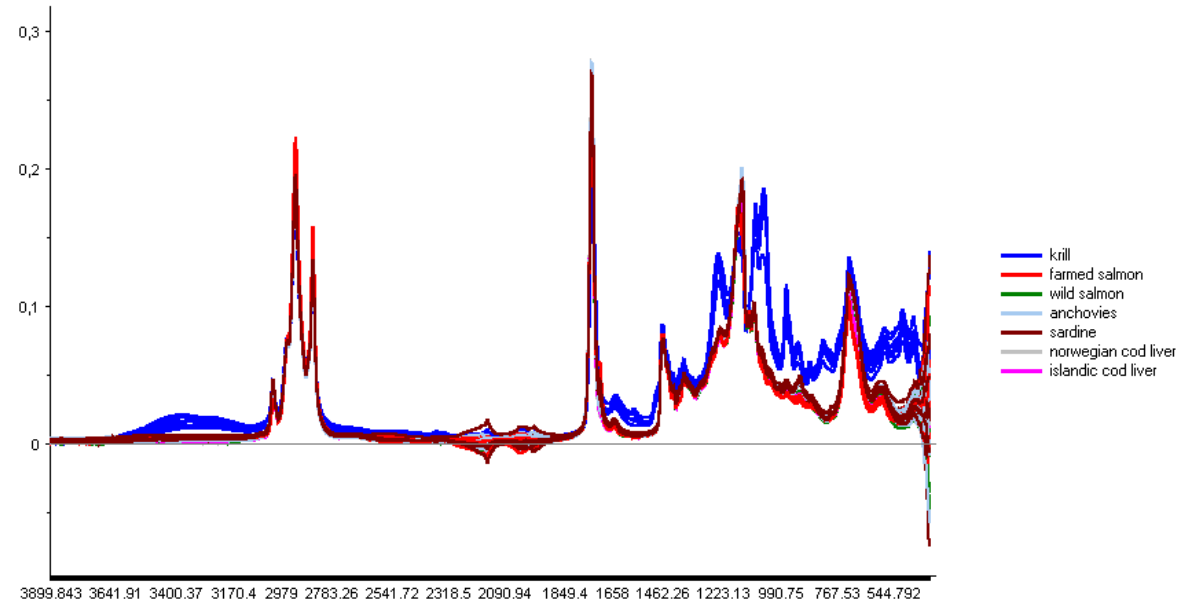


*Figure 11 – Average (n=3) FTIR spectra for the 72 samples of marine oils from Orivo. The spectra are colour-coded based on type of oil.*

The area between 2700 – 1800 $cm^{-1}$ and < 450 $cm^{-1}$ did not contain any relevant information for fats and oils. However, as can be seen in figure 11, these two areas showed a lot of variation for the different oils. As this was no relevant chemical information, it was decided to remove these areas before performing further data analysis.

### 4.1.3 Classification using FTIR spectra and PCA

After preprocessing the data, a PCA was run and the score plot for PC-1 and PC-2 can be seen in figure 12. The samples within each group were clustered together, which means they contain the same spectral information. However, the group of krill was clearly distinguished from all other groups. One significant difference between krill and other fish is that the lipid fraction of fish mainly consists of TAGs, while a large portion of this fraction in krill consists of phospholipids. Typically, about 43 g/100 g of krill oil are phospholipids (Burri & Johnsen, 2015). Such a difference in chemical composition is not ideal for this type of classification, as the goal here was to differentiate marine oils based on FA composition.

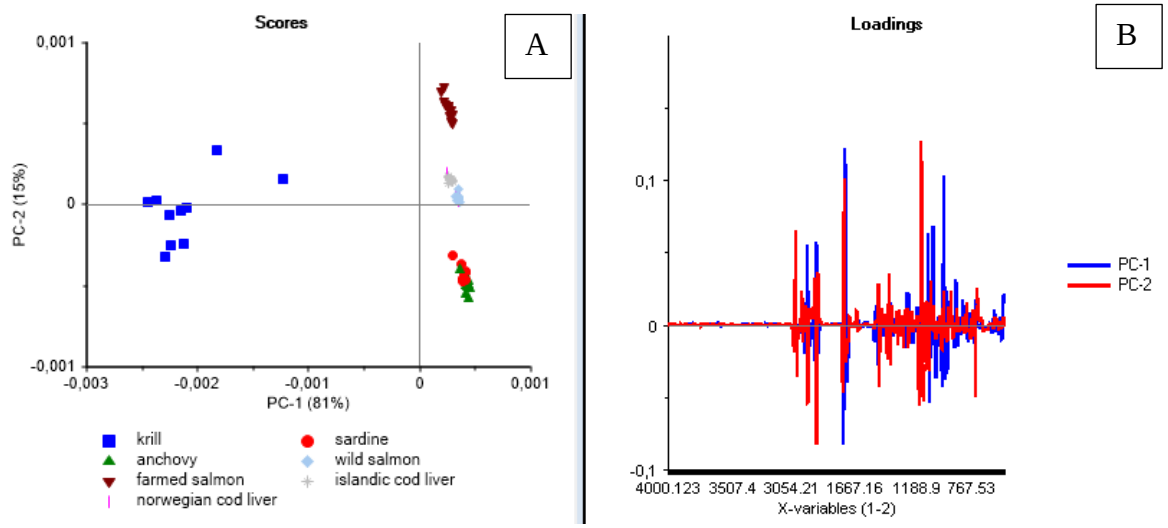


*Figure 12 – Principal component analysis for all samples of marine oils from Orivo. Figure 12A shows the score plot for PC-1 and PC-2, and figure 12B shows the loading plot for PC-1 and PC-2. The oil samples were analysed with FTIR spectroscopy.*

The associated loading plot for PC-1 and PC-2 is provided in figure 12B. Based on PC-1 the main absorption frequencies that distinguished the groups were 2923 $cm^{-1}$, 2852 $cm^{-1}$, 1730 $cm^{-1}$, 1090 $cm^{-1}$, 1050 $cm^{-1}$ and 968 $cm^{-1}$. For PC-2 the main bands in the loading plot were found at wavelengths 3012 $cm^{-1}$, 2850 $cm^{-1}$, 1737 $cm^{-1}$ and 1142 $cm^{-1}$. The characteristic absorption areas for FA in FTIR are mentioned in section 2.3.6. Phospholipids do have

characteristic stretches at ~1230 $cm^{-1}$, ~1085 $cm^{-1}$, ~1045 $cm^{-1}$ and ~820 $cm^{-1}$ due to the asymmetric and symmetric stretches of $PO_2^-$, the stretch of C–O–P and the P–O asymmetric stretch, respectively (Socrates, 2004). Nevertheless, a lack of reference values for the marine oils made proper interpretation of the loading plot for the PCAs difficult and was not attempted.

Since the difference between krill and the other oils dominated the initial PCA, a new PCA was performed leaving out the krill samples. Removal of the krill oil samples resulted in the score plot for PC-1 and PC-2 that is provided in figure 13A. Here the samples of farmed salmon were separated from all other oil types, while the groups of wild salmon, norwegian cod liver and islandic cod liver were located close together. The clusters of sardine and anchovy were positioned away from the other groups, but they did somewhat overlap. According to this score plot the six fish oils could be classified into three different groups based on the associated loading plot in figure 13B. For PC-1 the main absorption frequencies that differentiated these three groups were at 3012 $cm^{-1}$, 2853 $cm^{-1}$, 1739 $cm^{-1}$ and 1141 $cm^{-1}$. Based on PC-2 the main differences were found at wavenumbers 3010 $cm^{-1}$, 2930 $cm^{-1}$, 2847 $cm^{-1}$, 1709 $cm^{-1}$, 1145 $cm^{-1}$ and 1136 $cm^{-1}$.

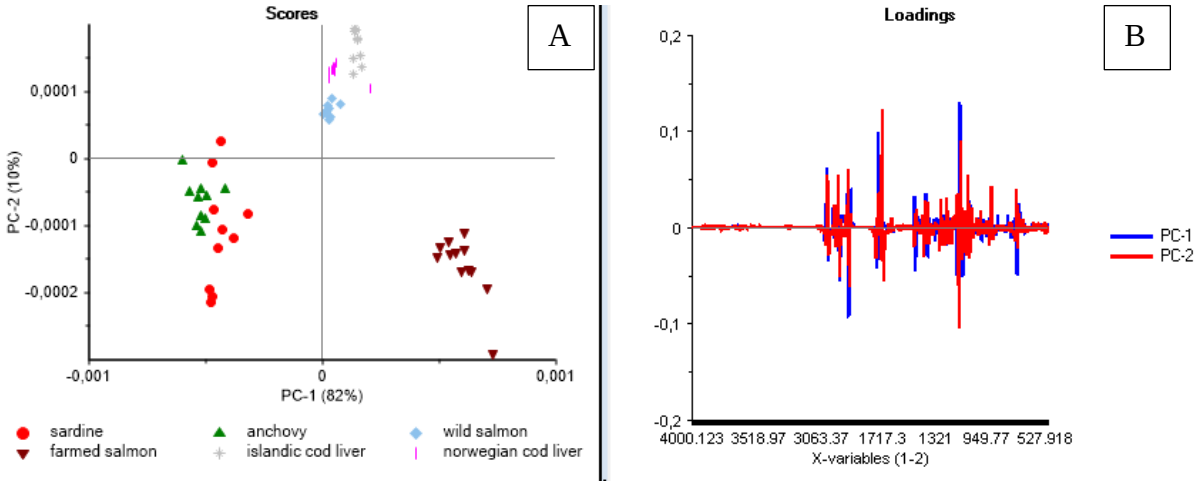


*Figure 13 - Principal component analysis for all samples from Orivo, except krill. Figure 13A shows the score plot for PC-1 and PC-2 and figure 13B shows the loading plot for PC-1 and PC-2. The oil samples were analysed with FTIR spectroscopy.*

PC-4, presented in figure 14, seemed to add some information on how to separate the group of wild salmon a bit better from norwegian and islandic cod liver. The most important bands in the loading plot for PC-4, which can be seen in figure 14B, were at wavenumbers 3014 $cm^{-1}$,

1746 $cm^{-1}$, 1091 $cm^{-1}$ and 723 $cm^{-1}$. Based on PC-1 and PC-4 the fish oils could be divided into four different classes.

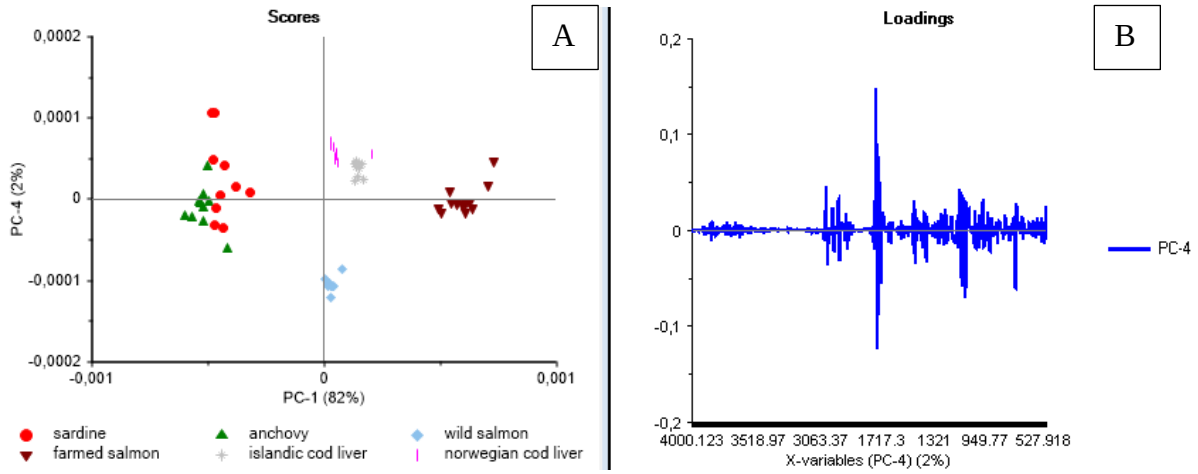


*Figure 14 - Principal component analysis for all samples from Orivo, except krill. Figure 14A shows the score plot for PC-1 and PC-4 and figure 14B shows the loading plot for PC-4. The oil samples were analysed with FTIR spectroscopy.*

Based on PCA with all six groups of marine oils it was not possible to distinguish the fish oil samples any further. Thus, a PCA was run based only on the groups that were hard to separate. Figure 15 displays a score and loading plot for sardine and anchovy, and here the samples could only be partly separated based on PC-1. The most prominent bands in the loading plot of PC-1 were at wavenumbers 2921 $cm^{-1}$, 2853 $cm^{-1}$, 1738 $cm^{-1}$, 1710 $cm^{-1}$, 1472 and 1144 $cm^{-1}$. The samples of sardine were quite scattered while the samples of anchovy were more clustered. Although the separation of these two groups was not perfect, the PCA in figure 15A still shows some separation.

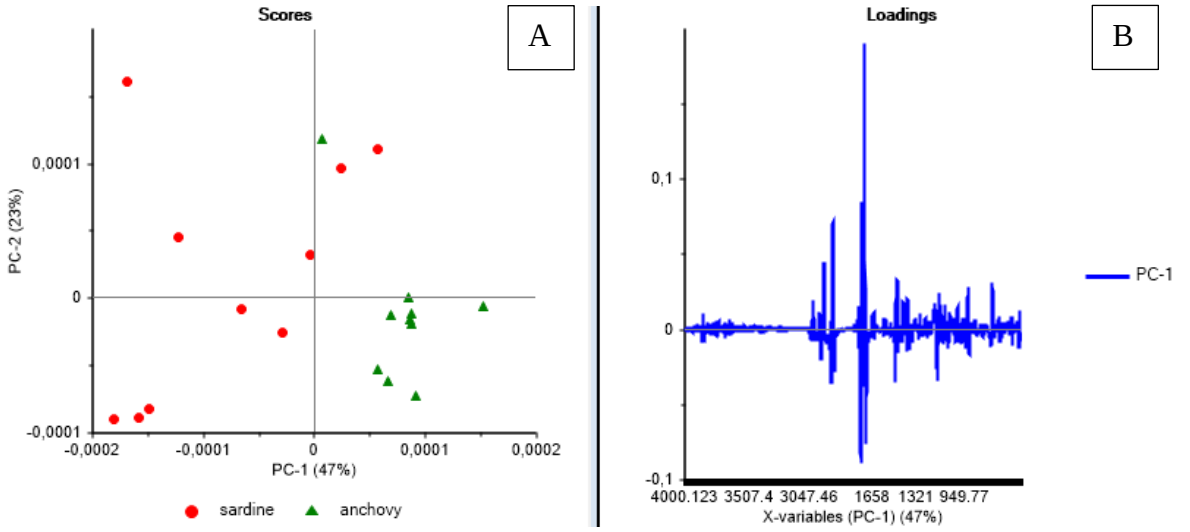


*Figure 15 - Principal component analysis for the samples of sardine and anchovy. Figure 15A shows the score plot for PC-1 and PC-2, and figure 15B shows the loading plot for PC-1. The oil samples were analysed with FTIR spectroscopy.*

A PCA of the samples of wild salmon, norwegian cod liver and islandic cod liver gave better results, as can be seen in figure 16. All samples of the same type of marine oil were clustered and placed apart from the other groups, except for one sample of norwegian cod liver oil that seemed to be an outlier. The most prominent bands in the loading plot for PC-1 were at 3012 $cm^{-1}$, 1746 $cm^{-1}$, 1137 $cm^{-1}$, 1119 $cm^{-1}$, 1090 $cm^{-1}$ and 722 $cm^{-1}$. For PC-2 the main peaks in the loading plot were at wavenumbers 2922 $cm^{-1}$, 2850 $cm^{-1}$ and 1740 $cm^{-1}$.

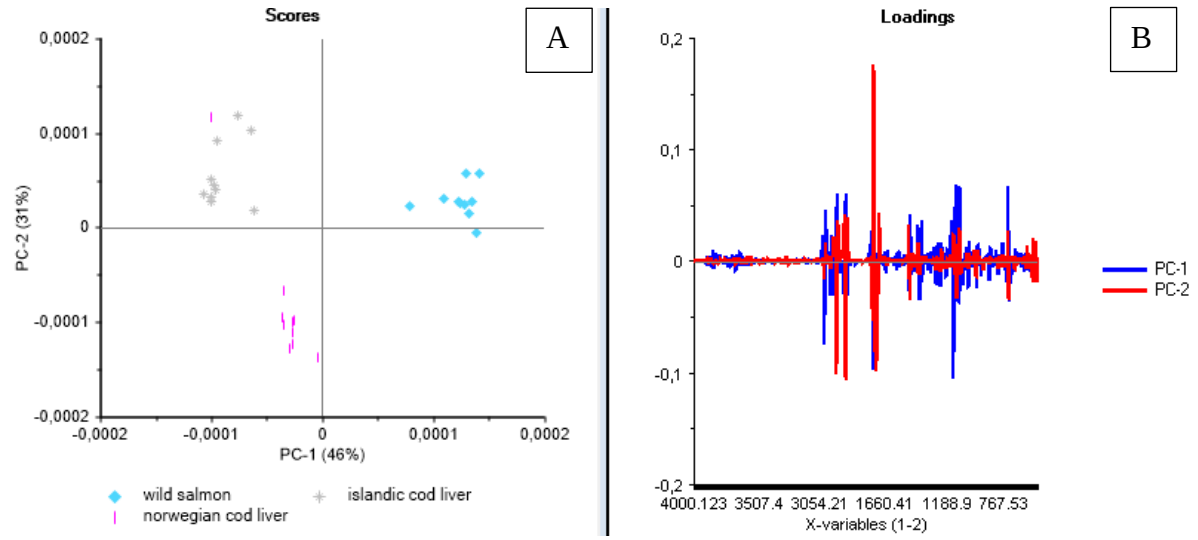


*Figure 16 - Principal component analysis for all oil samples of the types of wild salmon, islandic cod liver and norwegian cod liver. Figure 16A shows the score plot for PC-1 and PC-2 and figure 16B shows the loading plot for PC-1 and PC-2.*

Overall, PCA showed that each of the seven different marine oils could be separated from the other groups. Interpretation of the spectral bands was not attempted because no reference values were at hand, but the results seemed promising, and further classification with other classification methods should be pursued.

## 4.2 Part II – Method development

### 4.2.1 FA composition in reference oils – determined with GC-MS

In order to make a sample design with low correlation between the different FAs, the FA profiles of 18 reference oils were determined. A test run of FAME samples made from the reference oils and fats without added IS showed that there appeared to be some C19:0 present in three of the fish oils. The amounts present were however low and should not have any noteworthy impact on the results. Using C19:0 as IS will give quite accurate results for the FAs of similar chain length, but somewhat less accurate results for the shorter chain FAs such as C8:0 and C10:0. Out of the selected oils only coconut oil had significant amounts of shorter chain FAs.

Two series of samples with different IS concentration had to be prepared in order to accurately quantify both the large peaks and the smaller ones. In the 18 reference oils (table 7) 32 different FAs could be identified based on a comparison with the reference mix and the NIST 2017 database. Furthermore 12 unknown isomers of unsaturated FA were determined by using the NIST database. All FAs are listed in appendix C.

However, due to an unidentified mistake or problem, the quantification of FAs in the reference oils using the method with IS and calculations (Eq. 3) for the mass of each FA in the samples was not successful. In theory the sum of all identified FAs should have been close to 90g/100g of oil, but this was not the case. Thus, the FA profiles were used instead. The FA profiles for each oil were found by looking at the area in percent for the peaks of identified FAs in the chromatogram for each oil. By comparison with reference values for the FA composition of edible oils (matportalen.no, 2019), it could be seen that these values gave an accurate representation of the expected FA composition. All six sample replicates (from series one and two) were used for each reference oil, but some minor FAs were only identified in one of the two series of samples. This was mostly the case for the FAs present in small amounts, which could only be identified in the series with higher FAME concentration. The more unusual FAs were also only identified in the series with high FAME concentration.

The FA profile for the different reference oils (appendix E) showed that the FAs C16:0, C18:1n-9 and C18:2n-6 were generally present in large amounts in many of the oils. The FAs C20:5n-3 and C22:6n-3, which represent EPA and DHA respectively, were only found in the fish oils, as expected. The content of these valuable n-3 FAs was especially high in the oils 0370, 3040 and 4030, which are all fish oils enriched in EPA and DHA. C14:0, C18:0 and C18:3n-3 were also detected in larger amounts in most of the oils. These 8 FAs are the main FAs in the reference oils. Table 9 is an excerpt of appendix E and shows the FA profile for the reference oils including only the main FA, given in % FA of the total FA content.

*Table 9 – Fatty acid content in % (based on area in % of the assigned peaks in the chromatograms) for the 18 reference oils. This table is an excerpt from the table on appendix E. Numbers marked in red are only based on three replicates (n=3), for all other values n=6.*

| | 14:0 [%] | 16:0 [%] | 18:0 [%] | 18:1n-9 [%] | 18:2n-6 [%] | 18:3n-3 [%] | 20:5n-3 [%] | 22:6n-3 [%] |
|---|---|---|---|---|---|---|---|---|
| Rapeseed oil | 0.06 ±0.03 | 4.97 ±0.14 | 1.73 ±0.08 | 61.64 ±1.00 | 19.06 ±0.33 | 6.72 ±0.07 | n.d. | n.d. |
| Peanut oil | 0.02 ±0.00 | 6.90 ±0.11 | 2.12 ±0.13 | 67.59 ±1.48 | 15.36 ±0.35 | 0.47 ±0.05 | n.d. | n.d. |
| Sesame oil | 0.02 ±0.00 | 9.72 ±0.16 | 6.10 ±0.31 | 41.09 ±0.16 | 40.97 ±0.55 | 0.20 ±0.02 | n.d. | n.d. |
| Olive oil | 0.01 ±0.00 | 12.51 ±0.11 | 3.30 ±0.13 | 71.29 ±0.61 | 8.33 ±0.19 | 0.53 ±0.06 | n.d. | n.d. |
| Linseed oil | 0.04 ±0.00 | 6.73 ±0.07 | 4.32 ±0.14 | 20.50 ±0.31 | 15.31 ±0.39 | 51.92 ±0.92 | n.d. | n.d. |
| Soybean oil | 0.07 ±0.01 | 11.17 ±0.11 | 4.85 ±0.14 | 23.09 ±0.42 | 52.02 ±1.26 | 5.93 ±0.20 | n.d. | n.d. |
| Sunflower oil | 0.06 ±0.00 | 6.61 ±0.044 | 3.46 ±0.14 | 31.99 ±0.66 | 56.04 ±0.91 | 0.12 ±0.03 | n.d. | n.d. |
| Vita hjertegó | 0.04 ±0.00 | 6.24 ±0.09 | 2.31 ±0.07 | 56.39 ±0.79 | 25.75 ±0.44 | 5.24 ±0.13 | n.d. | n.d. |
| Frying oil | 0.05 ±0.00 | 5.70 ±0.06 | 2.48 ±0.08 | 45.47 ±0.15 | 38.23 ±0.35 | 4.52 ±0.13 | n.d. | n.d. |
| Møllers tran | 3.77 ±0.09 | 10.21 ±0.30 | 2.14 ±0.06 | 15.20 ±0.15 | 2.39 ±0.21 | 0.72 0.05 | 7.74 ±0.08 | 9.68 ±0.58 |
| Rice bran oil | 0.41 ±0.01 | 20.45 ±0.35 | 2.04 ±0.07 | 40.72 ±0.13 | 32.51 ±0.16 | 1.05 ±0.07 | n.d. | n.d. |
| Salmon oil | 2.19 ±0.06 | 9.96 ±0.34 | 2.68 ±0.09 | 42.58 ±0.41 | 13.78 ±0.19 | 4.91 ±0.08 | 1.99 ±0.34 | 2.80 ±0.17 |
| Herring oil | 8.91 ±0.19 | 14.25 ±0.35 | 1.09 ±0.04 | 6.99 ±0.11 | 1.52 ±0.09 | 1.12 ±0.07 | 7.00 ±0.08 | 6.14 ±0.18 |
| Coconut oil | 25.71 ±0.93 | 11.62 ±0.82 | 4.96 ±0.67 | 7.23 ±0.77 | 1.15 ±0.16 | n.d. | n.d. | n.d. |
| 0370 | 0.36 ±0.18 | 0.63 ±0.08 | 0.29 ±0.02 | 0.55 ±0.06 | 0.16 ±0.02 | n.d. | 12.89 ±1.50 | 62.32 ±3.55 |
| 4030 | 0.37 ±0.03 | 0.51 ±0.06 | 2.03 ±0.23 | 2.60 ±0.34 | n.d. | 0.19 ±0.04 | 44.08 ±0.94 | 28.21 ±2.67 |
| 3040 | 0.16 ±0.02 | 0.38 ±0.02 | 1.30 ±0.15 | 1.70 ±0.18 | 0.24 ±0.02 | 0.09 ±0.01 | 40.30 ±0.27 | 34.52 ±2.94 |
| Camelina oil | 0.04 ±0.01 | 6.12 ±0.13 | 2.93 ±0.09 | 16.79 ±0.11 | 19.32 ±0.33 | 37.97 ±0.48 | n.d. | n.d. |

Although a few of the FAs are dominating these profiles, important variations in FA composition can be found in the reference oils. As can be seen in figure 17 coconut oil is unique in regard to chain length because it contains many of the shorter chain FAs, the shortest being C6:0. The content of 12:0 in coconut oil is especially high compared to the other oils, with 35,82 ±2,91 % FA as opposed to a content of <0,2 % in the other samples. The longest FAs detected were C24:0 and C24:1n-9. C24:0 was mainly found in the plant oils and C24:1n-9 in the fish oils. Nevertheless, the amounts detected of these two long chain FAs were <1,2 % in all reference oils. C22:6n-3 was the long chain FA present in largest amounts, ranging from 2,80 ±0,17 % in salmon oil to 64,32 ±3,55 % in 0370. By dividing all the FA found in the reference oils into three categories based on chain length (C6 to C13, C14 to C19 and C20 to C24), one could see that the plant oils consisted of mainly FAs in the medium fraction, while the fish oils also contained large amounts of the longest chain fraction. Coconut oil was the only oil with significant amounts of FAs in the shortest chain fraction. Chain length of the reference oils is visualized in figure 17.

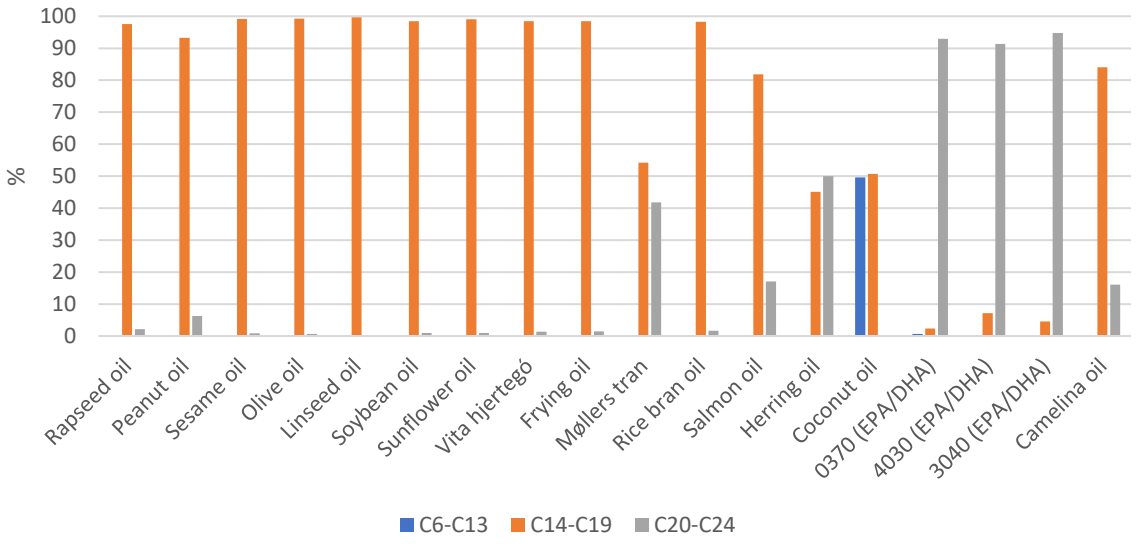


*Figure 17 – Illustration of fatty acid composition in the 18 reference oils. The fatty acids are summarized into the categories of fatty acids with 6-13 carbon atoms, 14-19 carbon atoms and 20-24 carbon atoms. The figure is based on table F2 in appendix F.*

The degree of unsaturation in the reference oils is shown in figure 18, where the sum of SFAs, MUFAs and PUFAs are presented for each oil. Coconut oil has the highest content of SFAs, followed by rice bran oil and herring oil. Olive, peanut and rapeseed oil have the highest

content of MUFAs, while the largest quantity of PUFAs can be found in 0730, 3040, and 4030.

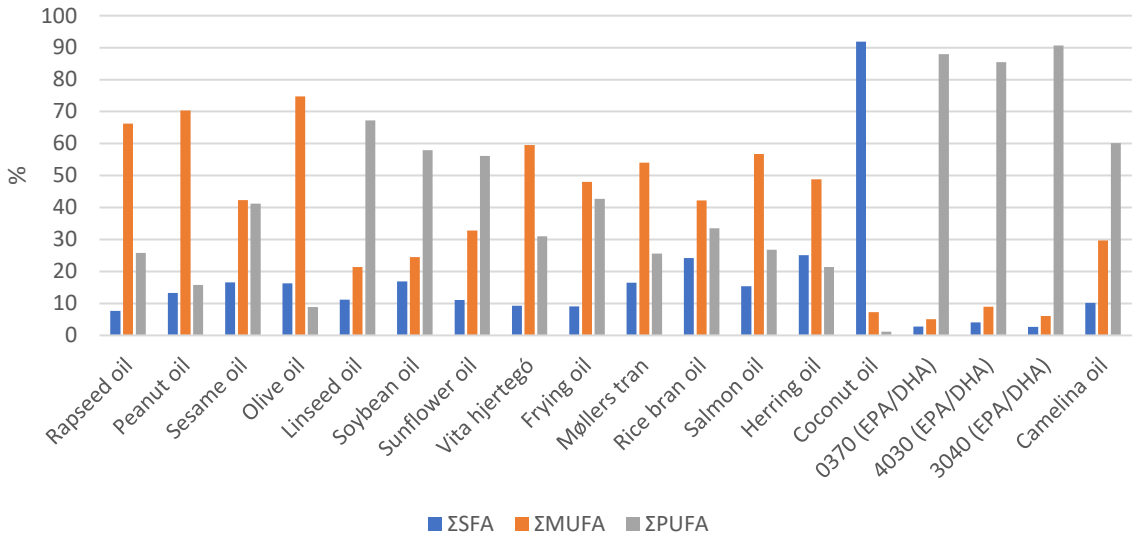


*Figure 18 – Illustration of the FA composition in the 18 reference oils. The FAs are displayed as ΣSFA, ΣMUFA and ΣPUFA. The figure is based on table F1 in appendix F.*

### 4.2.2 Calculated FA composition in the calibration set

The analyses of the reference oils showed that there were eight FAs that dominated the FA profiles. They included the SFAs C14:0, C16:0 and C18:0, the common FAs C18:1n-9, C18:2n-6 and C18:3n-3 as well as the valuable n-3 FAs C20:5n-3 and C22:6n-3. The set of mixtures that was chosen for the calibration set contained 80 mixtures of reference oils in different ratios. The details for these 80 mixtures can be found in appendix D.

The upper right part of figure 19 shows all possible mixtures (blue dots) of the sample design and the 80 samples that were chosen for the calibration set (red dots). Here one can see that the chosen mixtures do span the whole area of variation between two and two FAs quite well. The correlation between the different FAs in this set of samples should ideally be as low as possible. As can be seen in the lower left part of figure 19, correlations for the theoretical set were in the region between 0.03 – 0.65 (absolute values), which was acceptable for the purpose of the present study. C18:2n-6 and C18:3n-3 were the two FAs that were the least correlated, as could be seen from the correlation coefficient of -0.03. Many of the other FA combinations had correlation coefficients between ± 0.1– 0.3, while a few were above ± 0.5. This indicated that some of the FAs were correlated to some extent. However, as the samples

of the calibration set were made by mixing natural oils, some degree of correlation between different FAs in the samples was expected.

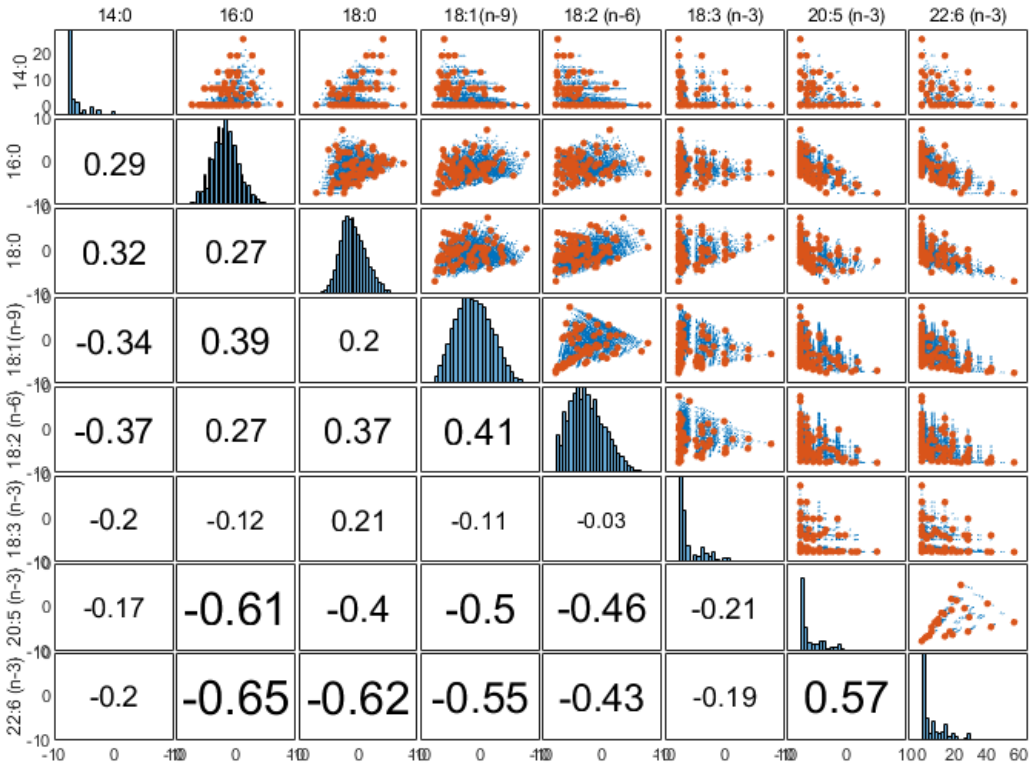


*Figure 19 – The numbers in the lower left part of the figure express the correlation between two and two FAs of the theoretical calibration set. The blue dots in the upper right part of the figure represent the possible mixtures, while the red dots represent the 80 samples that were chosen for the calibration set.*

The correlation values for the main FAs in the prepared samples of the calibration set are presented in table 10. By comparing these values with the theoretical values above, one could see that some of the calculated values deviated with ± 0.02 while most values deviated with ± 0.01 or were identical to the theoretical value. The small changes that could be seen for some of the correlation coefficients were likely since these calculated values were based on FA profiles from multiple replicates of each sample, and because the actual mixing ratios were slightly differing from the theoretical values. In table 10 the FA features are also included (i.e. ΣSFA, ΣMUFA, ΣPUFA and UI). The correlation coefficients for these features could be described as logic: ΣSFA was highly correlated C14:0, ΣMUFA was highly correlated to C18:1n-9 and the UI was highly correlated to C22:6n-3 (DHA) and ΣPUFA. One could also see that ΣSFA had low correlations with the unsaturated FAs and ΣMUFA had correlation

coefficients ≤ (± 0.55) for all other FAs than C18:1n-9. For ΣPUFA and the UI no further trends in the correlation coefficients could be observed.

*Table 10 – Correlation between the parameters of the prepared samples of the calibration set, expressed as Pearson's correlation coefficients.*

| | C4:0 | C16:0 | C18:0 | C18:1 n-9 | C18:2 n-6 | C18:3 n-3 | C20:5 n-3 | C22:6 n-3 | Σ SFA | Σ MUFA | Σ PUFA | UI |
|---|---|---|---|---|---|---|---|---|---|---|---|---|
| C14:0 | | | | | | | | | | | | |
| C16:0 | 0.27 | | | | | | | | | | | |
| C18:0 | 0.34 | 0.27 | | | | | | | | | | |
| C18:1n-9 | -0.35 | 0.38 | 0.18 | | | | | | | | | |
| C18:2n-6 | -0.37 | 0.27 | 0.36 | 0.40 | | | | | | | | |
| C18:3n-3 | -0.20 | -0.11 | 0.20 | -0.11 | -0.04 | | | | | | | |
| C20:5n-3 | -0.17 | -0.58 | -0.39 | -0.48 | -0.45 | -0.20 | | | | | | |
| C22:6n-3 | -0.20 | -0.66 | -0.61 | -0.55 | -0.43 | -0.19 | 0.55 | | | | | |
| ΣSFA | 0.97 | 0.43 | 0.48 | -0.18 | -0.21 | -0.19 | -0.32 | -0.35 | | | | |
| ΣMUFA | -0.35 | 0.45 | -0.03 | 0.89 | 0.27 | -0.14 | -0.41 | -0.55 | -0.25 | | | |
| ΣPUFA | -0.57 | -0.71 | -0.36 | -0.51 | 0.00 | 0.28 | 0.58 | 0.69 | -0.67 | -0.55 | | |
| UI | -0.45 | -0.76 | -0.60 | -0.54 | -0.35 | 0.02 | 0.74 | 0.90 | -0.60 | -0.51 | 0.89 | |

The calculated FA profiles for the calibration set including the eight main FAs and the parameters ΣSFA, ΣMUFA, ΣPUFA as well as the UI are presented in appendix G. The variation in FA composition in these samples is illustrated in figure 20, where the FAs are shown as ΣSFA, ΣMUFA, ΣPUFA. This figure clearly illustrated the sample variation in terms of types FAs they contained.

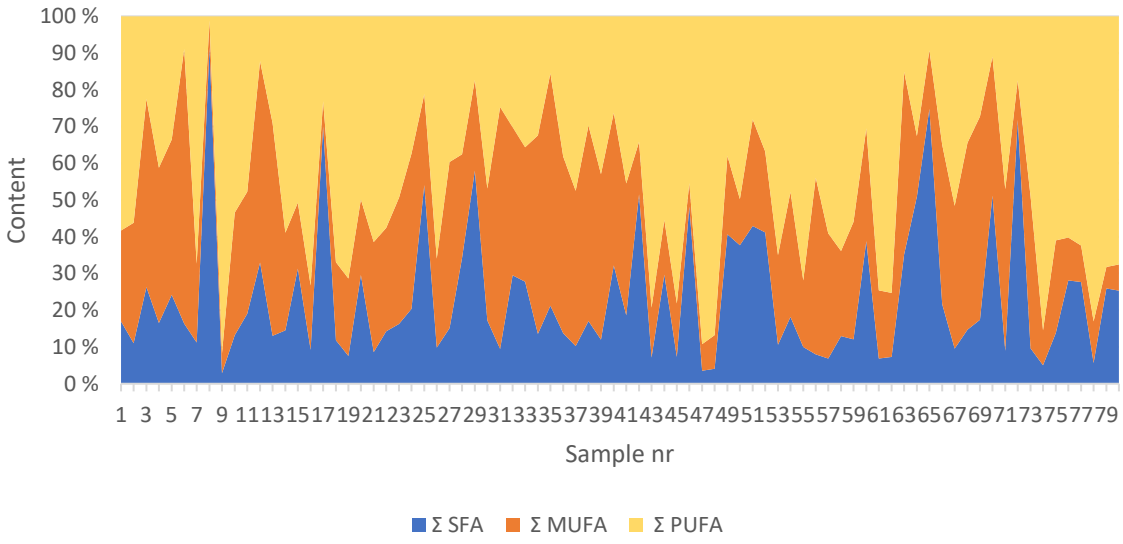


*Figure 20 – Illustration of the FA composition in the 80 samples of the calibration set. The FAs are displayed as ΣSFA, ΣMUFA and ΣPUFA.*

Based on the unsaturation index for each sample, the total degree of unsaturation is visualized in figure 21. Since the FA profiles were used to calculate the unsaturation values for each sample, a value of 1 will mean that each FA has one double bond on average. Sample nr eight was found to be the sample with the lowest degree of unsaturation, with a value of 0.10. This sample consisted of pure coconut oil. The highest unsaturation value was found for sample nr nine, which consisted of only 0370. All other samples had values spanning the area between these two values.

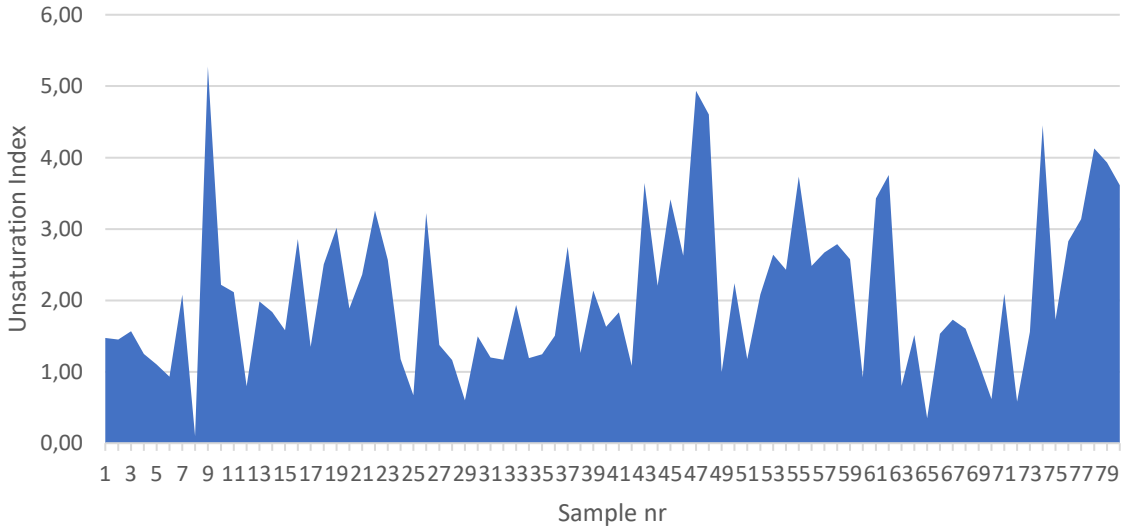


*Figure 21 – Illustration of the variation in total degree of unsaturation in the 80 samples of the calibration set, expressed as values of the unsaturation index.*

The goal of this thesis was to find calibration models that enable the use of vibrational spectroscopy to predict the FA composition in oils. The main FAs as well as ΣSFA, ΣMUFA, ΣPUFA and the UI were the parameters of interest for these models. Table 11 sums up the range (min. and max. values) for these 12 parameters in the 80 calibration samples that were prepared, in addition to the mean values of all samples and the standard deviations. Together with the low internal correlations between FAs that were seen in table 10, this showed that the chosen calibration set of 80 samples provided a high variation of each of the eight FAs, and low correlations between them.

*Table 11 – Range, mean and standard deviation (SD) for the 12 parameters of interest in the samples of the calibration set.*

| Parameter | Min [%] | Max [%] | Mean [%] | SD [%] |
|---|---|---|---|---|
| C14:0 [%] | 0.01 | 25.71 | 4.23 | 5.69 |
| C16:0 [%] | 0.51 | 20.45 | 8.17 | 3.92 |
| C18:0 [%] | 0.29 | 6.10 | 3.02 | 1.19 |
| C18:1(n-9) [%] | 0.55 | 71.29 | 24.25 | 16.01 |
| C18:2(n-6) [%] | 0.00 | 56.04 | 15.65 | 12.40 |
| C18:3(n-3) [%] | 0.00 | 51.92 | 8.78 | 11.61 |
| C20:5(n-3) [%] | 0.00 | 44.08 | 6.97 | 9.32 |
| C22:6(n-3) [%] | 0.00 | 62.32 | 11.33 | 13.61 |
| Σ SFA [%] | 2.78 | 91.92 | 23.18 | 18.24 |
| Σ MUFA [%] | 5.11 | 74.73 | 29.59 | 16.05 |
| Σ PUFA [%] | 1.15 | 88.01 | 46.27 | 20.66 |
| UI | 0.10 | 5.27 | 2.09 | 1.11 |

### 4.2.3 Calibration models based on FTIR spectroscopy

A line plot of the preprocessed FTIR spectra for the 80 calibration samples is presented in figure 22. Here one can see the main absorption bands for the samples, these are found in the area of 3100 – 2750 $cm^{-1}$ and 1800 – 500 $cm^{-1}$. The bands are generally the same in all oils, but with small variations in intensity.

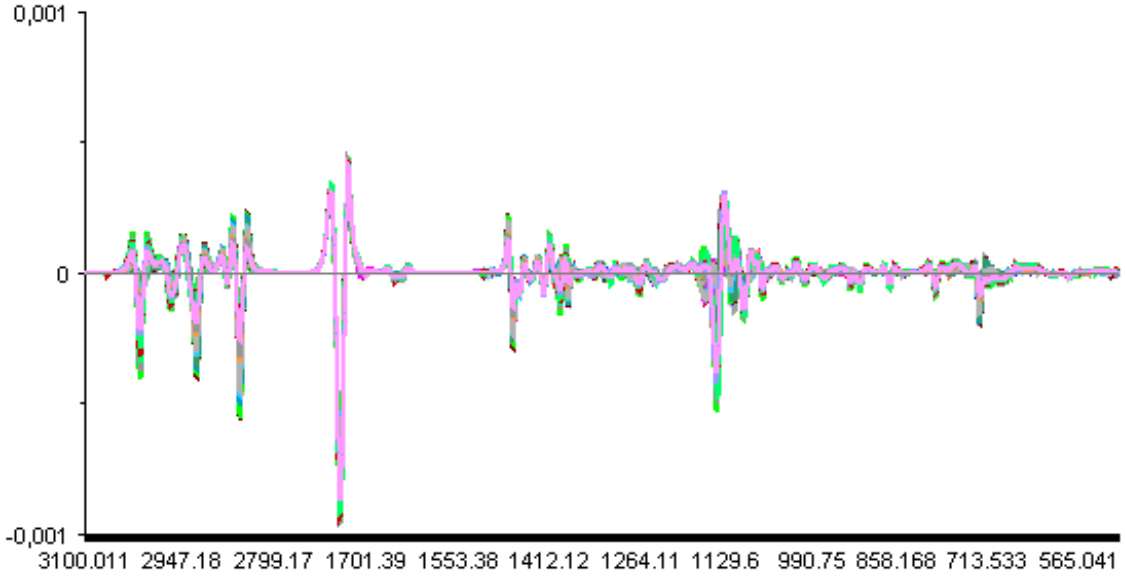


*Figure 22 - Line plot of the preprocessed FTIR spectra for the 80 calibration samples. The spectra have been preprocessed with Savitzky-Golay second derivatives and EMSC. The spectral area included is 3100 – 2750 $cm^{-1}$ and 1800 – 500 $cm^{-1}$.*

When making the PLSR models based on FTIR spectral data, the area of 1800 – 1700 $cm^{-1}$ was not included. In FTIR spectra of oils, as can be seen in figure 22, the carbonyl peak at around 1743 $cm^{-1}$ is quite dominant. As can be seen in the subsequent discussion, the C–O information in the FTIR spectrum can be indirectly related to FA composition. However, since different oils might have different glyceride composition, the band might in the worst case be indirectly correlated to the oils in the calibration set. In order to avoid any indirect link between the oils in the data set and the FA features, the carbonyl peak was not included when making the subsequent calibration models for the FTIR spectra.

PLSR with cross-validation was performed on the data from the 80 samples of the calibration set. The spectral data from FTIR analysis, which were preprocessed as described in section 3.4.3, served as predictor variables, and the different parameters listed in table 11 were response variables. All regression coefficients and predicted vs. reference plots for the calibration models with the 12 parameters of interest can be found in appendix K. A summary of the main information including the main bands of the regression coefficients for these analyses are presented in table 12.

The results of PLSR performed with 14:0 as response variable are provided in figure 23. Here the optimal number of factors was found to be four, and the correlation between the predictor

and response variables was good, as can be seen from the $R^2$-value of 0.98. RMSECV was found to be 0.8 %, which compared to the average C14:0 content in the calibration set (4.23 %) was an acceptable value. Thus, the overall fit of the model was good. The spectral bands for this regression can be seen in the regression coefficient plot of figure 23B, where the most prominent peaks were found at wavenumbers 1147 $cm^{-1}$, 1138 $cm^{-1}$, 1108 $cm^{-1}$ and 1083 $cm^{-1}$. An interpretation of these important wavelengths based on section 2.3.6 would suggest that the calibration model for C14:0 is largely based on the stretching of C–O in the ester part of the TAG structure. The vibration of C–O is based on two asymmetric coupled vibrations; primarily the vibration of C–C(=O)–O in addition to the vibration of O–C–C (Guillén & Cabo, 1997; Silverstein et al., 2015). FAs can thus be differentiated based on the vibration of C–O as this vibration is influenced by the length of the carbon chain that is bound to the glycerol part of the TAG by an ester linkage.

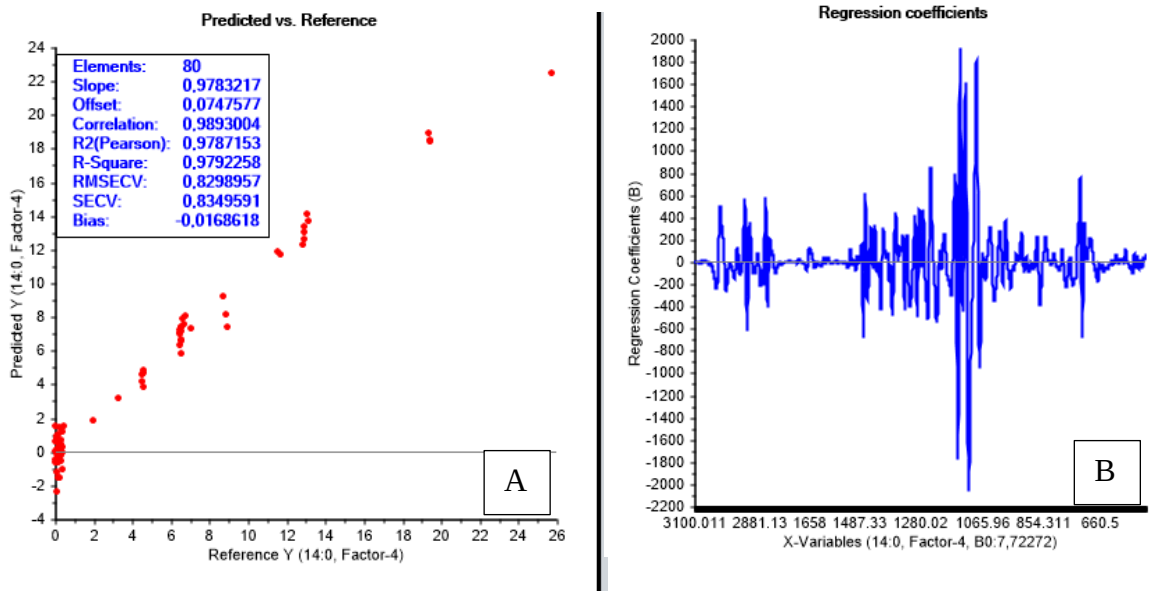


*Figure 2 – Predicted vs. Reference response values (A) and regression coefficients (B) for the calibration model obtained with 14:0 as response variable. The model was made using PLSR and was based on data from analysis of the calibration set with FTIR spectroscopy.*

Unfortunately, not all plots for the regression coefficients showed only few important spectral bands, as was seen in the model for C14:0. Especially the regression with C16:0 as response variable resulted in a PLSR plot where many of the spectral bands were of similar intensity, this can be seen in figure 24. The reason for this can partly be found by looking at the number of factors of this model, which was nine. Thus, the model for C16:0 was substantially more complex than the model for C14:0, which was based on only four factors. In the worst case,

an increase in model complexity might indicate more noise, which makes interpretation of the spectrum more difficult.

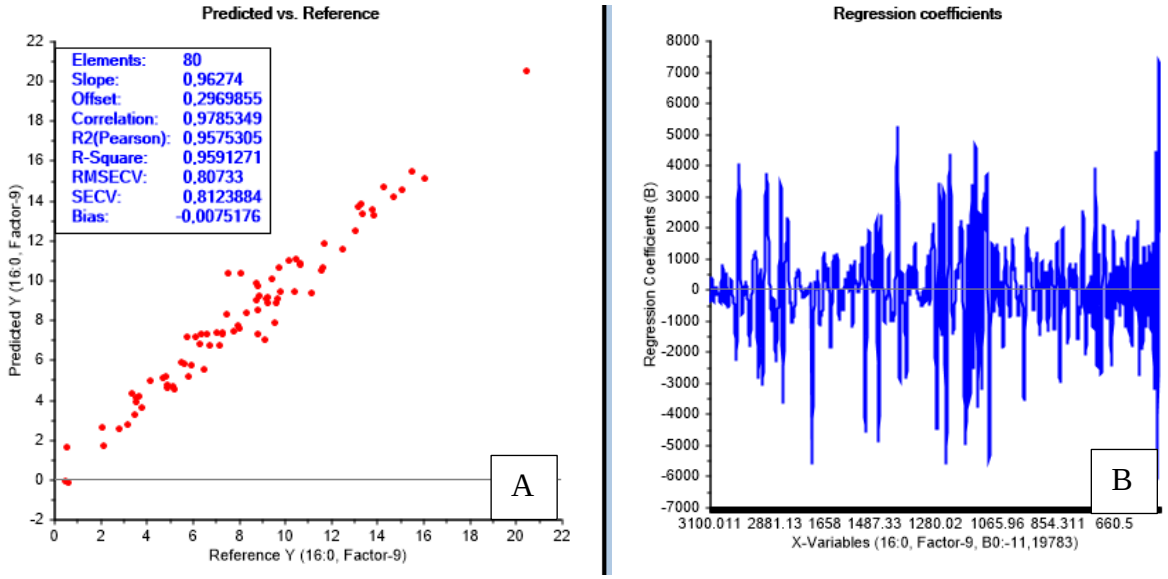


*Figure 3 – Predicted vs. reference values (A) and regression coefficients (B) for the calibration model obtained with 16:0 as response variable. The model was made using PLSR and was based on data from analysis of the calibration set with FTIR spectroscopy.*

For the calibration model of C16:0 the most prominent spectral bands were found at 1698 $cm^{-1}$, 1237 $cm^{-1}$, 1089 $cm^{-1}$, 510 $cm^{-1}$ and 503 $cm^{-1}$, but there were many other spectral bands of importance for this PLSR model. Interpretation of the bands of the regression coefficients was difficult due to the high model complexity and was thus not performed here.

For all the remaining parameters, the PLSR-plots can be found in appendix K. Table 12 summarizes the main information that was gathered from these analyses: $R^2$, RMSECV, number of factors and the main regression coefficients.

*Table 12 – Summary of RMSECV, $R^2$, number of factors and main spectral bands in the regression coefficient plots for the calibration models based on analysis with FTIR spectroscopy.*

| Parameter | RMSECV | $R^2$ | Factors | Main spectral bands ($cm^{-1}$) |
|---|---|---|---|---|
| C14:0 | 0.8 | 0.98 | 4 | 1147, 1138, 1108*, 1083 |
| C16:0 | 0.8 | 0.96 | 9 | 1698, 1237, 1089, 510, 503* |
| C18:0 | 0.3 | 0.93 | 7 | 1504*, 1497, 1490, 1040* |
| C18:1(n-9) | 2.2 | 0.98 | 5 | 2924, 1102, 1082*, 725 |
| C18:2(n-6) | 1.4 | 0.99 | 5 | 2954, 1397, 1111*, 1101*, 1067 |
| C18:3(n-3) | 1.3 | 0.99 | 5 | 2954, 1141*, 1131, 1067 |
| C20:5(n-3) | 1.4 | 0.98 | 5 | 1312, 1153*, 1137, 1110 |
| C22:6(n-3) | 1.6 | 0.99 | 4 | 3013, 1151, 1133*, 1120, 1109 |
| Σ SFA | 2.3 | 0.98 | 4 | 2926, 1145, 1138, 1120, 1108*, 1085 |
| Σ MUFA | 2.1 | 0.98 | 5 | 1468, 1403, 1396, 1118, 1103* |
| Σ PUFA | 2.5 | 0.99 | 4 | 2928, 2917, 2858, 2849*, 1112 |
| UI | 0.1 | 0.99 | 4 | 3015, 2926*, 2916, 2849, 713 |

* = strongest band in regression coefficient plot

In terms of model complexity, the simplest models were based on four factors. These were the models for C14:0, C22:6n-3, ΣSFA, ΣPUFA and UI. The models for C18:1n-9, C18:2n-6, C18:3n-3, C20:5n-3 and ΣMUFA were based on five factors and thus somewhat more complex. For C16:0 and C18:0 the models were more complex, with an optimal number of factors of nine and seven, respectively.

Based on $R^2$ alone, all models seemed to have high correlations. Depending on the model, 93 % to almost 100 % of the variation in the response variables could be explained from the spectral data. The regression model for C18:0 had the lowest fit with an $R^2$-value of 0.93, while the model for UI explained the largest amount of variation, close to 1.00. Regression analysis using C16:0 as response variable resulted in the second lowest $R^2$, with a value of 0.96. For the remaining models the $R^2$ value was 0.98 to 0.99.

The error of prediction for the PLSR models was here expressed as RMSECV. It estimates the deviations between the actual parameter-values in the samples that were left out during cross validation and the values predicted by the model based on the remaining samples. Although RMSECV has the same unit as the values for mean and range, direct comparison of the prediction error for the different models was not possible. The reason for this was that UI had a different unit than the other parameters, and the range and mean values for the parameters were quite diverse. Thus, RMSECV in percent of the mean value for each parameter in the 80 calibration samples was calculated to create better grounds for comparison, see table 13. UI clearly had the lowest prediction error, while C14:0 and C20:5n-3 had the largest with almost

20 % of the mean value. A relative prediction error >10 % of the mean value was also found for C18:0, C18:3n-3 and C22:6n-3. For C16:0, C18:1n-9, C18:2n-6, ΣSFA, ΣMUFA and ΣPUFA the prediction error was between 5 % and 10 %. The lowest prediction errors were found for the models based on the predictor variables ΣMUFA, ΣPUFA and UI.

*Table 13 – RMSECV for the calibration models based on FTIR spectroscopy, expressed in percent of the mean content for all samples of the calibration set. The mean values are based on the calculated FA content in the calibration samples.*

| Parameter | Mean | RMSECV | RMSECV [%] |
|---|---|---|---|
| C14:0 [%] | 4.23 | 0.8 | 19.6 |
| C16:0 [%] | 8.17 | 0.8 | 9.9 |
| C18:0 [%] | 3.02 | 0.3 | 10.6 |
| C18:1(n-9) [%] | 24.25 | 2.2 | 8.9 |
| C18:2(n-6) [%] | 15.65 | 1.4 | 9.0 |
| C18:3(n-3) [%] | 8.78 | 1.3 | 15.3 |
| C20:5(n-3) [%] | 6.97 | 1.4 | 19.5 |
| C22:6(n-3) [%] | 11.33 | 1.6 | 13.9 |
| Σ SFA [%] | 23.18 | 2.3 | 10.0 |
| Σ MUFA [%] | 29.59 | 2.1 | 6.9 |
| Σ PUFA [%] | 46.27 | 2.5 | 5.5 |
| UI | 2.09 | 0.1 | 2.4 |

Based on both RMSECV and $R^2$, the calibration model created using UI as response variable was the best model, followed by the models for ΣMUFA and ΣPUFA. These results indicated that the degree of unsaturation, ΣMUFA and ΣPUFA in edible oils could be predicted quite accurately using FTIR spectroscopy, while content of individual FAs and ΣSFA could be predicted with a somewhat larger error of prediction. Nevertheless, the calibration models for the single FAs did look promising. Considering the chemical structure of SFAs vs MUFAs or PUFAs, it seems logical that prediction of unsaturated FAs is easier than prediction of SFAs. Introduction of a double bond will give rise to a weak peak in the spectral area of 3010 $cm^{-1}$, while introduction of another C–C bond will only influence the intensity of the peaks that are already present in the region of 2800 – 3000 $cm^{-1}$. When a sample consists solely of SFAs, one way to distinguish them will be based on the relation between the different absorption bands for C–H stretching, or between C–H and C=O stretches, because this relation will vary with chain length (Socrates, 2004).

As mentioned before, the regression coefficient plots give information regarding what wavelengths are important when establishing a calibration model. More intense bands indicate larger spectral differences between the samples of the calibration set and show that the absorption at the given wavelength can be used for predictive purposes. Evaluation of the important bands a model is based on is a way to verify the model, by checking that the interpretation of the bands is meaningful. The PLSR models in appendix K show that for most of the models there was not one but a few bands that were intense. These main bands for all calibration models are summarized in table 12.

Many of the most important spectral bands were found in the area of 1040 – 1153 $cm^{-1}$, and for multiple models the main peak was also found in this area. Absorptions at wavenumbers in the area of 1037 – 1239 $cm^{-1}$ are caused by –C–O stretching in the TG and bending of –$CH_2$– in the case of vibrations around 1163 $cm^{-1}$. The vibration of C–O can be used to separate FAs based on their chain length, because this vibration consists of the two asymmetric coupled vibrations of C–C(=O)–O and O–C–C (Guillén & Cabo, 1997; Silverstein et al., 2015). Smaller variations in wavenumbers can generally be explained by differences in chemical surroundings.

For the models of ΣPUFA and UI the main peaks were found at 2849 $cm^{-1}$ and 2926 $cm^{-1}$, respectively, which means the symmetrical and asymmetrical stretching vibrations of –C–H in $CH_2$ were the most important absorptions. The spectral area of approximately 2800 $cm^{-1}$ to 3000 $cm^{-1}$ is important because it shows absorptions related to saturation of the FAs. Long chain FAs without any double bonds will show a strong absorption in this area, while FAs with one or more double bonds will have a less intense band in this area. It is expected, however, that the presence of C=C double bonds will also indirectly affect the symmetrical and asymmetrical stretches in this region, which is clearly visible from the interpretation of the regression models for UI and ΣPUFA.

For PUFAs the intensity of the peaks in area of 2800 – 3000 $cm^{-1}$ will be lower than for SFAs, so the total degree of unsaturation, here expressed as the UI, can be predicted based on the intensity of the peaks in this area. The same applies for prediction of ΣPUFA. The calibration set included samples of varying UI, ranging from 0.1 – 5.27, and with a ΣPUFA content ranging from 1.15 % – 88.01 %. Due to these large variations in UI and ΣPUFA for the samples of the calibration set, it makes sense that the main bands for this model were found in the spectral area of 2800 $cm^{-1}$ to 3000 $cm^{-1}$.

The models based on C18:1n-9, C18:2n-6, C18:3n-3, ΣSFA and ΣPUFA had a strong band in the spectral area of 2800 $cm^{-1}$ to 3000 $cm^{-1}$, which was to be expected, as they all deal with separating unsaturated FAs from SFAs. One would expect the models for C20:5n-3, C22:6n-3 and ΣMUFA to also have a main peak in this area, but this was not the case. However, the PLSR models for these three parameters (appendix K) did have less intense bands in this area. This means that the models are, to a smaller extent, built on the differences in absorption intensity at wavelengths in this area, but other bands were found to be more important.

One of the main bands for C22:6n-3 was found at 3013 $cm^{-1}$. Absorptions in the area of ~3008 $cm^{-1}$ are important in relation to the degree of unsaturation, because they are caused by the stretching vibration of =C–H in *cis* configuration. Besides the model for C22:6n-3 only the model for UI had one of the main bands in this area. Although the spectral band ~3008 $cm^{-1}$ is important in relation to distinguishing the SFAs from the unsaturated FAs, other spectral areas such as 2800 $cm^{-1}$ to 3000 $cm^{-1}$ seemed to be more important overall for the models based on the other parameters.

The main peak at 1504 $cm^{-1}$ in the model for C18:0 was somewhat difficult to interpret. Scissoring of –C–H in $CH_2$ and $CH_3$ found at 1465 $cm^{-1}$ was the closest value for interpretation, however such a large deviation means the observed band might be caused by some other vibration. As mentioned earlier, the large peak at 503 $cm^{-1}$ in the model for C16:0 cannot be explained based on the knowledge about interpretation of FTIR spectra. See section 2.3.6 for interpretation of the remaining bands listed in table 12.

### 4.2.4 Calibration models based on Raman spectroscopy

In figure 25 the preprocessed Raman spectra of the calibration set are presented. The shift values included were in the range of 500 – 1800 $cm^{-1}$, and various absorption peaks could be found in this area.

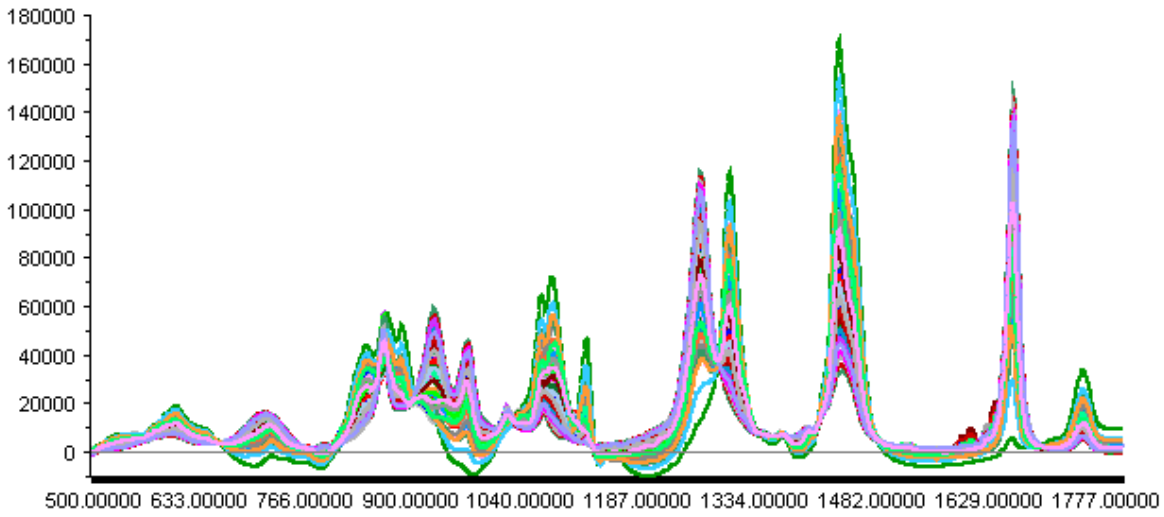


*Figure 25 - Line plot of the preprocessed Raman spectra for the 80 calibration samples. The spectra were baseline-corrected in Matlab and transformed with EMSC in Unscrambler. The spectral area included is 500 – 1800 $cm^{-1}$.*

PLSR with cross-validation was performed on the spectral data from the 80 samples of the calibration set. Details for the Raman analysis can be found in chapter 3.4.2. Prior to PLSR analysis the obtained Raman spectra were preprocessed as described in section 3.4.3. For PLSR analysis the spectral data served as predictor variable, while the same parameters as previously were used as response variables. All obtained regression plots can be found in appendix L, and a summary of $R^2$, RMSECV, number of factors and main spectral bands can be found in table 14.

PLSR plots for the regression performed with C14:0 as response variable are provided in figure 26. The regression model was built on five factors, which means that the model complexity is relatively low. $R^2$ was found to be 0.96, which means that 96 % of the variation in C14:0 content could be explained by the Raman spectral data. RMSECV is 1.10 %, which is an acceptable value compared to the range of C14:0 content in the calibration samples (0.01 – 25.71 %). Compared to the mean content of C14:0, 4.23 %, the prediction error was somewhat high. When taking both $R^2$ and RMSECV into consideration, the model for C14:0 seemed to be good, with a slightly high prediction error.

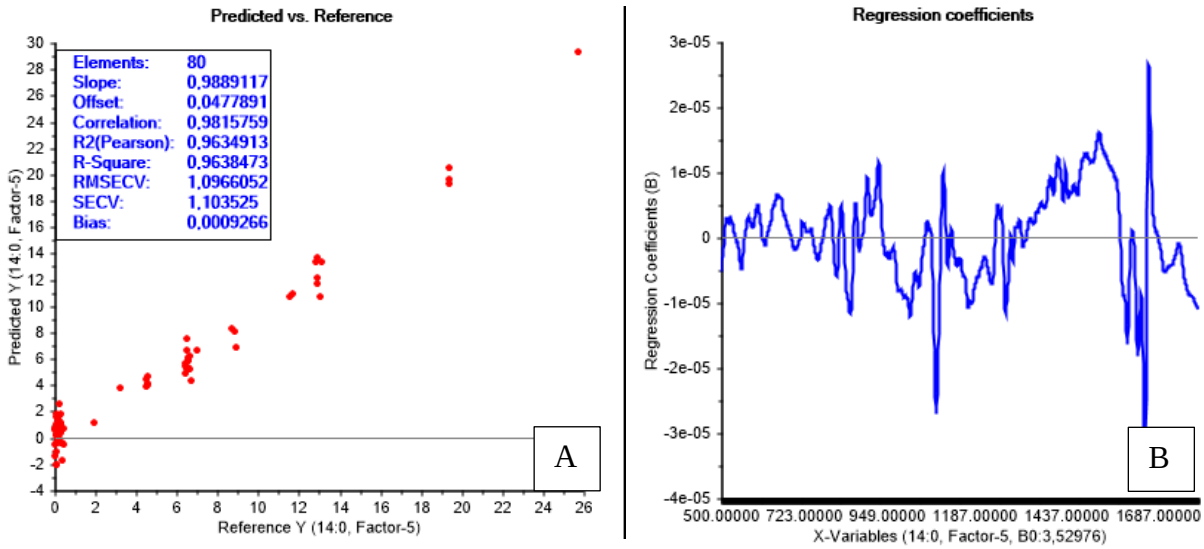


*Figure 4 – Predicted vs. reference values (A) and regression coefficients (B) for the calibration model obtained with C14:0 as response variable. The model was made using PLSR and was based on data from analysis of the calibration set with Raman spectroscopy.*

As can be seen from the regression coefficient plot in figure 26B, three of the bands are more intense than the others. These main bands are located at the Raman shifts of 1085 $cm^{-1}$, 1654 $cm^{-1}$ and 1665 $cm^{-1}$. The band at 1085 $cm^{-1}$ is most likely caused by a skeletal vibration such as a C–C or C–O stretch. The bands at 1654 $cm^{-1}$ and 1665 $cm^{-1}$ are both related to the C=C stretch. For an increase in degree of unsaturation, for example when going from MUFAs to PUFAs, the band for the C=C stretch will shift to a higher wavenumber. Figure 26B also shows how the regression coefficients shift from positive to negative in the area of 1400 – 1650 $cm^{-1}$, which indicates a shift in the degree of unsaturation (Afseth et al., 2005).

The model with C18:2n-6 as response variable, which is presented in figure 27, shows different main bands in the regression coefficient plot than the model for C14:0. Here the main bands are located at the wavenumbers of 837 $cm^{-1}$, 866 $cm^{-1}$, 959 $cm^{-1}$ and 1109 $cm^{-1}$. Based on the section about interpretation of Raman shifts, section 2.3.8, all these bands can be assigned to the skeletal vibrations of the C–C and C–O stretch that can be found in the $–(CH_2)_n-$ part of the FAs and in the C–O part of the TG structure. The band at 959 $cm^{-1}$ can potentially be assigned to the out of plane deformation of =C–H in the unsaturated part of C18:2n-6 (Afseth et al., 2006).

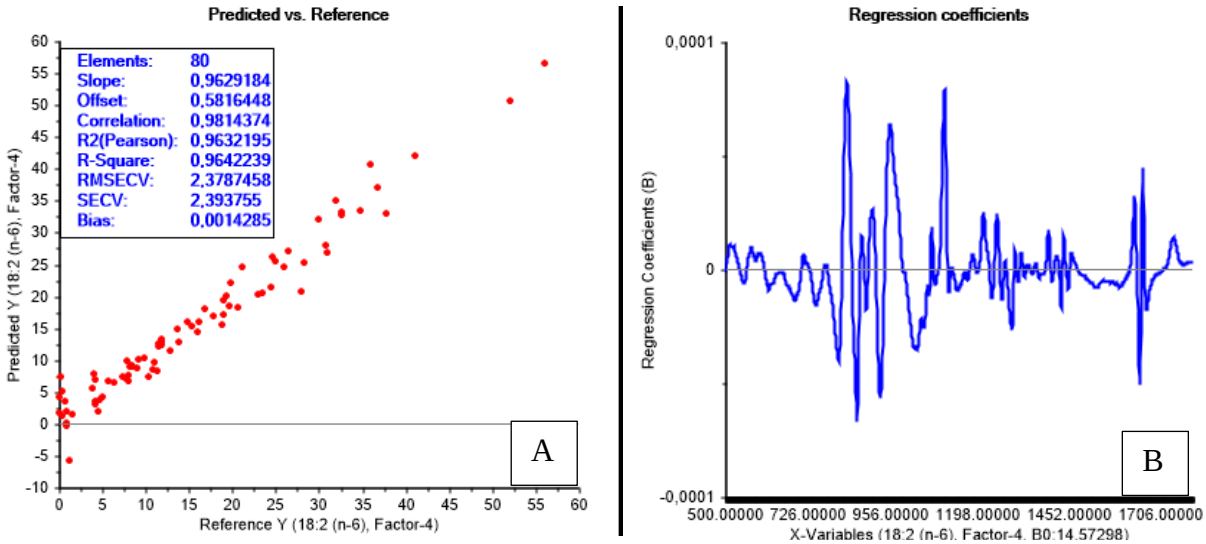


*Figure 5 – Predicted vs. reference values (A) and regression coefficients (B) for the calibration model obtained with C18:2n-6 as response variable. The model was made using PLSR and was based on data from analysis of the calibration set with Raman spectroscopy.*

As can be seen from the PLSR plots in figure 27, the model for C18:2n-6 is based on four factors, with an $R^2$ value of 0.96 and RMSECV of 2.3 %. Accordingly, the model complexity is low as the model is built on only four factors, and the overall fit is good, as can be seen from the correlation coefficient. 96 % of the variation in the spectral data could be explained by the response variable C18:2n-6. Considering the range of C18:2n-6 in the samples, 0.00 – 56.04 % with a mean content of 15.56 %, a prediction error of 2.3 % is low. Overall this seems like a good model for the prediction of C18:2n-6 content in oils.

The PLSR plots for the remaining parameters can be found in appendix L, and table 14 shows a summary of the main information that was gathered from these analyses, including number of factors the different models were based on, $R^2$ and RMSECV.

*Table 14 - Summary of RMSECV, $R^2$, number of factors and main spectral bands in the regression coefficient plots for the calibration models based on analysis with Raman spectroscopy.*

| Fatty acid | RMSECV | $R^2$ | Factors | Significant wavelengths/spectral bands ($cm^{-1}$) |
|---|---|---|---|---|
| C14:0 | 1.1 | 0.96 | 5 | 1085, 1654*, 1665 |
| C16:0 | 0.8 | 0.96 | 8 | 1096, 1117*, 1654 |
| C18:0 | 0.3 | 0.94 | 14 | 1625, 1638*, 1653 |
| C18:1n-9 | 3.3 | 0.96 | 6 | 1084*, 1103, 1660 |
| C18:2n-6 | 2.4 | 0.96 | 4 | 837*, 866, 959, 1109 |
| C18:3n-3 | 2.6 | 0.95 | 5 | 867*, 954, 1040 |
| C20:5n-3 | 1.9 | 0.96 | 7 | 857, 903, 928, 1038* |
| C22:6n-3 | 2.2 | 0.97 | 7 | 859, 929*, 990, 1035 |
| Σ SFA | 2.8 | 0.98 | 5 | 1654*, 1665 |
| Σ MUFA | 3.6 | 0.95 | 3 | 835, 868, 955, 1652*, 1661 |
| Σ PUFA | 2.6 | 0.98 | 5 | 955, 1658*, 1667 |
| UI | 0.2 | 0.97 | 4 | 931, 1438, 1655*, 1665 |

* = strongest band in regression coefficient plot

As shown in table 14, the complexity of the models based on Raman spectroscopy was quite diverse, ranging from three to 14 factors. The most complex model was the one for prediction of C18:0, with an optimal number of factors of 14. Eight factors were found to be optimal for C16:0, seven factors were optimal for C20:5n-3 and C22:6n-3 and six factors were optimal for C18:1n-9. For the models based on the parameters C14:0, C18:3n-3, ΣSFA and ΣPUFA five factors were found to be optimal, while the models for C18:2n-6 and UI were based on four factors. The simplest model was found for ΣMUFA, which was based on only three factors

The individual models had $R^2$ values in the range of 0.94 to 0.98. Thus, the overall fit of the models was good. Nevertheless, the model for C18:0 had the lowest fit with an $R^2$ value of 0.94, and the models for ΣSFA and ΣPUFA had the best fit with an $R^2$ value of 0.98. Calibration models for C18:3n-3 and ΣMUFA had $R^2$ values of 0.95, and the models for C14:0, C16:0, C18:1n-9, C18:2n-6 and C20:5n-3 had $R^2$-values of 0.96. Among the better models were C22:6n-3 and UI with $R^2$ of 0.97.

Again, RMSECV for the different models was calculated in percent of the mean value for the different parameters to achieve better grounds for comparison of the prediction errors. Table 15 summarizes the mean value for the parameters in the calibration samples, RMSECV for the calibration models and RMSECV in percent of the mean value.

*Table 15 - RMSECV for the calibration models based on Raman spectroscopy, expressed in percent of the mean value for all samples of the calibration set. The mean values are based on the calculated FA content in the calibration samples.*

| Parameter | Mean | RMSECV | RMSECV [%] |
|---|---|---|---|
| C14:0 [%] | 4,23 | 1,1 | 26,0 |
| C16:0 [%] | 8,17 | 0,8 | 10,3 |
| C18:0 [%] | 3,02 | 0,3 | 9,6 |
| C18:1(n-9) [%] | 24,25 | 3,3 | 13,4 |
| C18:2(n-6) [%] | 15,65 | 2,4 | 15,2 |
| C18:3(n-3) [%] | 8,78 | 2,6 | 29,3 |
| C20:5(n-3) [%] | 6,97 | 1,9 | 27,3 |
| C22:6(n-3) [%] | 11,33 | 2,2 | 19,5 |
| Σ SFA [%] | 23,18 | 2,8 | 12,2 |
| Σ MUFA [%] | 29,59 | 3,6 | 12,3 |
| Σ PUFA [%] | 46,27 | 2,6 | 5,6 |
| UI | 2,09 | 0,2 | 8,6 |

These calculations reveal that RMSECV had values equivalent to 5.6 – 29.3 % of the mean values for the respective parameters in the calibration samples. ΣPUFA had the lowest RMSECV with a relative value of 8.6 %, while C18:3n-3 had the highest RMSECV with a relative value of 29.3 %. Other parameters with a relative RMSECV of >20% were found for C14:0 and C20:5n-3, values between 10 – 20 % were found for the models of C16:0, C18:1n-9, C18:2n-6, C22:6n-3, ΣSFA and ΣMUFA. Only the models for C18:0, ΣPUFA and UI had a relative RMSECV <10 %.

Based on both $R^2$ and RMSECV it looks looked the PLSR model for ΣPUFA was the best, because it had an $R^2$ value of 0.98 and the lowest relative RMSECV. The model for UI was also quite promising, with an $R^2$ of 0.97 and relative RMSECV of 8.6 %. The remaining models either had a lower fit, as the model for C18:0 with $R^2$ of 0.94, or an RMSECV that was >10 % of the mean value. Especially the models for C14:0, C18:3n-3 and C20:5n-3 had high RMSECV values relative to the mean values, which means that the prediction error was quite large.

For all calibration models, except the ones for single PUFAs (C18:2n-6, C18:3n-3, C20:5n-3, C22:6n-3), one of the main bands in the regression coefficient plots was found in the area of 1638 – 1667 $cm^{-1}$. As can be seen in section 2.3.8, this area corresponds to the –C=C– *cis* stretch, and the higher shifts in this area indicate a higher degree of unsaturation. A prominent band in this area is logical for the models of ΣSFA, ΣMUFA, ΣPUFA and the UI, as these

models all deal with unsaturation. For the single FAs a strong peak in this area was only found for the SFAs and C18:1n-9. One explanation for this might be that an absorption in the area of 1638 – 1667 $cm^{-1}$ indirectly gives information whether a FA is saturated or not.

The calibration models for C14:0, C16:0, C18:1n-9, C18:3n-3, C20:5n-3 and C22:6n-6 had a main band in the spectral range of 1035 – 1096 $cm^{-1}$. A main band in the area of 929 – 990 $cm^{-1}$ was found for the calibration models for C18:2n-6, C18:3n-3, C20:5n-3, C22:6n-3, ΣMUFA, ΣPUFA and UI. Lastly, the calibration models for C18:2n-6, C18:3n-3, C20:5n-3, C22:6n-3 and ΣMUFA had a main band in the area of 835 – 867 $cm^{-1}$. Spectral bands in all three of these regions arise from skeletal stretching vibrations such as –C–C– and –C–O–. Differences in chain length and the number of C–C single bonds (as opposed to C=C double bonds) might give small differences in these bands, and it is thus reasonable to find main bands in this area for all calibration models.

Only the calibration model for UI showed a main peak in the area of 1438 $cm^{-1}$. Such a band arises from the scissoring vibration of $CH_2$. Considering that the number of $CH_2$ groups present in PUFAs < MUFAs < SFAs (if the number of carbon atoms in the FAs is the same), an absorption in this area for the UI is reasonable.

Three of the calibration models also had a main absorption band in the area of 1103 – 1117 $cm^{-1}$, these were the models for C16:0, C18:1n-9 and C18:2n-6. Raman shift values in this area could not be assigned to any FA stretching vibrations.

## 4.3 Part III – Method validation

### 4.3.1 Validation of calculated FA profiles in calibration samples

The last objective concerned the validation of the established calibration models. Prior to this, the calculated FA profiles of the calibration set were validated. Analysis of four samples from the calibration set with GC-MS showed that the calculated FA profiles were acceptable. Appendix H presents the calculated vs reference values of the eight main FAs in the calibration samples with numbers 32, 54, 58 and 77. The deviations of the calculated values from the reference values are also presented. Generally, the calculated FA profiles were good, however the calculated values for C14:0 and C20:5n-3 showed larger deviations from the reference values than the other FAs. One reason for the observed deviations was that the standard deviations for the FAs in the reference oils were not considered when the FA profiles

of the calibration set were calculated. Nevertheless, this can only explain a small part of the observed deviations.

### 4.3.2 Validation of calibration models for FTIR spectroscopy

PCA of the preprocessed data from the 80 samples of the calibration set, the 10 samples of norwegian cod liver oil and the four validation samples resulted in the score plot that is provided in figure 28. All points for the validation oils and norwegian cod liver samples (red and green dots) could be found within the area spanned by the calibration samples (blue dots). Thus, the spectral composition of the validation samples and the samples of norwegian cod liver oil did not differ from the calibration set. This is good, as all the predictions are based solely on the spectral signatures of the validation samples.

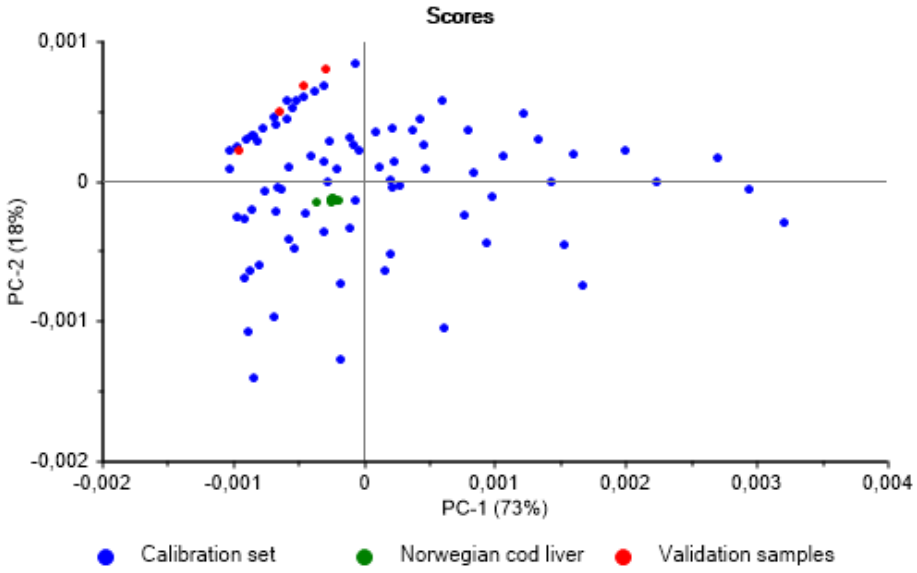


*Figure 28 – Score plot for PCA of the preprocessed samples of the calibration set, validation set and samples of norwegian cod liver oil. The score plot consists of PC-1 and PC-2.*

Table 16 provides the results for the predicted FA content and the equivalent reference values for the validation samples in addition to samples of norwegian cod liver oil. Reference values for the Norwegian cod liver oil were taken from matvaretabellen.no (matportalen.no, 2019). Deviations of the predicted values from the reference values are presented in percentage.

*Table 16 – Predicted and reference values for the 12 parameters in the validation samples and the sample of norwegian cod liver oil. The predicted values were found by using the calibration models that were established for FTIR spectroscopy, while the reference values were determined using GC-MS. The deviation in percent expresses the difference in predicted value compared to the reference value.*

| Type of oil | | C14:0 | C16:0 | C18:0 | C18:1n-9 | C18:2n-6 | C18:3n-3 | C20:5n-3 | C22:6n-3 | Σ SFA | Σ MUFA | Σ PUFA | UI |
|---|---|---|---|---|---|---|---|---|---|---|---|---|---|
| **Grapeseed oil** | Predicted | -2.7 | 5.7 | 3.9 | 23.1 | 64.9 | 1.1 | 2.9 | 3.2 | 10.1 | 20.0 | 68.12 | 1.66 |
| | Reference | 0.0 | 7.3 | 4.3 | 20.9 | 65.2 | 0.3 | 0.0 | 0.0 | 12.0 | 22.0 | 65.52 | 1.54 |
| | Deviation [%] | - | -21.7 | -9.4 | 10.5 | -0.6 | 304.6 | - | - | -15.8 | -9.2 | 4.0 | 7.9 |
| **Frying oil** | Predicted | -0.7 | 6.4 | 2.7 | 76.2 | 11.2 | 1.3 | 1.9 | 0.0 | 12.2 | 76.3 | 19.0 | 1.0 |
| | Reference | 0.0 | 4.0 | 2.9 | 80.5 | 10.0 | 0.1 | 0.0 | 0.0 | 8.2 | 81.7 | 10.1 | 1.0 |
| | Deviation [%] | - | 59.6 | -6.9 | -5.3 | 13.0 | 782.0 | - | - | 48.8 | -6.6 | 87.9 | 2.1 |
| **Walnut oil** | Predicted | -2.7 | 6.1 | 4.3 | 17.8 | 60.6 | 12.9 | 2.9 | 2.5 | 9.0 | 13.8 | 75.3 | 1.9 |
| | Reference | 0.0 | 7.4 | 2.9 | 15.4 | 60.0 | 12.5 | 0.0 | 0.0 | 10.5 | 16.5 | 72.4 | 1.8 |
| | Deviation [%] | - | -17.2 | 46.2 | 15.7 | 1.1 | 3.4 | - | - | -14.1 | -16.4 | 4.0 | 6.4 |
| **Cooking oil** | Predicted | -1.5 | 5.2 | 3.4 | 44.9 | 38.1 | 4.8 | 2.7 | 1.4 | 10.9 | 44.1 | 47.4 | 1.5 |
| | Reference | 0.1 | 5.7 | 2.8 | 45.3 | 38.2 | 3.5 | 0.0 | 0.0 | 9.5 | 48.4 | 41.7 | 1.4 |
| | Deviation [%] | - | -8.0 | 19.4 | -0.9 | -0.3 | 35.7 | - | - | 14.2 | -8.8 | 13.5 | 6.6 |
| **Norwegian** | Predicted | 5.2 | 10.5 | 1.3 | 24.7 | 3.4 | 0.3 | 9.0 | 8.1 | 20.8 | 49.1 | 26.9 | 1.9 |
| **Cod liver oil** | Reference | 4.0 | 10.4 | 2.5 | 20.8 | 1.7 | 1.0 | 8.7 | 13.0 | - | - | - | - |

The predicted values for 14:0 were negative for all samples except for the norwegian cod liver oil. Such a prediction makes no sense, and future models should include a factor that excludes predictions below zero. The models for 16:0 and 18:0 are promising, with deviations ranging from ± 0.7 – 59.0 % and ± 6.9 – 46.6 %, respectively. Predictions for C18:1n-9 were good, with predicted values differing ± 0.9 – 18.3 % of the reference values. C18:2n-3 showed very good predictions for three out of four oils, with deviations of ± 0.3 – 13.0 %. For the sample of norwegian cod liver the deviation was 93.8 %. The model for C18:3n-3 showed the largest deviations, up to 782 % for frying oil. Predicted values for C20:5n-3 and C22:6n-3 resulted in positive predictions for the four validation oils, although none of them contained any of these two FAs. In norwegian cod liver oil C20:5n-3 content seemed to be predicted quite accurately, while C22:6n-3 content was predicted less accurately. Content of ΣSFAs was predicted with acceptable deviations for all samples, ranging from ± 14.1 – 48.8 %. The models for the remaining parameters, ΣMUFA, ΣPUFA and UI were good, with prediction deviations ranging from ± 4.0 – 16.4 %, except for frying oil prediction where ΣPUFA was predicted to be 87.9 % higher than the actual content. For norwegian cod liver oil the predictions for the last four parameters were not evaluated, since the FA composition of these oils were only obtained online from Matvaretabellen.no.

Out of all the calibration models for FTIR spectroscopy, UI had the smallest differences between predicted and reference values for all five samples. UI is a parameter that considers the FA composition of the complete samples, which means it is indirectly based on all models. Thus, good predictions for UI as well as Σ MUFA and Σ PUFA were as expected. The calibration models for the single FAs did overall look promising. The prediction accuracy for the FAs C18:1n-9 and C18:2n-6 was found to be good, while the other FAs were predicted with a lower accuracy. The model for C18:3n-3 gave the least accurate predictions. The overall trend in the predictions does indicate that FTIR and the design approach used in the present thesis may be a suitable method for prediction of individual FAs.

### 4.3.3 Validation of calibration models for Raman spectroscopy

The score plot for PCA of the preprocessed spectral data for the calibration samples, the validation samples and the norwegian cod liver oil is presented in figure 29. The reference values for cod liver oil were taken from matvaretabellen.no, since no reference analyses were done for these samples. Here one can see that the samples of norwegian cod liver oil (green dots) are placed far away from the calibration samples (blue dots). The spectral information in these samples is thus different from the calibration set and will not be included for the

prediction. Most likely, this is related to the sample background and noise levels, which were difficult to completely remove with the preprocessing techniques used. The validation samples (red dots) are within the area spanned by the calibration set, meaning that the calibration models can be applied for these samples.

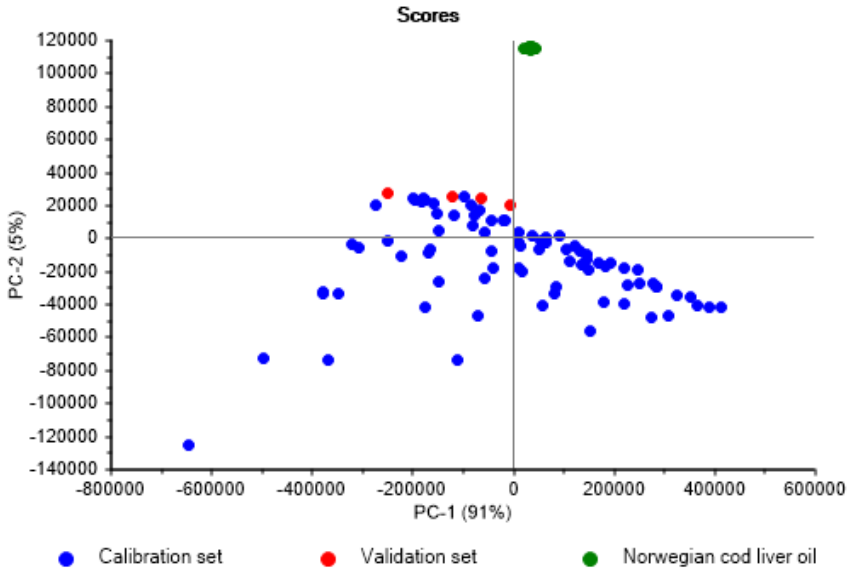


*Figure 29 - Score plot for PCA of the preprocessed data from the samples of the calibration set, validation set and samples of norwegian cod liver oil. The score plot consists of PC-1 and PC-2.*

The predicted and reference values for the FAs in the validation oils are presented in table 17. The deviations of the predicted values from the reference values are presented in percentage.

*Table 17 - Predicted and reference values for the 12 parameters in the validation samples. The predicted values were found by using the calibration models that were established for Raman spectroscopy, while the reference values were determined using GC-MS. The deviation in percent expresses the difference in predicted value compared to the reference value.*

| Sample nr. | | C14:0 | C16:0 | C18:0 | C18:1n-9 | C18:2n-6 | C18:3n-3 | C20:5n-3 | C22:6n-3 | Σ SFA | Σ MUFA | Σ PUFA | UI |
|---|---|---|---|---|---|---|---|---|---|---|---|---|---|
| Grapeseed oil | Predicted | -3.6 | 9.2 | 5.1 | 25.7 | 66.1 | 1.2 | 1.8 | 1.3 | 11.5 | 21.2 | 62.1 | 1.7 |
| | Reference | 0.0 | 7.3 | 4.3 | 20.9 | 65.2 | 0.3 | 0.0 | 0.0 | 12.0 | 22.0 | 65.5 | 1.5 |
| | Deviation [%] | - | 25.8 | 17.5 | 23.2 | 1.4 | 352.8 | - | - | -4.0 | -3.5 | -5.2 | 8.2 |
| Frying oil | Predicted | 0.2 | 2.5 | 0.6 | 78.6 | 11.8 | -0.3 | 1.6 | 1.6 | 9.2 | 78.7 | 16.1 | 1.0 |
| | Reference | 0.0 | 4.0 | 2.9 | 80.5 | 10.0 | 0.1 | 0.0 | 0.0 | 8.2 | 81.7 | 10.1 | 1.0 |
| | Deviation [%] | 296.1 | -39.2 | -78.4 | -2.3 | 18.3 | - | - | - | 12.2 | -3.7 | 59.9 | -1.2 |
| Walnut oil | Predicted | -4.0 | 5.5 | 4.8 | 22.3 | 58.9 | 13.5 | 3.8 | -0.4 | 7.1 | 18.3 | 69.7 | 1.9 |
| | Reference | 0.0 | 7.4 | 2.9 | 15.4 | 60.0 | 12.5 | 0.0 | 0.0 | 10.5 | 16.5 | 72.4 | 1.8 |
| | Deviation [%] | - | -25.5 | 64.6 | 44.9 | -1.7 | 7.8 | - | - | -32.1 | 11.2 | -3.9 | 9.3 |
| Cooking oil | Predicted | -2.0 | 5.9 | 3.8 | 48.3 | 40.7 | 4.0 | 2.2 | -0.7 | 9.3 | 46.9 | 42.9 | 1.4 |
| | Reference | 0.1 | 5.7 | 2.8 | 45.3 | 38.2 | 3.5 | 0.0 | 0.0 | 9.5 | 48.4 | 41.8 | 1.4 |
| | Deviation [%] | - | 3.8 | 32.6 | 6.6 | 6.3 | 12.6 | - | - | -2.2 | -3.1 | 2.6 | 1.3 |

As can be seen in table 17, some of the predicted FA values were negative. These were predicted values mainly for C14:0, but C18:3n-3 and C22:6n-3 did also have one negative prediction value. The model for C16:0 showed variations between predicted and reference values of ± 3.8-39.2 %, and for prediction of 18:0 the deviations were in the range of ± 17.5 – 78,4 %. Content of C18:1n-3 was predicted to be ± 2.3 – 44.9 % smaller/larger than the reference values, and prediction of C18:2n-6 resulted in good predictions with deviations in the range of ± 1.4 – 18.3 %. Predicted content of C18:3n-3 in grapeseed oil was 352.8 % larger than the reference value, while the two remaining positive prediction values were 7.8 – 12.6 % larger than the respective reference values. All predictions for C20:5n-3 were positive, although this FA was not present in any samples. For C22:6n-3 two of the predicted values were negative, and two were positive, but this FA was also not present in any of the validation samples. The predicted values for Σ SFA and Σ MUFA had deviations from the reference values in the ranges of ± 2.2 – 32.1 % and ± 3.1 – 11.2 %, respectively. For ΣPUFA and UI the predicted values showed differences ranging from ± 2.6 – 59.9 % and ± 1.2 – 9.3 % of predicted vs reference values.

Overall the model for UI gave the most accurate predictions, closely followed by the model for prediction of ΣMUFA. The models for ΣSFA and ΣPUFA gave somewhat less accurate predictions. Good predictive abilities for the models of the FA parameters were expected, as these parameters are indirectly based on the models for the individual FAs. The model for C18:2n-6 gave the most accurate predictions of the models for single FAs, while the models for C16:0 and C18:1n-9 also gave good predictions. The predictive abilities of the models for C18:0 and C18:3n-3 were less accurate, and the predictive abilities for C20:5n-3 and C22:6n-3 could not be evaluated as none of the validation samples contained any of these n-3 FAs.

## 4.4 General discussion and future work

The first objective of this study was to classify marine oils using vibrational spectroscopy. The results showed that FTIR was a suitable method for separating all seven types of oils from each other, while the spectral data obtained with Raman spectroscopy could not be used due to fluorescence background. PCA was used to perform classification, and this is an unsupervised method. This means that there is no *a priori* information about class membership included in the model and thus PCA will give the least optimistic results, compared to supervised classification methods. Supervised classification methods generally

are better suited for classifying samples, and in future work such methods should be applied. Examples of supervised classification methods are partial least squares discriminant analysis (PLS-DA) and soft independent modelling of class analogies (SIMCA). For future classification of oils based on FTIR spectroscopy, the sample set should ideally also be larger than the sample set that was used here.

Raman spectroscopy was shown to be an unsuitable method for use in classification. There was a lot of background information in the spectra which might have influenced the classification despite preprocessing of the data. The background noise will however not add any information regarding chemical differences in the samples, but rather make it harder to achieve robust classification. Fluorescence background was also a recurring problem.

For the classification performed with FTIR spectroscopy, the spectral area of 4000 – 2700 $cm^{-1}$ and 1800 – 500 $cm^{-1}$ was used. These two areas include all spectral information regarding FA composition, TG structure and phospholipid structure that can be obtained using FTIR. When looking for class membership in oil samples, the type of lipids as well as FA composition can give relevant information, which is why a wide range of spectral information was included.

The second objective was to make calibration models for the prediction of FA composition based on analysis of a calibration set. 18 reference oils were analysed with GC-MS, and their FA composition was determined. Originally the idea was to quantify the FAs in the reference oils by using an IS and RRF-values in addition to the information obtained from the GC-MS analyses. However, due to an unidentified problem or miscalculation the total amount of FAs that were quantified in each oil was much lower than expected. Fats and oils generally contain about 90 % FAs, the remaining 10 % being the glycerol backbone (Lichtenstein, 2013). The amounts of FAs that were quantified in the reference oils were in the range of 40 – 80 g/100 g of oil. Thus, it was decided to use the FA profiles based on the peak areas in the chromatograms in percentage instead. A quick comparison with previously determined FA profiles for these oils (Matvaretabellen.no) showed that the obtained results seemed realistic. These FA profiles were then used to make 80 calibration samples.

Calibration models were established based on analysis of a set of 80 calibration samples. The samples were created based on reference analysis of 18 oils and contained one to three different oils in various ratios. The calibration set showed little correlation between the main FAs in the samples; the highest correlation was found to be -0.66. When working with

biological samples as basis for sample mixtures it is impossible to avoid correlation altogether. The created samples were also shown to span out the area of varying FA composition, with differing FA chain lengths and varying degrees of unsaturation.

For the calibration models based on FTIR, the spectral ranges of 3100 – 2750 $cm^{-1}$ and 1700 – 500 $cm^{-1}$ were the areas included. Thus, a narrower range of the spectral information was used for PLSR than for PCA. The reason for this was that the purpose of the calibration models was to predict single FAs and some FA features, so the information >3100 $cm^{-1}$ and 2750 – 1800 $cm^{-1}$ did not contain any relevant information. Spectral information of the carbonyl group was also excluded when making the calibration models. The reason for this was that the carbonyl-signal was quite strong in all spectra, and it influenced in the calibration models when the area of 1800 – 1700 $cm^{-1}$ was included for PLSR analysis. Since the carbonyl-band might be indirectly correlated to the oils in the calibration set, it was decided to exclude the area of 1800 – 1700 $cm^{-1}$ when establishing the calibration models.

The calibration models based on FTIR spectroscopy were found to be slightly better than the models based on Raman spectroscopy. $R^2$ values for FTIR models were in the range of 0.96 – 0.99, only one model had $R^2$ = 0.93. For Raman spectroscopy the range included 0.94 – 0.98. RMSECV values were overall lower for FTIR models than for Raman. For both FTIR and Raman the highest number of factors were found for the models of C16:0 and C18:0, they were nine and seven for FTIR and eight and 14 for Raman. It is generally accepted that the signal-to-noise ratio provided by FTIR is higher than for Raman for samples that are easily analysed using FTIR spectroscopy (for instance edible oils). It is thus to be expected that the FTIR models are slightly better than the models obtained for Raman (Larkin, 2011).

Evaluation of the established calibration models is important. The main steps are interpretation of the regression coefficients and their charge, as was shown in section 4.2.3 and 4.2.4. Such interpretation might indicate whether the models are built on relevant chemical information in the data or not. Nevertheless, there are also limitations to such interpretations. Firstly, one should always keep in mind that the observed regression coefficients might not be caused by actual differences in the data but are caused by the modelling. Thus, it is important not to read too much into the regression coefficients and their corresponding intensities. Secondly, rising complexity of the models, observable as the number of optimal factors, will make interpretation of the regression coefficients more difficult.

The third objective of the thesis dealt with validation of the established calibration models. Overall the deviations between predicted and reference values for FTIR spectroscopy were in the range of ± 0.3 – 782.0 % and for Raman spectroscopy they were in the range of ± 1.2 – 367.8 %. Many of the models showed very good predictions, with deviation of < 10 %. Few predictions had deviations > 100 %, but these were all for FAs that were present in small amounts in the respective oils. Some of the predicted values might seem very inaccurate based on the percentwise deviations from the reference values, but the values obtained with the calibration models clearly reflect the actual FA profiles. Through the eyes of a chromatographer the predictions might not seem very accurate, but from the view of a spectroscopist the results are very good and promising. A specific challenge with Raman spectroscopy is the fluctuating baseline features caused by e. g. fluorescence, which is clearly visible from the raw Raman spectra. When existing mathematical correction methods fail in removing these features completely, this will also affect prediction accuracies.

Regarding future work, the classification of marine oils should be repeated with a larger sample set for more representative results, and a supervised classification method such as SIMCA or PLS-DA should be used. It would also be interesting to have reference values for the FA profiles and different lipid fractions in the marine oil samples, so that the classification results can be better understood. In relation to the calibration models, the FAs in the reference oils should be quantified so that the FA profiles can be based on masses. A larger calibration set would also make the models more accurate and robust. Ideally the FA profiles for all samples of the calibration would also be determined using GC-MS. The size of the validation set should also be increased to further test the accuracy and robustness of the established calibration models. Anyhow, an intriguing aspect with the presented calibration design is to explore the use of this calibration to predict individual FAs in new samples, from oils to fat-containing tissues and microorganisms. If this works, this low-cost design approach could find many new applications in the future.

# 5. Conclusion

The objective of this work was to study and develop a robust method for the determination of single FAs in edible oils using vibrational spectroscopy, by creating a sample design with low correlation between the FAs. In the first sub-objective it was shown that FTIR is a suitable method for the classification of oils, while Raman spectroscopy could not be applied for this purpose due to a strong fluorescence background in the samples. Next, the calibration set that was made based on the sample design was shown to have low correlations between the different FAs. The calibration models that were established after analysis of the calibration set with FTIR and Raman spectroscopy seemed to be good. All models had $R^2$-values $\geq 0.93$. The models for FA features such as ΣMUFA and UI showed good results, as expected, but the models for single FAs did also look very promising. Overall FTIR spectroscopy was better suited for the prediction of FAs than Raman spectroscopy, in part due to the background noise that was present in Raman spectra. Validation with a small set of independent samples showed that good predictions were achieved for the calibration models of both FTIR and Raman spectroscopy.

# References


Afseth, N. K., Segtnan, V. H., Marquardt, B. J. & Wold, J. P. (2005). Raman and Near-Infrared Spectroscopy for Quantification of Fat Composition in a Complex Food Model System. Applied Spectroscopy, 59 (11): 1324-1332. doi: 10.1366/000370205774783304.

Afseth, N. K., Wold, J. P. & Segtnan, V. H. (2006). The potential of Raman spectroscopy for characterisation of the fatty acid unsaturation of salmon. Analytica Chimica Acta, 572 (1): 85-92. doi: https://doi.org/10.1016/j.aca.2006.05.013.

Afseth, N. K., Martens, H., Randby, Å., Gidskehaug, L., Narum, B., Jørgensen, K., Lien, S. & Kohler, A. (2010). Predicting the Fatty Acid Composition of Milk: A Comparison of Two Fourier Transform Infrared Sampling Techniques. Applied Spectroscopy, 64 (7): 700-707. doi: 10.1366/000370210791666200.

Afseth, N. K. & Kohler, A. (2012). Extended multiplicative signal correction in vibrational spectroscopy, a tutorial. Chemometrics and Intelligent Laboratory Systems, 117: 92-99. doi: https://doi.org/10.1016/j.chemolab.2012.03.004.

Akoglu, H. (2018). User's guide to correlation coefficients. Turkish journal of emergency medicine, 18 (3): 91-93. doi: 10.1016/j.tjem.2018.08.001.

Baeten, V., Hourant, P., Morales, M. T. & Aparicio, R. (1998). Oil and Fat Classification by FT-Raman Spectroscopy. Journal of Agricultural and Food Chemistry, 46 (7): 2638-2646. doi: 10.1021/jf9707851.

Balić, A., Vlašić, D., Žužul, K., Marinović, B. & Mokos, Z. B. (2020). Omega-3 versus Omega-6 polyunsaturated fatty acids in the prevention and treatment of inflammatory skin diseases. International Journal of Molecular Sciences, 21 (3). doi: 10.3390/ijms21030741.

Bekhit, M. Y., Grung, B. & Mjøs, S. A. (2014). Determination of Omega-3 Fatty Acids in Fish Oil Supplements Using Vibrational Spectroscopy and Chemometric Methods. Applied Spectroscopy, 68 (10): 1190-1200. doi: 10.1366/13-07210.

Berghian-Grosan, C. & Magdas, D. A. (2020). Raman spectroscopy and machine-learning for edible oils evaluation. Talanta, 218: 121176. doi: https://doi.org/10.1016/j.talanta.2020.121176.

Boulesteix, A.-L. & Strimmer, K. (2006). Partial least squares: a versatile tool for the analysis of high-dimensional genomic data. Briefings in Bioinformatics, 8 (1): 32-44. doi: 10.1093/bib/bbl016.

Burri, L. & Johnsen, L. (2015). Krill products: an overview of animal studies. Nutrients, 7 (5): 3300-3321. doi: 10.3390/nu7053300.

Christie, W. W. (1997). Structural Analysis of Fatty Acids. In Christie, W. W. (ed.) vol. 8 Advances in Lipid Methodology - Four, pp. 120-123. Dundee: The Oily Press.

Coltro, W. K. T., Ferreira, M. M. C., Macedo, F. A. F., Oliveira, C. C., Visentainer, J. V., Souza, N. E. & Matsushita, M. (2005). Correlation of animal diet and fatty acid content in young goat meat by gas chromatography and chemometrics. Meat Science, 71 (2): 358-363. doi: https://doi.org/10.1016/j.meatsci.2005.04.016.

Daszykowski, M., Walczak, B. & Massart, D. L. (2002). Representative subset selection. Analytica Chimica Acta, 468 (1): 91-103. doi: https://doi.org/10.1016/S0003-2670(02)00651-7.

Davidson, B. C. & Cantrill, R. C. (1985). Fatty acid nomenclature. A short review. S Afr Med J, 67 (16): 633-4. doi: 10.1002/chin.198542383.

Didham, M., Truong, V. K., Chapman, J. & Cozzolino, D. (2020). Sensing the Addition of Vegetable Oils to Olive Oil: The Ability of UV–VIS and MIR Spectroscopy Coupled

with Chemometric Analysis. Food Analytical Methods, 13 (3): 601-607. doi: 10.1007/s12161-019-01680-8.
Esbensen, K. H. (2002). Multivariate Data Analysis - In Practice: CAMO Process AS.
Eskildsen, C. E., Rasmussen, M. A., Engelsen, S. B., Larsen, L. B., Poulsen, N. A. & Skov, T. (2014). Quantification of individual fatty acids in bovine milk by infrared spectroscopy and chemometrics: Understanding predictions of highly collinear reference variables. Journal of Dairy Science, 97 (12): 7940-7951. doi: https://doi.org/10.3168/jds.2014-8337.
Eurofins. (2020). QTA/Hurtiganalyser. Available at: https://www.eurofins.no/food-feed-testing/vaare-tjenester/service-og-kompetanse/marin-industri/qtahurtiganalyser.
Guillén, M. D. & Cabo, N. (1997). Characterization of edible oils and lard by fourier transform infrared spectroscopy. Relationships between composition and frequency of concrete bands in the fingerprint region. JAOCS, Journal of the American Oil Chemists' Society, 74 (10): 1281-1286. doi: 10.1007/s11746-997-0058-4.
Guillén, M. D. & Goicoechea, E. (2007). Detection of Primary and Secondary Oxidation Products by Fourier Transform Infrared Spectroscopy (FTIR) and 1H Nuclear Magnetic Resonance (NMR) in Sunflower Oil during Storage. Journal of Agricultural and Food Chemistry, 55 (26): 10729-10736. doi: 10.1021/jf071712c.
Halvorsen, K. B. (2019). Karakterisering av lipider i villaks, oppdrettslaks (Salmo salar) og fiskefôr med GC-MS Ås: Norwegian University of Life Sciences.
Hamilton, H. A., Newton, R., Auchterlonie, N. A. & Müller, D. B. (2020). Systems approach to quantify the global omega-3 fatty acid cycle. Nature Food, 1 (1): 59-62. doi: 10.1038/s43016-019-0006-0.
Hart, D. J., Hadad, Christopher M., Craine, Leslie E., Hart, Harold. (2012). Organic Chemistry, a brief course. 13th edition.: Brooks/Cole.
Jollife, I. T. & Cadima, J. (2016). Principal component analysis: A review and recent developments. Philosophical Transactions of the Royal Society A: Mathematical, Physical and Engineering Sciences, 374 (2065). doi: 10.1098/rsta.2015.0202.
Kostamovaara, J., Tenhunen, J., Kögler, M., Nissinen, I., Nissinen, J. & Keränen, P. (2013). Fluorescence suppression in Raman spectroscopy using a time-gated CMOS SPAD. Optics Express, 21 (25): 31632-31645. doi: 10.1364/OE.21.031632.
Krauss, R. M. & Kris-Etherton, P. M. (2020a). Public health guidelines should recommend reducing saturated fat consumption as much as possible: Debate Consensus. The American Journal of Clinical Nutrition. doi: 10.1093/ajcn/nqaa134.
Krauss, R. M. & Kris-Etherton, P. M. (2020b). Public health guidelines should recommend reducing saturated fat consumption as much as possible: NO. The American Journal of Clinical Nutrition. doi: 10.1093/ajcn/nqaa111.
Kris-Etherton, P. M. & Krauss, R. M. (2020). Public health guidelines should recommend reducing saturated fat consumption as much as possible: YES. The American Journal of Clinical Nutrition. doi: 10.1093/ajcn/nqaa110.
Li-Chan, E., Ismail, A. A., Sedman, J. & Voort, F. R. (2006). Vibrational Spectroscopy of Food and Food Products. In.
Li-Chan, E. C. Y. (2010). Introduction to Vibrational Spectroscopy in Food Science. In Applications of Vibrational Spectroscopy in Food Science, pp. 3-29.
Li, Q., Chen, J., Huyan, Z., Kou, Y., Xu, L., Yu, X. & Gao, J.-M. (2018). Application of Fourier transform infrared spectroscopy for the quality and safety analysis of fats and oils: A review. Critical Reviews in Food Science and Nutrition: 1-15. doi: 10.1080/10408398.2018.1500441.
Lichtenstein, A. H. (2013). Fats and Oils. In Caballero, B. (ed.) Encyclopedia of Human Nutrition (Third Edition), pp. 201-208. Waltham: Academic Press.

Lieber, C. A. & Mahadevan-Jansen, A. (2003). Automated method for subtraction of fluorescence from biological Raman spectra. Appl Spectrosc, 57 (11): 1363-7. doi: 10.1366/000370203322554518.
matportalen.no. (2019). Matvaretabellen - Margarin, Smør, Matolje o.l. Available at: https://www.matvaretabellen.no/margarin-smoer-matolje-ol-g8.
Matsakidou, A., Papadopoulou, D., Nenadis, N. & Tsimidou, M. Z. (2020). Getting inside on virgin olive oil (VOO) photooxidation kinetics through combined generalized 2D correlation analysis and moving window 2D correlation analysis of ATR-FTIR spectra. Talanta, 215: 120917. doi: https://doi.org/10.1016/j.talanta.2020.120917.
Matthews, C. K., van Holde, K. E., Appling, D. R. & Anthony-Cahill, S. J. (2013). Biochemistry. 4th ed.: Pearson Canada Inc.
Miller, J. M. (2005). Chromatography: Concepts and Contrasts. 2nd ed ed. New Yersey: John Wiley & Sons, Inc.
Molversmyr, E. (2020). Identification and Quantitation of Lipids in Atlantic Mackerel (Scomber scombrus), Wild and Farmed Atlantic Salmon (Salmo salar) and Salmon Feed by GC-MS. Ås: NMBU. Unpublished manuscript.
Moss, G. P., Smith, P. A. S. & Tavernier, D. (1995). Glossary of class names of organic compounds and reactivity intermediates based on structure (IUPAC Recommendations 1995). Pure and Applied Chemistry, 67, 8-9. p. 1307.
Nettleton, J. A., Brouwer, I. A., Mensink, R. P., Diekman, C. & Hornstra, G. (2018). Fats in Foods: Current Evidence for Dietary Advice. Annals of nutrition & metabolism, 72 (3): 248-254. doi: 10.1159/000488006.
Olkin, I. & Sampson, A. R. (2001). Multivariate Analysis: Overview. In Smelser, N. J. & Baltes, P. B. (eds) International Encyclopedia of the Social & Behavioral Sciences, pp. 10240-10247. Oxford: Pergamon.
Orsavova, J., Misurcova, L., Ambrozova, J. V., Vicha, R. & Mlcek, J. (2015). Fatty Acids Composition of Vegetable Oils and Its Contribution to Dietary Energy Intake and Dependence of Cardiovascular Mortality on Dietary Intake of Fatty Acids. International journal of molecular sciences, 16 (6): 12871-12890. doi: 10.3390/ijms160612871.
Pereira, A. F. C., Pontes, M. J. C., Neto, F. F. G., Santos, S. R. B., Galvão, R. K. H. & Araújo, M. C. U. (2008). NIR spectrometric determination of quality parameters in vegetable oils using iPLS and variable selection. Food Research International, 41 (4): 341-348. doi: https://doi.org/10.1016/j.foodres.2007.12.013.
PerkinElmer. (2005). FT-IR Spectroscopy - Attenuated Total Reflectance (ATR). perkinelmer.com.
Punia, S., Sandhu, K. S., Siroha, A. K. & Dhull, S. B. (2019). Omega 3-metabolism, absorption, bioavailability and health benefits–A review. PharmaNutrition, 10: 100162. doi: https://doi.org/10.1016/j.phanu.2019.100162.
Rajalahti, T. & Kvalheim, O. M. (2011). Multivariate data analysis in pharmaceutics: A tutorial review. International Journal of Pharmaceutics, 417 (1): 280-290. doi: https://doi.org/10.1016/j.ijpharm.2011.02.019.
Reich, G. (2005). Near-infrared spectroscopy and imaging: Basic principles and pharmaceutical applications. Advanced Drug Delivery Reviews, 57 (8): 1109-1143. doi: https://doi.org/10.1016/j.addr.2005.01.020.
Rinnan, Å., Berg, F. v. d. & Engelsen, S. B. (2009). Review of the most common pre-processing techniques for near-infrared spectra. TrAC Trends in Analytical Chemistry, 28 (10): 1201-1222. doi: https://doi.org/10.1016/j.trac.2009.07.007.

Rohman, A. & Irnawati. (2020). Pumpkin (Cucurbita maxima) seed oil: Chemical composition, antioxidant activities and its authentication analysis. Food Research, 4 (3): 578-584. doi: 10.26656/fr.2017.4(3).242.
Ross, S. M. (2010). CHAPTER 12 - Linear Regression. In Ross, S. M. (ed.) Introductory Statistics (Third Edition), pp. 537-604. Boston: Academic Press.
Sacks, F. M., Lichtenstein, A. H., Wu, J. H. Y., Appel, L. J., Creager, M. A., Kris-Etherton, P. M., Miller, M., Rimm, E. B., Rudel, L. L., Robinson, J. G., et al. (2017). Dietary fats and cardiovascular disease: A presidential advisory from the American Heart Association. Circulation, 136 (3): e1-e23. doi: 10.1161/CIR.0000000000000510.
Saini, R. K. & Keum, Y.-S. (2018). Omega-3 and omega-6 polyunsaturated fatty acids: Dietary sources, metabolism, and significance — A review. Life Sciences, 203: 255-267. doi: https://doi.org/10.1016/j.lfs.2018.04.049.
Schuchardt, U., Sercheli, R. & Vargas, R. M. (1998). Transesterification of vegetable oils: a review. Journal of the Brazilian Chemical Society, 9 (3): 199-210.
Silverstein, R. M., Webster, F. X., Kiemle, D. J. & Bryce, D. L. (2015). Spectrometric Identification of Organic Compounds. 8th ed.: John Wiley & Sons, Inc.
Socrates, G. (2004). Infrared and Raman Characteristic Group Frequencies - Tables and Charts: John Wiley & Sons, Inc.
Suutari, M. (1995). Effect of growth temperature on lipid fatty acids of four fungi (Aspergillus niger, Neurospora crassa, Penicillium chrysogenum, and Trichoderma reesei). Archives of Microbiology, 164 (3): 212-216. doi: 10.1007/BF02529973.
Tao, F. F. & Ngadi, M. (2018). Recent advances in rapid and nondestructive determination of fat content and fatty acids composition of muscle foods. Critical Reviews in Food Science and Nutrition, 58 (9): 1565-1593. doi: 10.1080/10408398.2016.1261332.
U.S. National Library of Medicine. PubChem - Explore Chemistry. Available at: https://pubchem.ncbi.nlm.nih.gov/ (accessed: 18.02).
Viscarra Rossel, R. A., Walvoort, D. J. J., McBratney, A. B., Janik, L. J. & Skjemstad, J. O. (2006). Visible, near infrared, mid infrared or combined diffuse reflectance spectroscopy for simultaneous assessment of various soil properties. Geoderma, 131 (1): 59-75. doi: https://doi.org/10.1016/j.geoderma.2005.03.007.
Wang, M., Wang, C. & Han, X. (2017). Selection of internal standards for accurate quantification of complex lipid species in biological extracts by electrospray ionization mass spectrometry-What, how and why? Mass spectrometry reviews, 36 (6): 693-714. doi: 10.1002/mas.21492.
WHO, W. H. O. (2020). Healthy diet. Available at: https://www.who.int/news-room/fact-sheets/detail/healthy-diet (accessed: 29.06).
Wijendran, V. & Hayes, K. C. (2004). DIETARY n-6 AND n-3 FATTY ACID BALANCE AND CARDIOVASCULAR HEALTH. Annual Review of Nutrition, 24 (1): 597-615. doi: 10.1146/annurev.nutr.24.012003.132106.
Williams, D. H. & Fleming, I. (2008). Spectroscopic Methods in Organic Chemistry: McGraw-Hill.
Yoshida, S. & Yoshida, H. (2003). Nondestructive Analyses of Unsaturated Fatty Acid Species in Dietary Oils by Attenuated Total Reflectance with Fourier Transform IR Spectroscopy. Biopolymers, 70 (4): 604-613. doi: 10.1002/bip.10505.

# Appendix A – Fatty acids

*Summary of the IUPAC names, trivial names and shorthand notation for all the FA relevant to this study. The IUPAC nomenclature is based on the entries in the online database PubChem (U.S. National Library of Medicine).*

| IUPAC Nomenclature | Trivial Nomenclature | Shorthand Notation |
|---|---|---|
| Hexanoic acid | Caproic acid | C6:0 |
| Octanoic acid | Caprylic acid | C8:0 |
| Decanoic acid | Capric acid | C10:0 |
| Undecanoic acid | | C11:0 |
| Dodecanoic | Lauric acid | C12:0 |
| Tridecanoic acid | | C13:0 |
| Tetradecanoic acid | Myristic acid | C14:0 |
| (Z)-tetradec-9-enoic acid | Myristoleic acid | C14:1n-5 |
| Pentadecanoic acid | | C15:0 |
| Hexadecanoic acid | Palmitic acid | C16:0 |
| (Z)-hexadec-9-enoic acid | Palmitoleic acid | C16:1n-7 |
| Heptadecanoic acid | Margaric acid | C17:0 |
| Octadecanoic acid | Stearic acid | C18:0 |
| (Z)-octadec-9-enoic acid | Oleic acid | C18:1n-9 |
| Nonadecanoic acid | | C19:0 |
| (9Z,12Z)-octadeca-9,12-dienoic acid | Linoleic acid | C18:2n-6 |
| Eicosanoic acid | Arachidic acid | C20:0 |
| (9Z,12Z,15Z)-octadeca-9,12,15-trienoic acid | Linolenic acid | C18:3n-3 |
| (Z)-icos-11-enoic acid | Gondoic acid | C20:1n-9 |
| Heneicosanoic acid | | C21:0 |
| (11Z,14Z)-icosa-11,14-dienoic acid | | C20:2n-6 |
| (8Z,11Z,14Z)-icosa-8,11,14-trienoic acid | Dihomo-gamma-linolenic acid | C20:3n-6 |
| Docosanoic acid | Behenic acid | C22:0 |
| (11Z,14Z,17Z)-icosa-11,14,17-trienoic acid | | C20:3n-3 |
| (5Z,8Z,11Z,14Z)-icosa-5,8,11,14-tetraenoic acid | Arachidonic acid | C20:4n-6 |
| (Z)-docos-13-enoic acid | Erucic acid | C22:1n-9 |
| Tricosanoic acid | | C23:0 |
| (5Z,8Z,11Z,14Z,17Z)-icosa-5,8,11,14,17-pentaenoic acid | EPA | C20:5n-3 |
| (13Z,16Z)-docosa-13,16-dienoic aid | | C22:2n-6 |
| Tetracosanoic acid | Lignoceric acid | C24:0 |
| (Z)-tetracos-15-enoic acid | Nervonic acid | C24:1n-9 |
| (4Z,7Z,10Z,13Z,16Z,19Z)-docosa-4,7,10,13,16,19-hexaenoic acid | DHA | C22:6n-3 |

# Appendix B – Internal standard

*Exact amounts of trinonadecanoin and chloroform used to make stock solutions of the internal standard.*

| | Trinonadecanoin | Chloroform | Concentration | Mole IS (TG) | Mole IS (FA) |
|---|---|---|---|---|---|
| IS 1 | 80.7 mg | 8.0 mL | 10.1 mg/mL | $1.08*10^{-6}$ | $3.24*10^{-6}$ |
| IS 2 | 81.3 mg | 8.0 mL | 10.2 mg/mL | $1.09*10^{`-6}$ | $3.26*10^{-6}$ |

# Appendix C – Relative response factors

*Relative response factors and molecular weight for all fatty acids in this study, including the unidentified isomers (u.i.).*

| Fatty acid | Molecular weight [g/mol] | RRF |
|---|---|---|
| C6:0 | 116.16 | 0.62 |
| C8:0 | 144.21 | 0.88 |
| C10:0 | 172.26 | 1.00 |
| C11:0 | 186.29 | 0.94 |
| C12:0 | 200.32 | 1.08 |
| C13:0 | 214. 34 | 1.01 |
| C14:0 | 228.37 | 1.11 |
| C14:1n-5 | 226.35 | 0.97 |
| C15:0 | 242.20 | 1.01 |
| C16:0 | 256.42 | 1.10 |
| C16:1n-7 | 254.41 | 0.86 |
| C17:0 | 270.50 | 0.92 |
| C18:0 | 284.50 | 1.00 |
| C18:1n-9 | 282.50 | 1.04 |
| C19:0 | 298.50 | 1.00 |
| C18:2n-6 | 280.40 | 1.15 |
| C20:0 | 312.50 | 1.15 |
| C18:3n-3 | 278.40 | 1.15 |
| C20:1n-9 | 310.50 | 1.00 |
| C21:0 | 326.60 | 0.97 |
| C20:2n-6 | 308.50 | 1.02 |
| C22:0 | 340.60 | 1.04 |
| C20:3n-6 | 306.50 | 0.96 |
| C20:4n-6 | 304.50 | 1.26 |
| C20:3n-3 | 306.50 | 1.15 |
| C22:1n-9 | 338.60 | 1.03 |
| C23:0 | 354.60 | 1.08 |
| C20:5n-3 | 302.50 | 1.32 |
| C22:2n-6 | 336.60 | 1.41 |
| C24:0 | 368.60 | 1.38 |
| C24:1n-9 | 366.60 | 1.24 |
| C22:6n-3 | 328.50 | 1.24 |
| C16:1 u.i. | 254.41 | 0.86 |
| C17:1 u.i. | 268.40 | 0.88 |
| C18:1 u.i. | 282.50 | 1.04 |
| C18:2 u.i. | 280.40 | 1.15 |
| C18:3 u.i. | 278.40 | 1.15 |
| C18:4 u.i. | 276.40 | 1.00* |
| C20:1 u.i. | 310.50 | 1.00 |
| C20:2 u.i. | 308.50 | 1.02 |
| C20:4 u.i. | 304.50 | 1.26 |

| | | |
|---|---|---|
| C21:5 u.i. | 316.50 | 1.00* |
| C22:1 u.i. | 338.60 | 1.03 |
| C22:5 u.i. | 330.50 | 1.00* |

* = RRF value set to one for the unidentified FAs with no standard of equivalent isomer.

# Appendix D – Calibration set

*Samples of the calibration set with composition and mixing ratios of reference oils.*

| Sample nr. | Contents |
|---|---|
| 1 | 100 % Soybean |
| 2 | 100 % Sunflower |
| 3 | 100 % Herring |
| 4 | 100 % Sesame |
| 5 | 100 % Rice bran |
| 6 | 100 % Olive |
| 7 | 100 % Flaxseed |
| 8 | 100 % Coconut |
| 9 | 100 % 0370 (EPA/DHA) |
| 10 | 75 % Sesame + 25 % 0370 (EPA/DHA) |
| 11 | 75 % Rice bran + 25 % 0370 (EPA/DHA) |
| 12 | 75 % Peanut + 25 % Coconut |
| 13 | 75 % Olive + 25 % 0370 (EPA/DHA) |
| 14 | 75 % Flaxseed + 25 % Rice bran |
| 15 | 75 % Flaxseed + 25 % Coconut |
| 16 | 75 % Flaxseed + 25 % 0370 (EPA/DHA) |
| 17 | 75 % Coconut + 25 % 0370 (EPA/DHA) |
| 18 | 50 % Soybean + 25 % 0370 (EPA/DHA) + 25 % Camelina |
| 19 | 50 % Sunflower + 50 % 4030 (EPA/DHA) |
| 20 | 50 % Sunflower + 25 % Coconut + 25 % 4030 (EPA/DHA) |
| 21 | 50 % Sunflower + 25 % Frying oil + 25 % 0370 (EPA/DHA) |
| 22 | 50 % Herring + 50 % 3040 (EPA/DHA) |
| 23 | 50 % Herring + 25 % 0370 (EPA/DHA) + 25 % Camelina |
| 24 | 50 % Sesame + 50 % Rice bran |
| 25 | 50 % Sesame + 50 % Coconut |
| 26 | 50 % Sesame + 50 % 0370 (EPA/DHA) |
| 27 | 50 % Sesame + 25 % Olive + 25 % Flaxseed |
| 28 | 50 % Sesame + 25 % Flaxseed + 25 % Coconut |
| 29 | 50 % Rice bran + 50 % Coconut |
| 30 | 50 % Rice bran + 50 % Camelina |
| 31 | 50 % Rapeseed +25 % Peanut + 25 % Vita hjertgó |
| 32 | 50 % Rapeseed +25 % Flaxseed + 25 % Coconut |
| 33 | 50 % Rapeseed +25 % Coconut + 25 % 0370 (EPA/DHA) |
| 34 | 50 % Peanut +25 % Sesame + 25 % Sunflower |
| 35 | 50 % Olive +50 % Herring |
| 36 | 50 % Olive +50 % Flaxseed |
| 37 | 50 % Olive +50 % 4030 (EPA/DHA) |
| 38 | 50 % Olive +25 % Flaxseed + 25 % Rice bran |
| 39 | 50 % Olive +25 % Flaxseed + 25 % 4030 (EPA/DHA) |
| 40 | 50 % Olive +25 % Coconut + 25 % 4030 (EPA/DHA) |
| 41 | 50 % Flaxseed + 50 % Herring |

| | |
|---|---|
| 42 | 50 % Flaxseed + 50 % Coconut |
| 43 | 50 % Flaxseed + 50 % 0370 (EPA/DHA) |
| 44 | 50 % Flaxseed + 25 % Coconut + 25 % 4030 (EPA/DHA) |
| 45 | 50 % Flaxseed + 25 % 4030 (EPA/DHA) + 25 % 3040 (EPA/DHA) |
| 46 | 50 % Coconut + 50 % 0370 (EPA/DHA) |
| 47 | 50 % 0370 (EPA/DHA) + 50 % 4030 (EPA/DHA) |
| 48 | 100 % 4030 (EPA/DHA) |
| 49 | 33 % Soybean + 33 % Sunflower + 33 % Coconut |
| 50 | 33 % Soybean + 33 % Coconut + 33 % 0370 (EPA/DHA) |
| 51 | 33 % Herring + 33 % Coconut + 33 % Camelina |
| 52 | 33 % Herring + 33 % Coconut + 33 % 4030 (EPA/DHA) |
| 53 | 33 % Sesame + 33 % Flaxseed + 33 % 4030 (EPA/DHA) |
| 54 | 33 % Rice bran + 33 % Herring + 33 % 4030 (EPA/DHA) |
| 55 | 33 % Rice bran + 33 % 0370 (EPA/DHA) + 33 % 3040 (EPA/DHA) |
| 56 | 33 % Rapeseed + 33 % Peanut + 33 % 0370 (EPA/DHA) |
| 57 | 33 % Rapeseed + 33 % 3040 (EPA/DHA) + 33 % Camelina |
| 58 | 33 % Flaxseed + 33 % Rice bran + 33 % 0370 (EPA/DHA) |
| 59 | 33 % Frying oil + 33 % Rice bran + 33 % 0370 (EPA/DHA) |
| 60 | 25 % Sunflower + 50 % Rice bran + 25 % Coconut |
| 61 | 25 % Sunflower + 50 % 0370 (EPA/DHA) + 25 % Camelina |
| 62 | 25 % Sesame + 75 % 4030 (EPA/DHA) |
| 63 | 25 % Sesame + 50 % Olive + 25 % Coconut |
| 64 | 25 % Sesame + 50 % Coconut + 25 % 4030 (EPA/DHA) |
| 65 | 25 % Rice bran + 75 % Coconut |
| 66 | 25 % Rice bran + 50 % Herring + 25 % Camelina |
| 67 | 25 % Rapeseed + 75 % Camelina |
| 68 | 25 % Rapeseed + 25 % Soybean + 50 % Møllers tran |
| 69 | 25 % Rapeseed + 25 % Peanut + 50 % Rice bran |
| 70 | 25 % Rapeseed + 25 % Peanut + 50 % Coconut |
| 71 | 25 % Peanut + 50 % Frying oil + 25 % 4030 (EPA/DHA) |
| 72 | 25 % Flaxseed + 75 % Coconut |
| 73 | 25 % Flaxseed + 75 % Frying oil |
| 74 | 25 % Flaxseed + 75 % 0370 (EPA/DHA) |
| 75 | 25 % Flaxseed + 50 % Soybean + 25 % Camelina |
| 76 | 25 % Flaxseed + 25 % Coconut + 50 % 4030 (EPA/DHA) |
| 77 | 25 % Flaxseed + 25 % Coconut + 50 % 0370 (EPA/DHA) |
| 78 | 25 % Flaxseed + 25 % 0370 (EPA/DHA) + 50 % 4030 (EPA/DHA) |
| 79 | 25 % Coconut + 75 % 0370 (EPA/DHA) |
| 80 | 25 % Coconut + 25 % 4030 (EPA/DHA) + 50 % 3040 (EPA/DHA) |

# Appendix E – Fatty acid profiles of the reference oils

*Fatty acid profiles in % of total area in the chromatogram, with standard deviations based on six replicate measurements. Numbers marked in red are only based on three replicates. n.d. = not detected. For numbers in red n=3, for all remaining values n=6.*

| Fatty acid | Rapeseed oil | Peanut oil | Sesame oil | Olive oil | Linseed oil | Soybean oil | Sunflower oil | Vita hjertego | Frying oil | Møllers tran | Rice bran oil | Salmon oil | Herring oil | Coconut oil | 0370 (EPA/DHA) | 4030 (EPA/DHA) | 3040 (EPA/DHA) | Camelina oil |
|---|---|---|---|---|---|---|---|---|---|---|---|---|---|---|---|---|---|---|
| C6:0 | n.d. | n.d. | n.d. | n.d. | n.d. | n.d. | n.d. | n.d. | n.d. | n.d. | n.d. | n.d. | n.d. | 0.47 ±0.05 | n.d. | n.d. | n.d. | n.d. |
| C8:0 | n.d. | n.d. | n.d. | n.d. | n.d. | n.d. | n.d. | n.d. | n.d. | n.d. | n.d. | n.d. | n.d. | 6.77 ±0.37 | 0.07 ±0.05 | n.d. | n.d. | n.d. |
| C10:0 | 0.01 ±0.0 | n.d. | n.d. | n.d. | n.d. | n.d. | n.d. | n.d. | n.d. | n.d. | n.d. | n.d. | 0.01 ±0.0 | 6.43 ±0.13 | 0.05 ±0.05 | n.d. | n.d. | n.d. |
| C11:0 | n.d. | n.d. | n.d. | n.d. | n.d. | n.d. | n.d. | n.d. | n.d. | n.d. | n.d. | n.d. | n.d. | 0.03 ±0.0 | n.d. | n.d. | n.d. | n.d. |
| C12:0 | 0.01 ±0.01 | n.d. | 0.01 ±0.0 | n.d. | n.d. | n.d. | n.d. | n.d. | n.d. | 0.02 ±0.01 | 0.01 ±0.0 | 0.03 ±0.01 | 0.12 ±0.02 | 35.82 ±2.91 | 0.50 ±0.46 | 0.04 ±0.05 | 0.05 ±0.07 | 0.01 ±0.01 |
| C13:0 | n.d. | n.d. | n.d. | n.d. | n.d. | n.d. | n.d. | n.d. | n.d. | 0.01 ±0.0 | n.d. | 0.03 ±0.03 | 0.04 ±0.0 | 0.05 ±0.01 | n.d. | n.d. | n.d. | n.d. |
| C14:0 | 0.06 ±0.03 | 0.02 ±0.00 | 0.02 ±0.01 | 0.01 ±0.00 | 0.04 ±0.00 | 0.07 ±0.01 | 0.06 ±0.00 | 0.04 ±0.00 | 0.05 ±0.00 | 3.77 ±0.09 | 0.41 ±0.01 | 2.19 ±0.06 | 8.91 ±0.19 | 25.71 ±0.93 | 0.36 ±0.18 | 0.37 ±0.03 | 0.16 ±0.02 | 0.04 ±0.01 |
| C14:1n-5 | n.d. | n.d. | n.d. | n.d. | n.d. | n.d. | n.d. | n.d. | n.d. | 0.12 ±0.01 | n.d. | n.d. | n.d. | n.d. | n.d. | n.d. | n.d. | n.d. |
| C15:0 | 0.02 ±0.01 | 0.01 ±0.00 | n.d. | n.d. | 0.02 ±0.01 | 0.01 ±0.00 | 0.01 ±0.00 | 0.01 ±0.00 | 0.01 ±0.00 | 0.31 ±0.01 | 0.02 ±0.01 | 0.14 ±0.04 | 0.45 ±0.01 | n.d. | n.d. | n.d. | n.d. | 0.01 ±0.00 |
| C16:0 | 4.97 ±0.14 | 6.90 ±0.11 | 9.72 ±0.16 | 12.51 ±0.11 | 6.73 ±0.07 | 11.17 ±0.11 | 6.61 ±0.04 | 6.24 ±0.09 | 5.70 ±0.06 | 10.21 ±0.30 | 20.45 ±0.35 | 9.96 ±0.34 | 14.25 ±0.35 | 11.62 ±0.82 | 0.63 ±0.08 | 0.51 ±0.06 | 0.38 ±0.02 | 6.12 ±0.13 |
| C16:1n-7 | 0.20 ±0.02 | 0.06 ±0.01 | 0.13 ±0.01 | 0.93 ±0.05 | 0.06 ±0.02 | 0.06 ±0.01 | 0.08 ±0.01 | 0.21 ±0.01 | 0.11 ±0.01 | 9.89 ±0.18 | 0.16 ±0.01 | 2.30 ±0.20 | 4.98 ±0.06 | n.d. | 0.20 ±0.03 | 0.24 ±0.03 | 0.13 ±0.01 | n.d. |
| C17:0 | 0.05 ±0.01 | 0.07 ±0.01 | 0.03 ±0.01 | 0.07 ±0.01 | 0.05 ±0.01 | 0.08 ±0.02 | 0.03 ±0.01 | 0.04 ±0.01 | 0.04 ±0.01 | n.d. | 0.04 ±0.01 | n.d. | n.d. | n.d. | n.d. | n.d. | n.d. | 0.04 ±0.0 |
| C18:0 | 1.73 ±0.08 | 2.12 ±0.13 | 6.10 ±0.31 | 3.30 ±0.13 | 4.32 ±0.14 | 4.85 ±0.14 | 3.46 ±0.14 | 2.31 ±0.07 | 2.48 ±0.08 | 2.14 ±0.06 | 2.04 ±0.07 | 2.68 ±0.09 | 1.09 ±0.04 | 4.96 ±0.67 | 0.29 ±0.02 | 2.03 ±0.23 | 1.30 ±0.15 | 2.93 ±0.09 |
| C18:1n-9 | 61.64 ±1.00 | 67.59 ±1.48 | 41.09 ±0.16 | 71.29 ±0.61 | 20.50 ±0.31 | 23.09 ±0.42 | 31.99 ±0.66 | 56.39 ±0.79 | 45.47 ±0.15 | 15.20 ±0.15 | 40.72 ±0.13 | 42.58 ±0.41 | 6.99 ±0.11 | 7.23 ±0.77 | 0.55 ±0.06 | 2.60 ±0.34 | 1.70 ±0.18 | 16.79 ±0.11 |

| | | | | | | | | | | | | | | | | | | |
|---|---|---|---|---|---|---|---|---|---|---|---|---|---|---|---|---|---|---|
| **C18:2n-6** | 19.06 ±0.33 | 15.36 ±0.35 | 40.97 ±0.55 | 8.33 ±0.19 | 15.31 ±0.39 | 52.02 ±1.26 | 56.04 ±0.91 | 25.75 ±0.44 | 38.23 ±0.35 | 2.39 ±0.21 | 32.51 ±0.16 | 13.78 ±0.19 | 1.52 ±0.09 | 1.15 ±0.16 | 0.16 ±0.02 | n.d. | 0.24 ±0.02 | 19.32 ±0.33 |
| **C20:0** | 0.52 ±0.05 | 0.92 ±0.09 | 0.58 ±0.06 | 0.37 ±0.03 | n.d. | 0.38 ±0.02 | 0.21 ±0.02 | 0.37 ±0.02 | 0.34 ±0.03 | n.d. | 0.80 ±0.05 | 0.29 ±0.04 | 0.16 ±0.01 | 0.08 ±0.01 | 0.34 ±0.06 | 0.81 ±0.11 | 0.55 ±0.08 | 0.89 ±0.01 |
| **C18:3n-3** | 6.72 ±0.07 | 0.47 ±0.05 | 0.20 ±0.02 | 0.53 ±0.06 | 51.92 ±0.92 | 5.93 ±0.20 | 0.12 ±0.03 | 5.24 ±0.13 | 4.52 ±0.13 | 0.72 0.05 | 1.05 ±0.07 | 4.91 ±0.08 | 1.12 ±0.07 | n.d. | n.d. | 0.19 ±0.04 | 0.09 ±0.01 | 37.97 ±0.48 |
| **C20:1n-9** | 1.12 ±0.09 | 1.90 ±0.13 | 0.12 ±0.01 | 0.18 ±0.02 | 0.09 ±0.01 | 0.14 ±0.01 | 0.11 ±0.01 | 0.66 ±0.04 | 0.57 ±0.05 | 13.13 ±0.07 | 0.43 ±0.02 | 4.47 ±0.05 | 12.15 ±0.15 | n.d. | 0.73 ±0.13 | 2.89 ±0.41 | 1.77 ±0.22 | 10.79 ±0.14 |
| **C21:0** | n.d. | n.d. | n.d. | n.d. | n.d. | 0.03 ±0.02 | n.d. | n.d. | 0.02 ±0.01 | n.d. | 0.04 ±0.01 | n.d. | 0.05 ±0.01 | n.d. | 0.14 ±0.03 | 0.10 ±0.02 | 0.08 ±0.02 | n.d. |
| **C20:2n-6** | 0.04 ±0.00 | n.d. | n.d. | n.d. | n.d. | 0.02 ±0.00 | n.d. | n.d. | n.d. | 0.27 ±0.02 | n.d. | 1.05 ±0.05 | 0.18 ±0.01 | n.d. | 0.14 ±0.04 | 0.48 ±0.09 | 0.28 ±0.07 | 1.66 ±0.11 |
| **C22:0** | 0.21 ±0.03 | 2.13 ±0.18 | 0.07 ±0.01 | 0.05 ±0.01 | 0.05 ±0.01 | 0.27 ±0.02 | 0.55 ±0.04 | 0.26 ±0.02 | 0.37 ±0.03 | n.d. | 0.18 ±0.02 | 0.09 ±0.01 | n.d. | n.d. | 0.41 ±0.01 | 0.19 ±0.01 | 0.16 ±0.02 | 0.13 ±0.02 |
| **C20:3n-6** | n.d. | n.d. | n.d. | n.d. | n.d. | n.d. | n.d. | n.d. | n.d. | 0.04 ±0.01 | n.d. | 0.23 ±0.02 | 0.05 ±0.00 | n.d. | 0.11 ±0.01 | 0.36 ±0.06 | 0.34 ±0.06 | n.d. |
| **C20:4n-6** | n.d. | n.d. | n.d. | n.d. | n.d. | n.d. | n.d. | n.d. | n.d. | 0.24 ±0.04 | n.d. | 0.10 ±0.02 | 0.31 ±0.03 | n.d. | 0.72 ±0.33 | 2.30 ±0.47 | 2.06 ±0.40 | n.d. |
| **C20:3n-3** | n.d. | n.d. | n.d. | n.d. | 0.02 ±0.01 | n.d. | n.d. | n.d. | n.d. | 0.07 ±0.01 | n.d. | 0.37 ±0.03 | 0.12 ±0.03 | n.d. | n.d. | 0.23 ±0.02 | 0.13 ±0.04 | 1.16 ±0.10 |
| **C22:1n-11** | 0.11 ±0.01 | 0.14 ±0.01 | n.d. | n.d. | n.d. | n.d. | n.d. | n.d. | 0.02 ±0.01 | 6.32 ±0.16 | n.d. | 0.44 ±0.08 | 21.32 ±0.47 | n.d. | 1.09 ±0.56 | 0.78 ±0.03 | 0.82 ±0.02 | 1.04 ±0.10 |
| **C23:0** | n.d. | 0.01 ±0.00 | n.d. | n.d. | n.d. | 0.01 ±0.00 | n.d. | n.d. | n.d. | n.d. | n.d. | n.d. | n.d. | n.d. | n.d. | n.d. | n.d. | n.d. |
| **C20:5n-3** | n.d. | n.d. | n.d. | n.d. | n.d. | n.d. | n.d. | n.d. | n.d. | 7.74 ±0.08 | n.d. | 1.99 ±0.34 | 7.00 ±0.08 | n.d. | 12.89 ±1.50 | 44.08 ±0.94 | 40.30 ±0.27 | n.d. |
| **C22:2n-6** | n.d. | n.d. | n.d. | n.d. | n.d. | n.d. | n.d. | n.d. | n.d. | n.d. | n.d. | 0.06 ±0.01 | n.d. | n.d. | n.d. | n.d. | n.d. | 0.04 ±0.01 |
| **C24:0** | 0.06 ±0.01 | 1.11 ±0.14 | 0.02 ±0.01 | 0.01 ±0.01 | 0.02 ±0.01 | 0.05 ±0.01 | 0.11 ±0.02 | 0.05 ±0.01 | 0.07 ±0.01 | n.d. | 0.24 ±0.03 | n.d. | n.d. | n.d. | n.d. | n.d. | n.d. | 0.04 ±0.01 |
| **C24:1n-9** | 0.05 ±0.01 | n.d. | n.d. | n.d. | n.d. | n.d. | n.d. | 0.03 ±0.01 | 0.02 ±0.01 | 0.19 ±0.01 | n.d. | 0.26 ±0.03 | 0.39 ±0.17 | n.d. | 1.00 ±0.16 | 0.27 ±0.08 | 0.30 ±0.07 | 0.28 ±0.03 |
| **C22:6n-3** | n.d. | n.d. | n.d. | n.d. | n.d. | n.d. | n.d. | n.d. | n.d. | 9.68 ±0.58 | n.d. | 2.80 ±0.17 | 6.14 ±0.18 | n.d. | 62.32 ±3.55 | 28.21 ±2.67 | 34.52 ±2.94 | n.d. |
| **C16:1. u.i.** | 0.03 ±0.01 | 0.04 ±0.00 | 0.02 ±0.01 | 0.09 ±0.01 | 0.02 ±0.00 | n.d. | 0.01 ±0.00 | 0.03 ±0.01 | 0.02 ±0.00 | 0.62 ±0.26 | 0.04 ±0.01 | 0.19 ±0.01 | 0.40 ±0.26 | n.d. | n.d. | n.d. | n.d. | n.d. |
| **C17:1 u.i.** | n.d. | n.d. | n.d. | n.d. | n.d. | n.d. | n.d. | n.d. | n.d. | 0.22 ±0.01 | n.d. | n.d. | 0.19 ±0.00 | n.d. | n.d. | n.d. | n.d. | n.d. |

| | | | | | | | | | | | | | | | | | | |
|---|---|---|---|---|---|---|---|---|---|---|---|---|---|---|---|---|---|---|
| **C18:1 u.i.** | 3.14 ±0.13 | 0.68 ±0.09 | 0.93 ±0.07 | 2.25 ±0.13 | 0.75 ±0.05 | 1.26 ±0.09 | 0.63 ±0.06 | 2.25 ±0.14 | 1.85 ±0.11 | 6.08 ±1.21 | 0.84 ±0.06 | 3.13 ±0.15 | 1.48 ±0.41 | 0.05 ±0.01 | 0.15 ±0.00 | 0.86 ±0.15 | 0.54 ±0.07 | 0.82 ±0.07 |
| **C18:2 u.i.** | n.d. | n.d. | n.d. | n.d. | n.d. | n.d. | n.d. | n.d. | n.d. | 0.14 ±0.01 | n.d. | n.d. | 0.08 ±0.01 | n.d. | n.d. | 0.33 ±0.01 | n.d. | n.d. |
| **C18:3 u.i.** | n.d. | n.d. | n.d. | n.d. | n.d. | n.d. | n.d. | n.d. | n.d. | 0.11 ±0.00 | n.d. | n.d. | 0.08 ±0.01 | n.d. | n.d. | n.d. | n.d. | n.d. |
| **C18:4 u.i.** | n.d. | n.d. | n.d. | n.d. | n.d. | n.d. | n.d. | n.d. | n.d. | 2.29 ±0.03 | n.d. | n.d. | 3.59 ±0.02 | n.d. | n.d. | n.d. | n.d. | n.d. |
| **C20:1 u.i.** | n.d. | n.d. | n.d. | n.d. | n.d. | n.d. | n.d. | n.d. | n.d. | 1.46 ±0.07 | n.d. | 0.42 ±0.03 | 0.90 ±0.01 | n.d. | n.d. | 1.17 ±0.01 | 0.59 ±0.01 | n.d. |
| **C20:2 u.i.** | n.d. | n.d. | n.d. | n.d. | n.d. | n.d. | n.d. | n.d. | n.d. | n.d. | n.d. | n.d. | n.d. | n.d. | n.d. | 0.65 ±0.02 | 0.55 ±0.01 | n.d. |
| **C20:4 u.i.** | n.d. | n.d. | n.d. | n.d. | n.d. | n.d. | n.d. | n.d. | n.d. | 0.56 ±0.01 | n.d. | 0.78 ±0.01 | 0.52 ±0.03 | n.d. | n.d. | 2.88 ±0.05 | 2.49 ±0.05 | n.d. |
| **C21:5 u.i.** | n.d. | n.d. | n.d. | n.d. | n.d. | n.d. | n.d. | n.d. | n.d. | 0.33 ±0.00 | n.d. | n.d. | n.d. | n.d. | n.d. | n.d. | 3.32 ±0.09 | n.d. |
| **C22:1 u.i.** | n.d. | n.d. | n.d. | n.d. | n.d. | n.d. | n.d. | n.d. | n.d. | 0.77 ±0.02 | n.d. | 2.92 ±0.06 | n.d. | n.d. | 1.39 ±0.09 | 0.18 ±0.01 | 0.19 ±0.01 | n.d. |
| **C22:5 u.i.** | n.d. | n.d. | n.d. | n.d. | n.d. | n.d. | n.d. | n.d. | n.d. | 1.01 ±0.01 | n.d. | 0.77 ±0.02 | 0.68 ±0.05 | n.d. | 11.67 ±0.12 | 5.73 ±0.58 | 6.35 ±0.15 | n.d. |

# Appendix F – Reference oils

*Table F1 - Sum of SFA, MUFA and PUFA in the reference oils (% based on total area in the chromatograms).*

| | Σ SFA | Σ MUFA | Σ PUFA |
|---|---|---|---|
| Rapeseed oil | 7.63 | 66.28 | 25.82 |
| Peanut oil | 13.28 | 70.40 | 15.83 |
| Sesame oil | 16.55 | 42.29 | 41.17 |
| Olive oil | 16.32 | 74.73 | 8.86 |
| Linseed oil | 11.23 | 21.41 | 67.25 |
| Soybean oil | 16.90 | 24.54 | 57.97 |
| Sunflower oil | 11.03 | 32.81 | 56.16 |
| Vita hjertegó | 9.31 | 59.57 | 30.98 |
| Frying oil | 9.08 | 48.06 | 42.75 |
| Møllers tran | 16.47 | 54.00 | 25.58 |
| Rice bran oil | 24.23 | 42.19 | 33.55 |
| Salmon oil | 15.39 | 56.71 | 26.84 |
| Herring oil | 25.07 | 48.80 | 21.38 |
| Coconut oil | 91.92 | 7.28 | 1.15 |
| 0370 (EPA/DHA) | 2.78 | 5.11 | 88.01 |
| 4030 (EPA/DHA) | 4.05 | 8.98 | 85.43 |
| 3040 (EPA/DHA) | 2.68 | 6.03 | 90.66 |
| Camelina oil | 10.21 | 29.71 | 60.15 |

*Table F2 - Sum of the FAs of different chain lengths in the reference oils (% based on total area in the chromatograms).*

| | C6-C13 | C14-C19 | C20-C24 |
|---|---|---|---|
| Rapeseed oil | 0.02 | 97.61 | 2.10 |
| Peanut oil | 0.00 | 93.30 | 6.20 |
| Sesame oil | 0.01 | 99.19 | 0.80 |
| Olive oil | 0.00 | 99.30 | 0.61 |
| Linseed oil | 0.00 | 99.71 | 0.18 |
| Soybean oil | 0.00 | 98.51 | 0.90 |
| Sunflower oil | 0.00 | 99.03 | 0.97 |
| Vita hjertegó | 0.00 | 98.51 | 1.36 |
| Frying oil | 0.00 | 98.48 | 1.41 |
| Møllers tran | 0.03 | 54.20 | 41.81 |
| Rice bran oil | 0.01 | 98.27 | 1.69 |
| Salmon oil | 0.06 | 81.85 | 17.03 |
| Herring oil | 0.17 | 45.12 | 49.96 |
| Coconut oil | 49.56 | 50.71 | 0.08 |
| 0370 (EPA/DHA) | 0.62 | 2.32 | 92.95 |
| 4030 (EPA/DHA) | 0.04 | 7.11 | 91.31 |
| 3040 (EPA/DHA) | 0.05 | 4.53 | 94.80 |
| Camelina oil | 0.01 | 84.04 | 16.02 |

# Appendix G – Calibration set

*Calculated fatty acid profiles of the calibration set. Only the eight main fatty acids are included, in addition to the parameters ΣSFA, ΣMUFA, ΣPUFA and UI.*

| Sample nr. | C14:0 | C16:0 | C18:0 | C18:1n-9 | C18:2n-6 | C18:3n-3 | C20:5n-3 | C22:6n-3 | Σ SFA | Σ MUFA | Σ PUFA | UI |
|---|---|---|---|---|---|---|---|---|---|---|---|---|
| 1 | 0.07 | 11.17 | 4.85 | 23.09 | 52.02 | 5.93 | 0.00 | 0.00 | 16.90 | 24.54 | 57.97 | 1.47 |
| 2 | 0.06 | 6.61 | 3.46 | 31.99 | 56.04 | 0.12 | 0.00 | 0.00 | 11.03 | 32.81 | 56.16 | 1.45 |
| 3 | 8.91 | 14.25 | 1.09 | 6.99 | 1.52 | 1.12 | 7.00 | 6.14 | 25.07 | 48.80 | 21.38 | 1.57 |
| 4 | 0.02 | 9.72 | 6.10 | 41.09 | 40.97 | 0.20 | 0.00 | 0.00 | 16.55 | 42.29 | 41.17 | 1.25 |
| 5 | 0.41 | 20.45 | 2.04 | 40.72 | 32.51 | 1.05 | 0.00 | 0.00 | 24.23 | 42.19 | 33.55 | 1.10 |
| 6 | 0.01 | 12.51 | 3.30 | 71.29 | 8.33 | 0.53 | 0.00 | 0.00 | 16.32 | 74.73 | 8.86 | 0.93 |
| 7 | 0.04 | 6.73 | 4.32 | 20.50 | 15.31 | 51.92 | 0.00 | 0.00 | 11.23 | 21.41 | 67.25 | 2.08 |
| 8 | 25.71 | 11.62 | 4.96 | 7.23 | 1.15 | 0.00 | 0.00 | 0.00 | 91.92 | 7.28 | 1.15 | 0.10 |
| 9 | 0.36 | 0.63 | 0.29 | 0.55 | 0.16 | 0.00 | 12.89 | 62.32 | 2.78 | 5.11 | 88.01 | 5.27 |
| 10 | 0.10 | 7.45 | 4.65 | 31.00 | 30.81 | 0.15 | 3.21 | 15.52 | 13.12 | 33.03 | 52.83 | 2.22 |
| 11 | 0.40 | 15.48 | 1.60 | 30.64 | 24.40 | 0.78 | 3.23 | 15.63 | 18.85 | 32.89 | 47.21 | 2.12 |
| 12 | 6.45 | 8.08 | 2.83 | 52.49 | 11.81 | 0.35 | 0.00 | 0.00 | 32.95 | 54.61 | 12.15 | 0.79 |
| 13 | 0.10 | 9.54 | 2.55 | 53.59 | 6.29 | 0.40 | 3.22 | 15.59 | 12.93 | 57.32 | 28.66 | 1.98 |
| 14 | 0.13 | 10.17 | 3.75 | 25.57 | 19.62 | 39.17 | 0.00 | 0.00 | 14.48 | 26.62 | 58.80 | 1.84 |
| 15 | 6.45 | 7.95 | 4.48 | 17.19 | 11.77 | 38.95 | 0.00 | 0.00 | 31.38 | 17.88 | 50.73 | 1.58 |
| 16 | 0.12 | 5.20 | 3.31 | 15.50 | 11.51 | 38.90 | 3.23 | 15.63 | 9.11 | 17.32 | 72.45 | 2.86 |
| 17 | 19.36 | 8.87 | 3.79 | 5.55 | 0.90 | 0.00 | 3.23 | 15.61 | 69.59 | 6.73 | 22.90 | 1.35 |
| 18 | 0.13 | 7.26 | 3.22 | 15.86 | 30.84 | 12.46 | 3.23 | 15.62 | 11.68 | 20.97 | 66.04 | 2.50 |
| 19 | 0.21 | 3.56 | 2.74 | 17.29 | 28.00 | 0.15 | 22.05 | 14.11 | 7.54 | 20.89 | 70.80 | 3.02 |
| 20 | 6.55 | 6.34 | 3.48 | 18.46 | 28.32 | 0.11 | 11.01 | 7.05 | 29.51 | 20.47 | 49.72 | 1.89 |
| 21 | 0.13 | 4.89 | 2.42 | 27.49 | 37.65 | 1.19 | 3.22 | 15.57 | 8.48 | 29.69 | 60.77 | 2.36 |
| 22 | 4.54 | 7.32 | 1.19 | 4.35 | 0.88 | 0.61 | 23.64 | 20.32 | 13.88 | 27.42 | 56.00 | 3.26 |

| | | | | | | | | | | | | |
|---|---|---|---|---|---|---|---|---|---|---|---|---|
| **23** | 4.54 | 8.80 | 1.36 | 7.87 | 5.69 | 10.18 | 6.69 | 18.55 | 15.76 | 33.10 | 47.77 | 2.57 |
| **24** | 0.21 | 15.08 | 4.07 | 40.90 | 36.74 | 0.62 | 0.00 | 0.00 | 20.39 | 42.24 | 37.36 | 1.18 |
| **25** | 12.85 | 10.67 | 5.53 | 24.18 | 21.08 | 0.10 | 0.00 | 0.00 | 54.19 | 24.80 | 21.18 | 0.67 |
| **26** | 0.19 | 5.17 | 3.19 | 20.80 | 20.54 | 0.10 | 6.45 | 31.19 | 9.65 | 23.68 | 64.61 | 3.22 |
| **27** | 0.02 | 9.67 | 4.96 | 43.51 | 26.40 | 13.19 | 0.00 | 0.00 | 15.16 | 45.20 | 39.59 | 1.38 |
| **28** | 6.50 | 9.45 | 5.37 | 27.42 | 24.53 | 13.06 | 0.00 | 0.00 | 34.21 | 28.25 | 37.60 | 1.16 |
| **29** | 13.07 | 16.03 | 3.50 | 23.95 | 16.81 | 0.52 | 0.00 | 0.00 | 58.11 | 24.71 | 17.33 | 0.60 |
| **30** | 0.23 | 13.28 | 2.49 | 28.75 | 25.91 | 19.51 | 0.00 | 0.00 | 17.22 | 35.95 | 46.85 | 1.50 |
| **31** | 0.05 | 5.77 | 1.97 | 61.81 | 19.81 | 4.79 | 0.00 | 0.00 | 9.46 | 65.63 | 24.62 | 1.20 |
| **32** | 6.45 | 7.07 | 3.18 | 37.76 | 13.65 | 16.40 | 0.00 | 0.00 | 29.53 | 40.32 | 30.07 | 1.17 |
| **33** | 6.54 | 5.54 | 2.17 | 32.72 | 9.84 | 3.36 | 3.24 | 15.65 | 27.45 | 36.19 | 35.28 | 1.94 |
| **34** | 0.03 | 7.54 | 3.46 | 52.02 | 31.98 | 0.31 | 0.00 | 0.00 | 13.54 | 53.93 | 32.29 | 1.19 |
| **35** | 4.48 | 13.39 | 2.19 | 38.98 | 4.91 | 0.83 | 3.52 | 3.08 | 20.72 | 61.70 | 15.15 | 1.24 |
| **36** | 0.03 | 9.62 | 3.81 | 45.86 | 11.82 | 26.26 | 0.00 | 0.00 | 13.77 | 48.03 | 38.09 | 1.51 |
| **37** | 0.19 | 6.52 | 2.67 | 36.97 | 4.17 | 0.36 | 22.02 | 14.09 | 10.19 | 41.88 | 47.11 | 2.75 |
| **38** | 0.12 | 13.05 | 3.24 | 50.94 | 16.11 | 13.52 | 0.00 | 0.00 | 17.02 | 53.26 | 29.64 | 1.26 |
| **39** | 0.11 | 8.04 | 3.23 | 41.26 | 7.96 | 13.25 | 11.14 | 7.13 | 11.95 | 44.82 | 42.77 | 2.14 |
| **40** | 6.52 | 9.28 | 3.40 | 38.07 | 4.45 | 0.31 | 11.05 | 7.07 | 32.12 | 41.40 | 26.14 | 1.63 |
| **41** | 4.47 | 10.49 | 2.71 | 13.75 | 8.42 | 26.54 | 3.50 | 3.06 | 18.14 | 35.09 | 44.33 | 1.83 |
| **42** | 12.89 | 9.18 | 4.64 | 13.86 | 8.22 | 25.93 | 0.00 | 0.00 | 51.62 | 14.34 | 34.16 | 1.08 |
| **43** | 0.20 | 3.68 | 2.30 | 10.53 | 7.73 | 25.96 | 6.45 | 31.16 | 7.00 | 13.26 | 77.63 | 3.64 |
| **44** | 6.55 | 6.40 | 3.91 | 12.70 | 7.94 | 25.99 | 11.02 | 7.05 | 29.63 | 14.77 | 55.25 | 2.20 |
| **45** | 0.15 | 3.56 | 2.99 | 11.25 | 7.65 | 25.82 | 21.28 | 15.79 | 7.27 | 14.41 | 77.71 | 3.41 |
| **46** | 13.04 | 6.13 | 2.62 | 3.89 | 0.65 | 0.00 | 6.44 | 31.15 | 47.37 | 6.19 | 44.56 | 2.62 |
| **47** | 0.36 | 0.57 | 1.16 | 1.58 | 0.08 | 0.09 | 28.49 | 45.26 | 3.41 | 7.05 | 86.72 | 4.93 |
| **48** | 0.37 | 0.51 | 2.03 | 2.60 | 0.00 | 0.19 | 44.08 | 28.21 | 4.05 | 8.98 | 85.43 | 4.60 |
| **49** | 8.84 | 9.82 | 4.43 | 20.59 | 35.93 | 1.99 | 0.00 | 0.00 | 40.65 | 21.35 | 37.92 | 0.99 |
| **50** | 8.70 | 7.80 | 3.36 | 10.29 | 17.77 | 1.98 | 4.30 | 20.79 | 37.17 | 12.31 | 49.06 | 2.24 |
| **51** | 11.54 | 10.66 | 2.99 | 10.34 | 7.34 | 13.06 | 2.33 | 2.05 | 42.34 | 28.61 | 27.61 | 1.18 |

| | | | | | | | | | | | | |
|---|---|---|---|---|---|---|---|---|---|---|---|---|
| **52** | 11.67 | 8.78 | 2.70 | 5.60 | 0.89 | 0.43 | 17.04 | 11.46 | 40.39 | 21.63 | 36.00 | 2.08 |
| **53** | 0.14 | 5.64 | 4.14 | 21.34 | 18.70 | 17.41 | 14.76 | 9.45 | 10.59 | 24.18 | 64.68 | 2.64 |
| **54** | 3.24 | 11.73 | 1.72 | 16.74 | 11.32 | 0.78 | 17.03 | 11.45 | 17.78 | 33.32 | 46.78 | 2.43 |
| **55** | 0.31 | 7.14 | 1.21 | 14.30 | 10.95 | 0.38 | 17.75 | 32.30 | 9.88 | 17.76 | 70.77 | 3.73 |
| **56** | 0.15 | 4.16 | 1.38 | 43.25 | 11.52 | 2.39 | 4.30 | 20.79 | 7.90 | 47.25 | 43.23 | 2.48 |
| **57** | 0.09 | 3.82 | 1.99 | 26.68 | 12.86 | 14.92 | 13.45 | 11.52 | 6.84 | 33.98 | 58.91 | 2.67 |
| **58** | 0.27 | 9.27 | 2.22 | 20.59 | 15.99 | 17.67 | 4.30 | 20.77 | 12.74 | 22.90 | 62.94 | 2.79 |
| **59** | 0.27 | 8.84 | 1.59 | 28.60 | 23.38 | 1.83 | 4.39 | 21.23 | 11.93 | 31.49 | 55.13 | 2.58 |
| **60** | 7.01 | 14.72 | 3.16 | 29.73 | 30.00 | 0.54 | 0.00 | 0.00 | 38.87 | 30.67 | 30.54 | 0.92 |
| **61** | 0.20 | 3.51 | 1.75 | 12.52 | 19.00 | 9.54 | 6.43 | 31.06 | 6.71 | 18.23 | 73.03 | 3.43 |
| **62** | 0.28 | 2.81 | 3.05 | 12.22 | 10.24 | 0.19 | 33.07 | 21.16 | 7.17 | 17.30 | 74.37 | 3.75 |
| **63** | 6.41 | 11.59 | 4.42 | 47.75 | 14.74 | 0.31 | 0.00 | 0.00 | 35.20 | 49.79 | 15.05 | 0.80 |
| **64** | 12.89 | 8.32 | 4.50 | 14.45 | 10.74 | 0.10 | 11.21 | 7.18 | 50.87 | 16.40 | 32.52 | 1.51 |
| **65** | 19.39 | 13.83 | 4.23 | 15.60 | 8.99 | 0.26 | 0.00 | 0.00 | 75.00 | 16.00 | 9.25 | 0.35 |
| **66** | 4.57 | 13.76 | 1.79 | 17.87 | 13.72 | 10.33 | 3.50 | 3.07 | 21.14 | 42.37 | 34.13 | 1.53 |
| **67** | 0.05 | 5.83 | 2.63 | 28.00 | 19.25 | 30.16 | 0.00 | 0.00 | 9.56 | 38.86 | 51.57 | 1.73 |
| **68** | 1.93 | 9.14 | 2.71 | 28.72 | 18.87 | 3.51 | 3.89 | 4.87 | 14.37 | 49.73 | 33.69 | 1.61 |
| **69** | 0.23 | 13.18 | 1.98 | 52.68 | 24.85 | 2.32 | 0.00 | 0.00 | 17.33 | 55.28 | 27.18 | 1.12 |
| **70** | 12.88 | 8.78 | 3.44 | 35.91 | 9.17 | 1.80 | 0.00 | 0.00 | 51.21 | 37.79 | 10.98 | 0.62 |
| **71** | 0.12 | 4.70 | 2.28 | 40.24 | 22.94 | 2.42 | 11.05 | 7.07 | 8.87 | 43.83 | 46.74 | 2.09 |
| **72** | 19.38 | 10.41 | 4.80 | 10.50 | 4.64 | 12.80 | 0.00 | 0.00 | 72.03 | 10.76 | 17.44 | 0.58 |
| **73** | 0.05 | 5.96 | 2.94 | 39.23 | 32.50 | 16.36 | 0.00 | 0.00 | 9.61 | 41.40 | 48.87 | 1.56 |
| **74** | 0.28 | 2.16 | 1.30 | 5.55 | 3.95 | 13.00 | 9.66 | 46.72 | 4.89 | 9.19 | 82.81 | 4.45 |
| **75** | 0.05 | 8.79 | 4.24 | 20.86 | 34.66 | 25.44 | 0.00 | 0.00 | 13.81 | 25.06 | 60.83 | 1.73 |
| **76** | 6.64 | 4.85 | 3.34 | 8.23 | 4.11 | 13.06 | 22.01 | 14.09 | 27.89 | 11.66 | 59.75 | 2.83 |
| **77** | 6.61 | 4.90 | 2.46 | 7.19 | 4.18 | 12.95 | 6.46 | 31.20 | 27.16 | 9.72 | 61.12 | 3.14 |
| **78** | 0.28 | 2.09 | 2.16 | 6.55 | 3.86 | 13.05 | 25.21 | 29.78 | 5.52 | 11.11 | 81.54 | 4.13 |
| **79** | 6.72 | 3.39 | 1.46 | 2.22 | 0.41 | 0.00 | 9.66 | 46.69 | 25.14 | 5.65 | 66.22 | 3.93 |
| **80** | 6.55 | 3.20 | 2.39 | 3.30 | 0.40 | 0.09 | 31.26 | 24.35 | 25.18 | 7.09 | 67.12 | 3.61 |

# Appendix H – Validation of calculated FA profiles of calibration set

*Calculated vs reference values for the FA profiles of four randomly picked samples from the calibration set. The deviations of the calculated values from the reference values in percent are included.*

| Sample nr. | | C14:0 | C16:0 | C18:0 | C18:1 n-9 | C18:2 n-6 | C18:3 n-3 | C20:5 n-3 | C22:6 n-3 | ΣSFA | ΣMUFA | ΣPUFA | UI |
|---|---|---|---|---|---|---|---|---|---|---|---|---|---|
| 32 | Predicted | 6,45 | 7,07 | 3,18 | 37,76 | 13,65 | 16,40 | 0 | 0 | 29,53 | 40,32 | 30,07 | 1,17 |
| | Reference | 4,52 | 6,11 | 2,89 | 40,34 | 14,07 | 16,53 | 0 | 0 | 25,72 | 43,28 | 30,60 | 1,21 |
| | Deviation [%] | 42,5 | 15,7 | 10,3 | -6,4 | -3,0 | -0,8 | - | - | 14,8 | -6,8 | -1,7 | -3,7 |
| 54 | Predicted | 3,24 | 11,73 | 1,72 | 16,74 | 11,32 | 0,78 | 17,03 | 11,45 | 17,78 | 33,32 | 46,78 | 2,43 |
| | Reference | 3,02 | 11,69 | 1,65 | 17,92 | 11,95 | 0,80 | 15,10 | 11,51 | 17,31 | 35,60 | 43,07 | 2,31 |
| | Deviation [%] | 7,0 | 0,3 | 4,3 | -6,5 | -5,2 | -2,4 | 12,8 | -0,5 | 2,7 | -6,4 | 8,6 | 5,1 |
| 58 | Predicted | 0,27 | 9,27 | 2,22 | 20,59 | 15,99 | 17,67 | 4,30 | 20,77 | 12,74 | 22,90 | 62,94 | 2,79 |
| | Reference | 0,18 | 9,78 | 2,43 | 22,71 | 16,97 | 18,55 | 2,60 | 19,81 | 13,35 | 24,85 | 60,29 | 2,61 |
| | Deviation [%] | 46,3 | -5,2 | -8,7 | -9,3 | -5,8 | -4,8 | 65,1 | 4,8 | -4,6 | -7,8 | 4,4 | 6,5 |
| 77 | Predicted | 6,61 | 4,90 | 2,46 | 7,19 | 4,18 | 12,95 | 6,46 | 31,20 | 27,16 | 9,72 | 61,12 | 3,14 |
| | Reference | 5,43 | 4,48 | 2,35 | 7,97 | 4,90 | 15,24 | 4,43 | 32,33 | 26,70 | 10,21 | 60,80 | 3,08 |
| | Deviation [%] | 21,8 | 9,4 | 4,7 | -9,7 | -14,6 | -15,1 | 45,8 | -3,5 | 1,8 | -4,8 | 0,5 | 1,9 |

# Appendix I – Data from GC-MS analyses of reference oils

| | Replicate 1 | | Replicate 2 | | Replicate 3 | |
|---|---|---|---|---|---|---|
| FA | RT (min) | MF | RT (min) | MF | RT (min) | MF |
| 18:1(n-9) | 59.60 | 941 | 59.48 | 941 | 59.63 | 940 |
| 18:2(n-6) | 65.52 | 898 | 65.38 | 904 | 65.47 | 903 |
| 10:0 | 12.60 | 834 | 12.55 | 882 | 12.56 | 830 |
| 12:0 | 15.68 | 847 | 15.63 | 809 | 15.63 | 837 |
| 14:0 | 21.65 | 869 | 21.55 | 885 | 21.55 | 871 |
| 15:0 | 26.61 | 838 | 26.49 | 787 | 26.50 | 785 |
| .16:0 | 34.01 | 905 | 33.84 | 923 | 33.88 | 902 |
| 16:1(n-7) | 38.68 | 883 | 38.48 | 875 | 38.50 | 891 |
| 17:0 | 43.96 | 807 | 43.72 | 770 | 43.75 | 783 |
| 18:0 | 55.03 | 924 | 54.88 | 920 | 55.03 | 924 |
| 20:0 | 71.81 | 889 | 71.69 | 889 | 71.73 | 887 |
| 18:3(n-3) | 72.41 | 935 | 72.24 | 939 | 72.32 | 936 |
| 20:1(n-9) | 75.03 | 863 | 74.86 | 882 | 74.93 | 884 |
| 20:2(n-6) | 80.98 | 799 | 80.84 | 783 | 80.88 | 775 |
| 22:0 | 85.78 | 880 | 85.70 | 875 | 85.71 | 887 |
| 22:1(n-11) | 87.72 | 801 | 87.63 | 844 | 87.65 | 844 |
| 24:0 | 93.88 | 843 | 93.81 | 848 | 93.82 | 844 |
| 24:1(n-9) | 94.99 | 809 | 94.06 | 805 | 94.96 | 816 |
| 18:1 u.i. | 59.88 | 907 | 59.74 | 919 | 59.87 | 920 |

*Figure I.1: Data for the various FAs identified in rapeseed oil by analysis with GC-MS. Information for the first three replicates is included. RT = Retention time, MF = Match factor, u.i. = Unidentified isomer.*

| | Replicate 1 | | Replicate 2 | | Replicate 3 | |
|---|---|---|---|---|---|---|
| FA | RT (min) | MF | RT (min) | MF | RT (min) | MF |
| 18:1(n-9) | 59.68 | 942 | 59.63 | 941 | 59.54 | 944 |
| 18:2(n-6) | 65.46 | 897 | 65.36 | 901 | 65.63 | 902 |
| 14:0 | 21.64 | 850 | 21.54 | 844 | 21.56 | 829 |
| 16:0 | 34.06 | 913 | 33.92 | 908 | 33.95 | 901 |
| 16:1(n-7) | 38.65 | 813 | 38.46 | 863 | 38.50 | 845 |
| 17:0 | 43.94 | 804 | 43.74 | 805 | 43.77 | 829 |
| 18:0 | 55.08 | 907 | 55.01 | 916 | 55.00 | 918 |
| 20:0 | 71.82 | 902 | 71.72 | 893 | 71.73 | 890 |
| 18:3(n-3) | 72.20 | 935 | 72.06 | 936 | 72.09 | 926 |
| 20:1(n-9) | 75.09 | 862 | 74.96 | 888 | 74.96 | 881 |
| 22:0 | 85.95 | 909 | 85.87 | 889 | 85.86 | 903 |
| 22:1(n-11) | 87.74 | 851 | 87.65 | 831 | 87.66 | 852 |
| 23:0 | 90.10 | 722 | 90.03 | 756 | 90.04 | 687 |
| 24:0 | 94.00 | 863 | 93.93 | 871 | 93.93 | 875 |
| 18:1 u.i. | 59.85 | 869 | 59.79 | 836 | 59.79 | 894 |

*Figure I.2: Data for the various FAs identified in peanut oil by analysis with GC-MS. Information for the first three replicates is included. RT = Retention time, MF = Match factor, u.i. = Unidentified isomer.*

| | Replicate 1 | | Replicate 2 | | Replicate 3 | |
|---|---|---|---|---|---|---|
| FA | RT (min) | MF | RT (min) | MF | RT (min) | MF |
| 16:0 | 34.12 | 911 | 34.00 | 902 | 34.00 | 908 |
| 18:1(n-9) | 59.36 | 948 | 59.25 | 942 | 59.22 | 948 |
| 18:2(n-6) | 65.36 | 896 | 65.66 | 905 | 65.63 | 901 |
| 12:0 | 15.68 | 799 | 15.63 | 850 | 15.63 | 820 |
| 14:0 | 21.63 | 794 | 21.55 | 828 | 21.55 | 817 |
| 16:1(n-7) | 38.66 | 857 | 38.49 | 872 | 38.49 | 881 |
| 17:0 | 43.93 | 749 | 43.73 | 772 | 43.76 | 739 |
| 18:0 | 55.16 | 934 | 55.08 | 925 | 55.03 | 930 |
| 20:0 | 71.77 | 899 | 71.67 | 904 | 71.66 | 881 |
| 18:3(n-3) | 72.19 | 934 | 72.07 | 930 | 72.06 | 925 |
| 20:1(n-9) | 74.91 | 816 | 74.79 | 837 | 74.80 | 818 |
| 22:0 | 85.75 | 860 | 85.68 | 869 | 85.68 | 872 |
| 24:0 | 93.85 | 778 | 93.79 | 759 | 93.81 | 806 |
| 18:1 u.i. | 59.63 | 899 | 59.51 | 886 | 59.50 | 899 |

*Figure I.3: Data for the various FAs identified in sesame oil by analysis with GC-MS. Information for the first three replicates is included. RT = Retention time, MF = Match factor, u.i. = Unidentified isomer.*

| | Replicate 1 | | Replicate 2 | | Replicate 3 | |
|---|---|---|---|---|---|---|
| RT (min) | MF | RT (min) | MF | RT (min) | MF | RT (min) |
| 16:0 | 34.19 | 908 | 34.07 | 904 | 34.05 | 912 |
| 18:1(n-9) | 59.61 | 944 | 59.65 | 944 | 59.54 | 941 |
| 18:2(n-2) | 65.32 | 904 | 65.21 | 891 | 65.17 | 897 |
| 14:0 | 21.64 | 769 | 21.55 | 834 | 21.56 | 760 |
| 16:1(n-7) | 38.72 | 891 | 38.54 | 890 | 38.56 | 886 |
| 17:0 | 43.93 | 840 | 43.76 | 824 | 43.76 | 829 |
| 18:0 | 55.13 | 922 | 55.12 | 919 | 54.97 | 917 |
| 20:0 | 71.74 | 888 | 71.63 | 892 | 71.63 | 882 |
| 18:3(n-3) | 72.21 | 931 | 72.09 | 939 | 72.07 | 933 |
| 20:1(n-9) | 74.92 | 843 | 74.79 | 826 | 74.80 | 830 |
| 22:0 | 85.75 | 871 | 85.68 | 860 | 85.69 | 858 |
| 24:0 | 93.84 | 763 | 93.79 | 759 | 93.80 | 721 |
| 18:1 u.i. | 59.91 | 916 | 59.87 | 924 | 59.74 | 916 |

*Figure I.4: Data for the various FAs identified in olive oil by analysis with GC-MS. Information for the first three replicates is included. RT = Retention time, MF = Match factor, u.i. = Unidentified isomer.*

| | Replicate 1 | | Replicate 2 | | Replicate 3 | |
|---|---|---|---|---|---|---|
| FA | RT (min) | MF | RT (min) | MF | RT (min) | MF |
| 18:1(n-9) | 59.05 | 941 | 58.90 | 944 | 58.88 | 944 |
| 18:2(n-6) | 65.41 | 895 | 65.28 | 896 | 65.28 | 896 |
| 18:3(n-3) | 72.92 | 934 | 72.83 | 934 | 72.83 | 934 |
| 14:0 | 21.64 | 868 | 21.56 | 863 | 21.56 | 852 |
| 15:0 | 26.60 | 778 | 26.50 | 791 | 26.49 | 792 |
| 16:0 | 34.03 | 915 | 33.90 | 904 | 33.88 | 913 |
| 16:1(n-5) | 38.66 | 849 | 38.49 | 853 | 38.49 | 828 |
| 17:0 | 43.92 | 777 | 43.74 | 801 | 43.77 | 780 |
| 18:0 | 54.96 | 909 | 54.81 | 935 | 54.77 | 925 |
| 20:1(n-9) | 74.91 | 805 | 74.79 | 812 | 74.78 | 792 |
| 22:0 | 85.75 | 838 | 85.67 | 829 | 85.69 | 879 |
| 20:3(n-3) | 86.17 | 753 | 86.09 | 812 | 86.09 | 813 |
| 24:0 | 93.86 | 782 | 93.80 | 782 | 93.80 | 780 |
| 18:1 u.i. | 59.43 | 882 | 59.28 | 888 | 59.27 | 883 |

*Figure I.5: Data for the various FAs identified in flaxseed oil by analysis with GC-MS. Information for the first three replicates is included. RT = Retention time, MF = Match factor, u.i. = Unidentified isomer.*

| | Replicate 1 | | Replicate 2 | | Replicate 3 | |
|---|---|---|---|---|---|---|
| FA | RT (min) | MF | RT (min) | MF | RT (min) | MF |
| 16:0 | 34.17 | 905 | 33.95 | 910 | 34.07 | 906 |
| 18:1(n-9) | 59.10 | 940 | 58.85 | 942 | 59.00 | 942 |
| 18:2(n-6) | 65.89 | 901 | 65.62 | 895 | 65.78 | 895 |
| 14:0 | 21.64 | 846 | 21.54 | 870 | 21.56 | 892 |
| 15:0 | 26.60 | 742 | 26.47 | 694 | 26.50 | 737 |
| 16:1(n-7) | 38.67 | 868 | 38.47 | 823 | 38.53 | 827 |
| 17:0 | 43.94 | 838 | 43.71 | 847 | 43.79 | 837 |
| 18:0 | 55.03 | 930 | 54.77 | 927 | 54.97 | 932 |
| 20:0 | 71.77 | 883 | 71.60 | 845 | 71.70 | 861 |
| 18:3(n-3) | 72.39 | 857 | 72.17 | 863 | 72.27 | 860 |
| 20:1(n-9) | 74.93 | 825 | 74.74 | 814 | 74.81 | 836 |
| 21:0 | 79.81 | 764 | 79.65 | 719 | 79.69 | 790 |
| 20:2(n-6) | 80.97 | 760 | 80.93 | 718 | 80.87 | 740 |
| 22:0 | 85.79 | 874 | 85.67 | 901 | 85.72 | 887 |
| 23:0 | 90.09 | 735 | 90.01 | 681 | 90.04 | 727 |
| 24:0 | 93.86 | 796 | 93.78 | 727 | 93.82 | 819 |
| 18:1 u.i. | 59.50 | 889 | 59.26 | 907 | 59.39 | 902 |

*Figure I.6: Data for the various FAs identified in soybean oil by analysis with GC-MS. Information for the first three replicates is included. RT = Retention time, MF = Match factor, u.i. = Unidentified isomer.*

| | Replicate 1 | | Replicate 2 | | Replicate 3 | |
|---|---|---|---|---|---|---|
| FA | RT (min) | MF | RT (min) | MF | RT (min) | MF |
| 18:1(n-9) | 59.20 | 946 | 59.14 | 941 | 59.10 | 945 |
| 18:2(n-6) | 65.89 | 899 | 65.80 | 906 | 65.80 | 897 |
| 14:0 | 21.63 | 866 | 21.54 | 814 | 21.56 | 847 |
| 15:0 | 26.59 | 734 | 26.50 | 728 | 26.52 | 693 |
| 16:0 | 34.02 | 901 | 33.89 | 898 | 33.91 | 908 |
| 16:1(n-7) | 38.66 | 763 | 38.46 | 822 | 38.49 | 836 |
| 17:0 | 43.92 | 752 | 43.74 | 748 | 43.77 | 752 |
| 18:0 | 55.00 | 927 | 59.94 | 922 | 54.92 | 925 |
| 20:0 | 71.71 | 885 | 71.62 | 874 | 71.62 | 891 |
| 18:3(n-3) | 72.21 | 853 | 72.06 | 879 | 72.08 | 910 |
| 20:1(n-9) | 74.90 | 811 | 74.78 | 808 | 74.78 | 817 |
| 22:0 | 85.81 | 886 | 85.73 | 898 | 85.73 | 885 |
| 24:0 | 93.87 | 826 | 93.81 | 835 | 93.82 | 830 |
| 18:1 u.i. | 59.50 | 886 | 59.41 | 876 | 59.40 | 883 |

*Figure I.7: Data for the various FAs identified in sunflower oil by analysis with GC-MS. Information for the first three replicates is included. RT = Retention time, MF = Match factor, u.i. = Unidentified isomer.*

| | Replicate 1 | | Replicate 2 | | Replicate 3 | |
|---|---|---|---|---|---|---|
| FA | RT (min) | MF | RT (min) | MF | RT (min) | MF |
| 18:1(n-9) | 59.49 | 947 | 59.37 | 947 | 59.37 | 942 |
| 18:2(n-6) | 65.56 | 905 | 65.45 | 901 | 65.45 | 896 |
| 12:0 | 15.67 | 786 | 15.62 | 740 | 15.63 | 748 |
| 14:0 | 21.62 | 843 | 21.53 | 871 | 21.56 | 873 |
| 15:0 | 26.59 | 741 | 26.47 | 786 | 26.51 | 762 |
| 16:0 | 33.99 | 912 | 33.85 | 907 | 33.91 | 908 |
| 16:1(n-7) | 38.62 | 875 | 38.47 | 895 | 38.51 | 876 |
| 17:0 | 43.88 | 743 | 43.71 | 778 | 43.77 | 755 |
| 18:0 | 54.98 | 906 | 54.88 | 920 | 54.92 | 928 |
| 20:0 | 71.74 | 865 | 71.64 | 911 | 71.69 | 893 |
| 18:3(n-3) | 72.32 | 864 | 72.18 | 892 | 72.24 | 865 |
| 20:1(n-9) | 74.93 | 861 | 74.82 | 862 | 74.85 | 856 |
| 22:0 | 85.75 | 884 | 85.69 | 866 | 85.72 | 876 |
| 23:0 | 90.07 | 665 | 90.03 | 647 | 90.04 | 670 |
| 24:0 | 93.84 | 810 | 93.79 | 812 | 93.82 | 793 |
| 24:1(n-9) | 94.98 | 758 | 94.95 | 777 | 94.96 | 791 |
| 18:1 u.i. | 59.76 | 897 | 59.64 | 912 | 59.70 | 907 |

*Figure I.8: Data for the various FAs identified in Vita Hjertegó by analysis with GC-MS. Information for the first three replicates is included. RT = Retention time, MF = Match factor, u.i. = Unidentified isomer.*

| | Replicate 1 | | Replicate 2 | | Replicate 3 | |
|---|---|---|---|---|---|---|
| FA | RT (min) | MF | RT (min) | MF | RT (min) | MF |
| 18:1(n-9) | 59.37 | 946 | 59.34 | 939 | 59.42 | 943 |
| 18:2(n-6) | 65.74 | 900 | 65.64 | 901 | 65.73 | 895 |
| 14:0 | 21.60 | 888 | 21.55 | 838 | 21.56 | 867 |
| 15:0 | 26.55 | 770 | 26.50 | 760 | 26.53 | 772 |
| 16:0 | 33.97 | 912 | 33.88 | 918 | 33.93 | 906 |
| 16:1(n-7) | 38.60 | 860 | 38.46 | 869 | 38.51 | 859 |
| 17:0 | 43.85 | 794 | 43.71 | 789 | 43.77 | 782 |
| 18:0 | 55.03 | 910 | 54.96 | 911 | 55.01 | 922 |
| 20:0 | 71.74 | 902 | 71.66 | 888 | 71.70 | 897 |
| 18:3(n-3) | 72.31 | 860 | 72.21 | 868 | 72.26 | 866 |
| 20:1(n-9) | 74.92 | 856 | 74.83 | 866 | 74.88 | 861 |
| 21:0 | 79.76 | 638 | 79.67 | 662 | 79.70 | 633 |
| 22:0 | 85.77 | 881 | 85.73 | 877 | 85.75 | 858 |
| 22:1(n-11) | 87.68 | 782 | 87.73 | 757 | 87.65 | 751 |
| 24:0 | 93.85 | 825 | 93.81 | 842 | 93.83 | 819 |
| 24:1(n-9) | 94.98 | 739 | 94.96 | 770 | 94.96 | 783 |
| 18:1 u.i. | 59.69 | 906 | 59.63 | 911 | 59.67 | 912 |

*Figure I.9: Data for the various FAs identified in frying oil by analysis with GC-MS. Information for the first three replicates is included. RT = Retention time, MF = Match factor, u.i. = Unidentified isomer.*

| | Replicate 1 | | Replicate 2 | | Replicate 3 | |
|---|---|---|---|---|---|---|
| FA | RT (min) | MF | RT (min) | MF | RT (min) | MF |
| 16:0 | 34.06 | 913 | 34.01 | 901 | 33.98 | 904 |
| 16:1(n-7) | 38.95 | 903 | 38.86 | 905 | 38.85 | 905 |
| 18:1(n-9) | 58.83 | 945 | 58.81 | 940 | 58.73 | 938 |
| 20:1(n-9) | 75.40 | 900 | 75.36 | 901 | 75.31 | 894 |
| 22:6(n-3) | 96.96 | 917 | 96.96 | 921 | 96.95 | 925 |
| 12:0 | 15.66 | 862 | 15.62 | 840 | 15.64 | 837 |
| 13:0 | 18.13 | 748 | 18.07 | 766 | 18.09 | 792 |
| 14:0 | 21.67 | 913 | 21.62 | 905 | 21.63 | 908 |
| 14:1(n-5) | 24.79 | 777 | 24.72 | 798 | 24.74 | 770 |
| 15:0 | 26.57 | 894 | 26.50 | 894 | 26.51 | 886 |
| 18:0 | 54.50 | 916 | 54.58 | 929 | 54.53 | 921 |
| 18:2(n-6) | 64.98 | 879 | 64.94 | 886 | 64.93 | 880 |
| 18:3(n-3) | 72.10 | 848 | 72.04 | 857 | 72.03 | 860 |
| 20:2(n-6) | 80.93 | 863 | 80.87 | 860 | 80.88 | 848 |
| 20:3(n-6) | 84.03 | 647 | 83.98 | 635 | 83.99 | 572 |
| 20:4(n-6) | 86.00 | 844 | 85.95 | 865 | 85.95 | 870 |
| 20:3(n-3) | 86.12 | 827 | 86.08 | 864 | 86.08 | 835 |
| 22:1(n-11) | 87.60 | 900 | 87.60 | 912 | 87.57 | 906 |
| 20:5(n-3) | 90.39 | 918 | 90.37 | 923 | 90.34 | 919 |
| 24:1(n-9) | 95.00 | 844 | 95.00 | 858 | 94.99 | 845 |
| 16:1 u.i. | 36.16 | 786 | 36.06 | 811 | 36.08 | 791 |
| 16:1 u.i. | 36.73 | 809 | 36.63 | 833 | 36.67 | 821 |
| 16:1 u.i. | 37.72 | 884 | 37.61 | 857 | 37.61 | 867 |
| 16:1 u.i. | 40.03 | 862 | 39.92 | 860 | 39.93 | 868 |
| 17:1 u.i. | 48.88 | 870 | 48.77 | 824 | 48.81 | 817 |
| 18:1 u.i. | 57.96 | 905 | 57.95 | 898 | 57.89 | 890 |
| 18:1 u.i. | 59.46 | 915 | 59.42 | 914 | 59.36 | 903 |
| 18:1 u.i. | 60.53 | 887 | 60.45 | 866 | 60.45 | 846 |
| 18:2 u.i. | 66.69 | 825 | 66.62 | 832 | 66.62 | 808 |
| 18:3 u.i. | 69.11 | 825 | 69.04 | 802 | 69.05 | 803 |
| 20:1 u.i. | 74.55 | 865 | 74.52 | 827 | 74.50 | 832 |
| 20:1 u.i. | 75.89 | 831 | 75.84 | 818 | 75.83 | 812 |
| 18:4 u.i. | 76.65 | 901 | 76.59 | 899 | 76.58 | 899 |
| 22:1 u.i. | 87.82 | 818 | 87.82 | 810 | 87.80 | 822 |
| 20:4 u.i. | 88.63 | 897 | 88.60 | 900 | 88.60 | 893 |
| 21:5 u.i. | 94.66 | 896 | 94.65 | 896 | 94.65 | 892 |
| 22:5 u.i. | 96.30 | 912 | 96.29 | 901 | 96.29 | 911 |

*Figure I.10: Data for the various FAs identified in Möller's Tran by analysis with GC-MS. Information for the first three replicates is included. RT = Retention time, MF = Match factor, u.i. = Unidentified isomer.*

| | Replicate 1 | | Replicate 2 | | Replicate 3 | |
|---|---|---|---|---|---|---|
| FA | RT (min) | MF | RT (min) | MF | RT (min) | MF |
| 16:0 | 34.24 | 906 | 34.27 | 898 | 34.18 | 901 |
| 18:1(n-9) | 59.23 | 947 | 59.26 | 945 | 59.18 | 941 |
| 18:2(n-6) | 65.57 | 900 | 65.58 | 925 | 65.51 | 901 |
| 12:0 | 15.65 | 815 | 15.63 | 839 | 15.63 | 845 |
| 14:0 | 21.59 | 890 | 21.56 | 892 | 21.55 | 904 |
| 15:0 | 26.52 | 824 | 26.52 | 807 | 26.49 | 783 |
| 16:1(n-7) | 38.59 | 874 | 38.55 | 884 | 38.51 | 882 |
| 17:0 | 43.80 | 766 | 43.76 | 789 | 43.72 | 784 |
| 18:0 | 54.83 | 917 | 54.84 | 927 | 54.76 | 919 |
| 20:0 | 71.70 | 897 | 71.71 | 891 | 71.66 | 901 |
| 18:3(n-3) | 72.11 | 858 | 72.10 | 862 | 72.08 | 850 |
| 20:1(n-9) | 74.84 | 828 | 74.84 | 861 | 74.81 | 855 |
| 21:0 | 79.68 | 609 | 79.69 | 604 | 79.67 | 571 |
| 22:0 | 85.70 | 888 | 85.70 | 868 | 85.70 | 875 |
| 24:0 | 93.83 | 852 | 93.85 | 859 | 93.85 | 855 |
| 18:1 u.i. | 59.50 | 901 | 59.52 | 902 | 59.44 | 898 |

*Figure I.11: Data for the various FAs identified in rice bran oil by analysis with GC-MS. Information for the first three replicates is included. RT = Retention time, MF = Match factor, u.i. = Unidentified isomer.*

| | Replicate 1 | | Replicate 2 | | Replicate 3 | |
|---|---|---|---|---|---|---|
| FA | RT (min) | MF | RT (min) | MF | RT (min) | MF |
| 16:0 | 34.03 | 899 | 34.02 | 910 | 33.97 | 900 |
| 18:1(n-9) | 59.24 | 945 | 59.27 | 942 | 59.16 | 945 |
| 18:2(n-6) | 65.28 | 896 | 65.30 | 896 | 65.23 | 896 |
| 12:0 | 15.64 | 742 | 15.63 | 807 | 15.63 | 859 |
| 13:0 | 18.09 | 750 | 18.08 | 771 | 18.08 | 751 |
| 14:0 | 21.63 | 897 | 21.60 | 891 | 21.60 | 896 |
| 15:0 | 26.53 | 894 | 26.51 | 878 | 26.50 | 884 |
| 16:1(n-7) | 38.65 | 896 | 38.64 | 893 | 38.62 | 900 |
| 18:0 | 54.81 | 905 | 54.84 | 908 | 54.77 | 907 |
| 20:0 | 71.68 | 769 | 71.70 | 876 | 71.68 | 847 |
| 18:3(n-3) | 72.23 | 871 | 72.20 | 862 | 72.18 | 870 |
| 20:1(n-9) | 75.10 | 859 | 75.10 | 859 | 75.04 | 848 |
| 20:2(n-6) | 80.95 | 886 | 80.94 | 893 | 80.90 | 894 |
| 20:3(n-6) | 84.02 | 831 | 84.00 | 826 | 83.99 | 837 |
| 22:0 | 85.78 | 824 | 85.78 | 838 | 85.78 | 825 |
| 20:4(n-6) | 85.96 | 776 | 85.95 | 744 | 85.95 | 750 |
| 20:3(n-3) | 86.12 | 894 | 86.10 | 835 | 86.10 | 885 |
| 22:1(n-11) | 87.73 | 874 | 87.73 | 867 | 87.72 | 858 |
| 20:5(n-3) | 90.30 | 894 | 90.27 | 899 | 90.26 | 896 |
| 22:2(n-6) | 90.84 | 777 | 90.83 | 697 | 90.83 | 668 |
| 24:1(n-9) | 94.99 | 854 | 94.98 | 863 | 94.98 | 858 |
| 22:6(n-3) | 96.92 | 874 | 96.91 | 876 | 96.91 | 920 |
| 18:1 u.i. | 59.60 | 901 | 59.63 | 917 | 59.54 | 911 |
| 18:1 u.i. | 60.57 | 733 | 60.57 | 712 | 60.51 | 718 |
| 20:1 u.i. | 74.41 | 832 | 74.41 | 781 | 74.36 | 793 |
| 20:1 u.i. | 75.75 | 706 | 75.75 | 693 | 75.73 | 688 |
| 22:1 u.i. | 87.46 | 850 | 87.46 | 844 | 87.45 | 848 |
| 20:4 u.i. | 88.62 | 890 | 88.62 | 854 | 88.58 | 889 |
| 22:5 u.i. | 96.30 | 895 | 96.30 | 921 | 96.28 | 916 |

*Figure I.12: Data for the various FAs identified in salmon oil by analysis with GC-MS. Information for the first three replicates is included. RT = Retention time, MF = Match factor, u.i. = Unidentified isomer.*

| | Replicate 1 | | Replicate 2 | | Replicate 3 | |
|---|---|---|---|---|---|---|
| FA | RT (min) | MF | RT (min) | MF | RT (min) | MF |
| 14:0 | 21.72 | 907 | 21.71 | 908 | 21.71 | 908 |
| 16:0 | 34.12 | 913 | 34.09 | 906 | 34.13 | 905 |
| 20:1(n-9) | 75.38 | 904 | 75.35 | 896 | 75.39 | 901 |
| 22:1(n-11) | 87.87 | 914 | 87.85 | 907 | 87.90 | 908 |
| 10:0 | 12.57 | 730 | 12.56 | 734 | 12.56 | 848 |
| 12:0 | 15.65 | 886 | 15.63 | 884 | 15.64 | 890 |
| 13:0 | 18.10 | 869 | 18.09 | 844 | 18.08 | 891 |
| 15:0 | 26.55 | 912 | 26.51 | 894 | 26.52 | 913 |
| 16:1(n-7) | 38.79 | 899 | 38.74 | 902 | 38.75 | 903 |
| 18:0 | 54.43 | 912 | 54.40 | 925 | 54.42 | 915 |
| 18:1(n-9) | 58.58 | 942 | 58.56 | 937 | 58.59 | 943 |
| 18:2(n-6) | 64.90 | 871 | 64.88 | 877 | 64.89 | 884 |
| 18:3(n-3) | 72.08 | 926 | 72.04 | 938 | 72.05 | 938 |
| 20:2(n-6) | 80.89 | 837 | 80.87 | 855 | 80.88 | 845 |
| 20:3(n-6) | 84.00 | 739 | 83.97 | 699 | 83.99 | 758 |
| 20:3(n-3) | 86.11 | 847 | 86.09 | 841 | 86.11 | 861 |
| 20:5(n-3) | 90.39 | 922 | 90.37 | 924 | 90.38 | 923 |
| 24:1(n-9) | 95.01 | 868 | 95.00 | 868 | 94.65 | 871 |
| 22:6(n-3) | 96.95 | 924 | 96.93 | 923 | 96.94 | 924 |
| 16:1 u.i. | 36.70 | 877 | 36.65 | 876 | 36.66 | 882 |
| 16:1 u.i. | 37.66 | 843 | 37.62 | 840 | 37.63 | 821 |
| 16:1 u.i. | 39.96 | 870 | 39.92 | 871 | 39.93 | 874 |
| 17:1 u.i. | 48.88 | 823 | 48.81 | 816 | 48.80 | 836 |
| 18:1 u.i. | 59.20 | 873 | 59.16 | 901 | 59.19 | 888 |
| 18:1 u.i. | 57.80 | 871 | 57.77 | 875 | 57.77 | 874 |
| 18:1 u.i. | 60.42 | 853 | 60.39 | 853 | 60.40 | 859 |
| 18:2 u.i. | 66.65 | 769 | 66.61 | 799 | 66.60 | 768 |
| 18:3 u.i. | 69.06 | 807 | 69.05 | 808 | 69.05 | 806 |
| 20:1 u.i. | 74.53 | 864 | 74.47 | 843 | 74.46 | 827 |
| 18:4 u.i. | 76.67 | 902 | 76.61 | 905 | 76.64 | 904 |
| 20:4 u.i. | 88.63 | 877 | 88.61 | 885 | 88.61 | 882 |
| 22:5 u.i. | 96.30 | 909 | 96.28 | 910 | 96.29 | 916 |

*Figure I.13: Data for the various FAs identified in herring oil by analysis with GC-MS. Information for the first three replicates is included. RT = Retention time, MF = Match factor, u.i. = Unidentified isomer.*

| | Replicate 1 | | Replicate 2 | | Replicate 3 | |
|---|---|---|---|---|---|---|
| FA | RT (min) | MF | RT (min) | MF | RT (min) | MF |
| 12:0 | 15.81 | 923 | 15.82 | 922 | 15.81 | 923 |
| 14:0 | 21.82 | 906 | 21.82 | 909 | 21.81 | 912 |
| 16:0 | 33.96 | 918 | 33.97 | 910 | 33.95 | 902 |
| 6:0 | 9.06 | 932 | 9.05 | 941 | 9.05 | 936 |
| 8:0 | 10.71 | 917 | 10.71 | 924 | 10.72 | 922 |
| 10:0 | 12.58 | 934 | 12.57 | 938 | 12.58 | 937 |
| 11:0 | 13.87 | 918 | 13.86 | 869 | 13.87 | 838 |
| 13:0 | 18.10 | 901 | 18.09 | 886 | 18.12 | 854 |
| 18:0 | 54.55 | 920 | 54.56 | 933 | 54.57 | 930 |
| 18:1(n-9) | 58.48 | 942 | 58.50 | 943 | 58.48 | 933 |
| 18:2(n-6) | 64.85 | 872 | 64.84 | 881 | 64.86 | 863 |
| 20:0 | 71.54 | 843 | 71.53 | 866 | 71.55 | 808 |
| 18:1 u.i. | 59.08 | 874 | 59.07 | 810 | 59.07 | 651 |

*Figure I.14: Data for the various FAs identified in coconut oil by analysis with GC-MS. Information for the first three replicates is included. RT = Retention time, MF = Match factor, u.i. = Unidentified isomer.*

| | Replicate 1 | | Replicate 2 | | Replicate 3 | |
|---|---|---|---|---|---|---|
| FA | RT (min) | MF | RT (min) | MF | RT (min) | MF |
| 20:5(n-3) | 90.36 | 922 | 90.35 | 914 | 90.37 | 917 |
| 22:6(n-3) | 97.11 | 929 | 97.11 | 933 | 97.11 | 931 |
| 8:0 | 10.70 | 778 | 10.70 | 901 | 10.70 | 909 |
| 10:0 | 12.56 | 643 | 12.55 | 884 | 12.56 | 882 |
| 12:0 | 15.64 | 856 | 15.63 | 907 | 15.65 | 896 |
| 14:0 | 21.56 | 883 | 21.55 | 888 | 21.58 | 880 |
| 16:0 | 33.62 | 893 | 33.58 | 889 | 33.64 | 917 |
| 16:1(n-7) | 38.47 | 853 | 38.44 | 841 | 38.53 | 842 |
| 18:0 | 54.27 | 873 | 54.24 | 861 | 54.30 | 858 |
| 18:1(n-9) | 58.21 | 858 | 58.19 | 890 | 58.28 | 888 |
| 18:2(n-6) | 64.79 | 794 | 64.76 | 806 | 64.81 | 819 |
| 20:0 | 71.57 | 877 | 71.56 | 846 | 71.61 | 833 |
| 20:1(n-9) | 74.77 | 848 | 74.76 | 836 | 74.80 | 840 |
| 21:0 | 79.74 | 777 | 79.74 | 803 | 79.79 | 830 |
| 20:2(n-6) | 80.84 | 795 | 80.82 | 788 | 80.87 | 806 |
| 20:3(n-6) | 83.98 | 766 | 83.95 | 750 | 84.00 | 743 |
| 20:4(n-6) | 85.93 | 775 | 85.92 | 748 | 85.96 | 753 |
| 22:1(n-11) | 87.43 | 877 | 87.44 | 852 | 87.46 | 874 |
| 24:1(n-9) | 95.14 | 854 | 95.14 | 867 | 95.16 | 859 |
| 18:1 u.i. | 59.00 | 766 | 58.97 | 770 | 59.02 | 774 |
| 22:1 u.i. | 87.78 | 757 | 87.77 | 732 | 87.79 | 719 |
| 22:1 u.i. | 88.30 | 845 | 88.29 | 802 | 88.33 | 831 |
| 22:5 u.i. | 96.34 | 900 | 96.34 | 926 | 96.36 | 932 |

*Figure I.15: Data for the various FAs identified in 0370 (cod liver oil enriched in EPA/DHA) by analysis with GC-MS. Information for the first three replicates is included. RT = Retention time, MF = Match factor, u.i. = Unidentified isomer.*

| | Replicate 1 | | Replicate 2 | | Replicate 3 | |
|---|---|---|---|---|---|---|
| FA | RT (min) | MF | RT (min) | MF | RT (min) | MF |
| 20:5(n-3) | 90.59 | 917 | 90.59 | 916 | 90.62 | 921 |
| 22:6(n-3) | 97.03 | 921 | 97.02 | 921 | 97.04 | 927 |
| 12:0 | 15.63 | 746 | 15.63 | 760 | 15.65 | 741 |
| 14:0 | 21.56 | 875 | 21.55 | 866 | 21.58 | 872 |
| 16:0 | 33.60 | 894 | 33.60 | 890 | 33.65 | 891 |
| 16:1(n-7) | 38.48 | 802 | 38.44 | 813 | 38.52 | 802 |
| 18:0 | 54.40 | 915 | 54.43 | 905 | 54.48 | 918 |
| 18:1(n-9) | 58.33 | 919 | 58.33 | 897 | 58.40 | 919 |
| 20:0 | 71.71 | 878 | 71.71 | 876 | 71.78 | 901 |
| 18:3(n-3) | 71.97 | 721 | 71.98 | 771 | 72.05 | 797 |
| 20:1(n-9) | 74.93 | 855 | 74.96 | 866 | 75.01 | 863 |
| 21:0 | 79.81 | 787 | 79.83 | 768 | 79.90 | 746 |
| 20:2(n-6) | 80.87 | 831 | 80.90 | 819 | 80.95 | 826 |
| 20:3(n-6) | 84.00 | 819 | 84.00 | 801 | 84.05 | 805 |
| 20:4(n-6) | 85.98 | 850 | 85.98 | 881 | 86.03 | 886 |
| 20:3(n-3) | 86.11 | 866 | 86.12 | 858 | 86.16 | 857 |
| 22:1(n-11) | 87.54 | 842 | 87.55 | 845 | 87.58 | 840 |
| 24:1(n-9) | 95.05 | 826 | 95.06 | 831 | 95.07 | 835 |
| 18:1 u.i. | 59.07 | 853 | 59.05 | 843 | 59.13 | 864 |
| 18:2 u.i. | 64.79 | 847 | 64.77 | 834 | 64.85 | 830 |
| 20:1 u.i. | 74.35 | 704 | 74.35 | 664 | 74.38 | 708 |
| 20:1 u.i. | 75.74 | 832 | 75.77 | 802 | 75.83 | 802 |
| 20:2 u.i. | 79.29 | 901 | 79.29 | 774 | 79.36 | 797 |
| 22:1 u.i. | 88.41 | 796 | 88.43 | 768 | 88.44 | 767 |
| 20:4 u.i. | 88.63 | 896 | 88.64 | 894 | 88.68 | 900 |
| 22:5 u.i. | 96.32 | 924 | 96.31 | 920 | 96.33 | 928 |

*Figure I.16: Data for the various FAs identified in 4030 (cod liver oil enriched in EPA/DHA) by analysis with GC-MS. Information for the first three replicates is included. RT = Retention time, MF = Match factor, u.i. = Unidentified isomer.*

| | Replicate 1 | | Replicate 2 | | Replicate 3 | |
|---|---|---|---|---|---|---|
| FA | RT (min) | MF | RT (min) | MF | RT (min) | MF |
| 20:5(n-3) | 90.54 | 921 | 90.54 | 925 | 90.62 | 918 |
| 22:6(n-3) | 97.03 | 922 | 97.04 | 922 | 97.07 | 926 |
| 12:0 | 15.69 | 815 | 15.63 | 722 | 15.65 | 679 |
| 14:0 | 21.65 | 870 | 21.54 | 883 | 21.59 | 842 |
| 16:0 | 33.81 | 885 | 33.57 | 868 | 33.67 | 892 |
| 16:1(n-7) | 38.66 | 720 | 38.44 | 744 | 38.54 | 743 |
| 18:0 | 54.51 | 902 | 54.35 | 900 | 54.47 | 904 |
| 18:1(n-9) | 58.39 | 891 | 58.25 | 906 | 58.37 | 906 |
| 18:2(n-6) | 65.04 | 807 | 64.76 | 802 | 64.85 | 772 |
| 20:0 | 71.74 | 868 | 71.64 | 870 | 71.76 | 867 |
| 20:1(n-9) | 74.96 | 837 | 74.85 | 850 | 74.97 | 847 |
| 21:0 | 79.41 | 703 | 79.80 | 744 | 79.91 | 752 |
| 20:2(n-6) | 81.00 | 797 | 80.85 | 791 | 80.95 | 778 |
| 20:3(n-6) | 84.11 | 820 | 83.98 | 758 | 84.06 | 807 |
| 20:4(n-6) | 86.08 | 881 | 85.97 | 886 | 86.03 | 881 |
| 20:3(n-3) | 86.22 | 807 | 86.09 | 829 | 86.14 | 807 |
| 22:1(n-11) | 87.87 | 836 | 87.49 | 848 | 87.59 | 851 |
| 24:1(n-9) | 94.93 | 796 | 95.06 | 839 | 95.11 | 829 |
| 18:1 u.i. | 59.00 | 825 | 59.02 | 821 | 59.14 | 812 |
| 20:1 u.i. | 75.68 | 833 | 75.70 | 775 | 75.82 | 787 |
| 20:2 u.i. | 79.25 | 890 | 79.26 | 794 | 79.39 | 803 |
| 22:1 u.i. | 88.35 | 789 | 88.37 | 755 | 88.46 | 766 |
| 20:4 u.i. | 88.61 | 900 | 88.62 | 888 | 88.68 | 903 |
| 21:5 u.i. | 94.66 | 921 | 94.66 | 918 | 94.69 | 920 |
| 22:5 u.i. | 96.31 | 928 | 96.32 | 846 | 96.35 | 929 |

*Figure I.17: Data for the various FAs identified in 3040 (cod liver oil enriched in EPA/DHA) by analysis with GC-MS. Information for the first three replicates is included. RT = Retention time, MF = Match factor, u.i. = Unidentified isomer.*

| | Replicate 1 | | Replicate 2 | | Replicate 3 | |
|---|---|---|---|---|---|---|
| FA | RT (min) | MF | RT (min) | MF | RT (min) | MF |
| 18:1(n-9) | 58.81 | 943 | 58.81 | 941 | 58.93 | 942 |
| 18:2(n-6) | 65.34 | 900 | 65.33 | 928 | 65.43 | 899 |
| 18:3(n-3) | 72.68 | 937 | 72.67 | 939 | 72.79 | 935 |
| 20:1(n-9) | 75.29 | 895 | 75.30 | 900 | 75.41 | 901 |
| 12:0 | 15.62 | 793 | 15.64 | 611 | 15.65 | 651 |
| 14:0 | 21.54 | 863 | 21.55 | 878 | 21.60 | 874 |
| 15:0 | 26.48 | 719 | 26.49 | 703 | 26.56 | 705 |
| 16:0 | 33.88 | 900 | 33.89 | 908 | 33.96 | 899 |
| 17:0 | 43.71 | 724 | 43.72 | 728 | 43.85 | 753 |
| 18:0 | 54.68 | 911 | 54.70 | 905 | 54.83 | 920 |
| 20:2(n-6) | 80.95 | 904 | 80.95 | 901 | 81.06 | 904 |
| 22:0 | 85.69 | 880 | 85.69 | 819 | 85.79 | 839 |
| 20:3(n-3) | 86.12 | 932 | 86.11 | 923 | 86.20 | 930 |
| 22:1(n-11) | 87.70 | 889 | 87.69 | 887 | 87.77 | 894 |
| 24:0 | 93.80 | 713 | 93.80 | 767 | 93.87 | 793 |
| 24:1(n-9) | 94.96 | 864 | 94.97 | 865 | 95.00 | 869 |
| 18:1 u.i. | 59.23 | 888 | 59.23 | 893 | 59.34 | 876 |

*Figure I.18: Data for the various FAs identified in camelina oil by analysis with GC-MS. Information for the first three replicates is included. RT = Retention time, MF = Match factor, u.i. = Unidentified isomer*

# Appendix J - Data from GC-MS analyses of validation oils

| | Replicate 1 | | Replicate 2 | | Replicate 3 | |
|---|---|---|---|---|---|---|
| FA | RT (min) | MF | RT (min) | MF | RT (min) | MF |
| 14:0 | 20.13 | 864 | 20.09 | 862 | 20.09 | 889 |
| 16:0 | 30.64 | 951 | 30.56 | 947 | 30.61 | 953 |
| 16:1(n-7) | 34.71 | 883 | 34.61 | 856 | 34.61 | 870 |
| 17:0 | 39.10 | 802 | 38.98 | 758 | 39.02 | 784 |
| 18:0 | 50.32 | 959 | 50.23 | 964 | 50.32 | 953 |
| 18:1(n-9) | 54.51 | 943 | 54.40 | 946 | 54.48 | 945 |
| 18:2(n-6) | 61.55 | 946 | 61.47 | 945 | 61.58 | 949 |
| 20:0 | 67.66 | 903 | 67.56 | 882 | 67.57 | 903 |
| 18:3(n-3) | 68.13 | 901 | 68.01 | 900 | 68.03 | 912 |
| 20:1(n-9) | 70.64 | 888 | 70.53 | 883 | 70.54 | 891 |
| 20:2(n-6) | 76.49 | 724 | 76.37 | 656 | 76.36 | 730 |
| 22:0 | 82.54 | 846 | 82.49 | 826 | 82.48 | 856 |
| 24:0 | 91.35 | 684 | 91.35 | 672 | 91.35 | 683 |
| 18:1 u.i. | 55.01 | 935 | 54.89 | 934 | 54.95 | 942 |

*Figure J.1: Data for the various FAs identified in grapeseed oil by analysis with GC-MS. Information for all three replicates is included. RT = Retention time, MF = Match factor, u.i. = Unidentified isomer.*

| | Replicate 1 | | Replicate 2 | | Replicate 3 | |
|---|---|---|---|---|---|---|
| FA | RT (min) | MF | RT (min) | MF | RT (min) | MF |
| 14:0 | 20.10 | 873 | 20.10 | 798 | 20.08 | 846 |
| 15:0 | 24.35 | 695 | 24.34 | 549 | 24.33 | 618 |
| 16:0 | 30.53 | 948 | 30.46 | 949 | 30.48 | 948 |
| 16:1(n-7) | 34.64 | 867 | 34.61 | 790 | 34.59 | 829 |
| 17:0 | 39.01 | 722 | 39.00 | 598 | 38.96 | 698 |
| 18:0 | 50.36 | 953 | 50.12 | 957 | 50.24 | 962 |
| 18:1(n-9) | 55.12 | 949 | 54.80 | 935 | 54.98 | 949 |
| 18:2(n-6) | 60.99 | 947 | 60.86 | 947 | 60.90 | 948 |
| 20:0 | 67.59 | 932 | 67.54 | 886 | 67.55 | 924 |
| 18:3(n-3) | 68.05 | 900 | 68.00 | 857 | 68.00 | 852 |
| 20:1(n-9) | 70.58 | 906 | 70.52 | 871 | 70.52 | 882 |
| 22:0 | 82.52 | 928 | 82.47 | 922 | 82.46 | 936 |
| 23:0 | 87.42 | 619 | 87.42 | 713 | 87.41 | 683 |
| 24:0 | 91.31 | 900 | 91.31 | 889 | 91.30 | 889 |
| 18:1 u.i. | 55.32 | 946 | 55.07 | 925 | 55.21 | 939 |

*Figure J.2: Data for the various FAs identified in frying oil (Coop) by analysis with GC-MS. Information for all three replicates is included. RT = Retention time, MF = Match factor, u.i. = Unidentified isomer.*

| | Replicate 1 | | Replicate 2 | | Replicate 3 | |
|---|---|---|---|---|---|---|
| FA | RT (min) | MF | RT (min) | MF | RT (min) | MF |
| 14:0 | 20.08 | 812 | 20.08 | 912 | 20.08 | 803 |
| 15:0 | 24.33 | 684 | 24.32 | 668 | 24.30 | 647 |
| 16:0 | 30.57 | 944 | 30.58 | 947 | 30.55 | 950 |
| 16:1(n-7) | 34.62 | 811 | 34.60 | 836 | 34.59 | 795 |
| 17:0 | 39.01 | 772 | 39.00 | 747 | 38.94 | 748 |
| 18:0 | 50.13 | 958 | 50.15 | 958 | 50.11 | 959 |
| 18:1(n-9) | 54.28 | 946 | 54.32 | 943 | 54.27 | 941 |
| 18:2(n-6) | 61.35 | 952 | 61.44 | 951 | 61.36 | 948 |
| 20:0 | 67.65 | 849 | 67.66 | 852 | 67.62 | 852 |
| 18:3(n-3) | 68.25 | 941 | 68.25 | 943 | 68.21 | 944 |
| 20:1(n-9) | 70.55 | 882 | 70.54 | 883 | 70.51 | 876 |
| 22:0 | 82.50 | 684 | 82.50 | 697 | 82.48 | 665 |
| 18:1 u.i. | 54.87 | 931 | 54.88 | 937 | 54.84 | 933 |

*Figure J.3: Data for the various FAs identified in walnut oil by analysis with GC-MS. Information for all three replicates is included. RT = Retention time, MF = Match factor, u.i. = Unidentified isomer.*

| | Replicate 1 | | Replicate 2 | | Replicate 3 | |
|---|---|---|---|---|---|---|
| FA | RT (min) | MF | RT (min) | MF | RT (min) | MF |
| 14:0 | 20.09 | 871 | 20.08 | 871 | 20.09 | 877 |
| 15:0 | 24.33 | 654 | 24.32 | 680 | 24.32 | 664 |
| 16:0 | 30.50 | 961 | 30.51 | 950 | 30.49 | 950 |
| 16:1(n-7) | 34.61 | 858 | 34.59 | 849 | 34.59 | 852 |
| 17:0 | 38.97 | 663 | 38.99 | 661 | 38.98 | 668 |
| 18:0 | 50.09 | 962 | 50.10 | 946 | 50.06 | 945 |
| 18:1(n-9) | 54.56 | 946 | 54.59 | 950 | 54.56 | 944 |
| 18:2(n-6) | 61.15 | 950 | 61.16 | 946 | 61.13 | 950 |
| 20:0 | 67.56 | 911 | 67.55 | 906 | 67.54 | 920 |
| 18:3(n-3) | 68.06 | 943 | 68.05 | 947 | 68.03 | 939 |
| 20:1(n-9) | 70.55 | 928 | 70.52 | 922 | 70.52 | 926 |
| 22:0 | 82.47 | 909 | 82.46 | 909 | 82.45 | 914 |
| 22:1(n-9) | 84.58 | 791 | 84.58 | 796 | 84.56 | 818 |
| 23:0 | 87.42 | 603 | 87.42 | 630 | 87.42 | 622 |
| 24:0 | 91.31 | 803 | 91.30 | 841 | 91.30 | 825 |
| 24:1(n-9) | 92.80 | 699 | 92.80 | 722 | 92.79 | 719 |
| 18:1 u.i. | 54.97 | 955 | 54.99 | 951 | 54.95 | 944 |

*Figure J.4: Data for the various FAs identified in cooking oil by analysis with GC-MS. Information for all three replicates is included. RT = Retention time, MF = Match factor, u.i. = Unidentified isomer.*

| | Replicate 1 | | Replicate 2 | | Replicate 3 | |
|---|---|---|---|---|---|---|
| FA | RT (min) | MF | RT (min) | MF | RT (min) | MF |
| 6:0 | 8.93 | 857 | 8.92 | 896 | 8.93 | 905 |
| 8:0 | 10.54 | 931 | 10.54 | 936 | 10.54 | 930 |
| 10:0 | 12.24 | 952 | 12.23 | 944 | 12.23 | 948 |
| 12:0 | 14.97 | 958 | 14.97 | 953 | 14.96 | 950 |
| 14:0 | 20.11 | 951 | 20.11 | 953 | 20.11 | 953 |
| 16:0 | 30.52 | 945 | 30.51 | 947 | 30.54 | 949 |
| 16:1(n-7) | 34.62 | 843 | 34.59 | 859 | 34.59 | 851 |
| 17:0 | 38.99 | 688 | 38.97 | 700 | 38.98 | 719 |
| 18:0 | 50.08 | 961 | 50.05 | 951 | 50.11 | 953 |
| 18:1(n-9) | 54.55 | 949 | 54.54 | 947 | 54.61 | 944 |
| 18:2(n-6) | 60.92 | 945 | 60.89 | 948 | 60.93 | 955 |
| 20:0 | 67.66 | 930 | 67.65 | 926 | 67.65 | 929 |
| 18:3(n-3) | 68.25 | 942 | 68.23 | 949 | 68.24 | 946 |
| 20:1(n-9) | 70.54 | 925 | 70.53 | 923 | 70.52 | 921 |
| 22:0 | 82.45 | 882 | 82.45 | 887 | 82.44 | 894 |
| 22:1(n-9) | 84.60 | 788 | 84.58 | 811 | 84.56 | 814 |
| 24:0 | 91.31 | 794 | 91.32 | 786 | 91.31 | 793 |
| 24:1(n-9) | 92.81 | 699 | 92.81 | 721 | 92.79 | 731 |

*Figure J.5: Data for the various FAs identified in sample nr. 32 of the calibration set by analysis with GC-MS. Information for all three replicates is included. RT = Retention time, MF = Match factor, u.i. = Unidentified isomer.*

| | Replicate 1 | | Replicate 2 | | Replicate 3 | |
|---|---|---|---|---|---|---|
| FA | RT (min) | MF | RT (min) | MF | RT (min) | MF |
| 12:0 | 14.96 | 870 | 14.95 | 848 | 14.95 | 869 |
| 14:0 | 20.10 | 954 | 20.09 | 949 | 20.10 | 955 |
| 15:0 | 24.33 | 913 | 24.32 | 900 | 24.31 | 923 |
| 16:0 | 30.63 | 950 | 30.60 | 951 | 30.61 | 941 |
| 16:1(n-7) | 34.67 | 916 | 34.65 | 940 | 34.64 | 941 |
| 18:0 | 49.96 | 950 | 49.93 | 953 | 49.93 | 945 |
| 18:1(n-9) | 54.30 | 946 | 54.25 | 944 | 54.27 | 947 |
| 18:2(n-6) | 60.89 | 946 | 60.94 | 797 | 60.87 | 945 |
| 20:0 | 67.59 | 929 | 67.58 | 920 | 67.57 | 936 |
| 18:3(n-3) | 67.99 | 932 | 67.98 | 932 | 67.97 | 931 |
| 20:1(n-9) | 70.69 | 944 | 70.65 | 944 | 70.66 | 941 |
| 20:2(n-6) | 76.34 | 858 | 76.31 | 856 | 76.29 | 882 |
| 20:3(n-6) | 80.27 | 821 | 80.24 | 833 | 80.25 | 841 |
| 20:4(n-6) | 82.63 | 906 | 82.60 | 907 | 82.60 | 894 |
| 20:3(n-3) | 82.73 | 825 | 82.72 | 817 | 82.73 | 822 |
| 22:1(n-9) | 84.43 | 949 | 84.38 | 949 | 84.40 | 942 |
| 20:5(n-3) | 87.65 | 962 | 87.62 | 953 | 87.63 | 954 |
| 24:0 | 91.30 | 669 | 91.29 | 655 | 91.29 | 661 |
| 24:1(n-9) | 92.81 | 879 | 92.79 | 875 | 92.79 | 886 |
| 22:6(n-3) | 95.75 | 961 | 95.74 | 956 | 95.75 | 957 |

*Figure J.6: Data for the various FAs identified in sample nr. 54 of the calibration set by analysis with GC-MS. Information for all three replicates is included. RT = Retention time, MF = Match factor, u.i. = Unidentified isomer.*

| | Replicate 1 | | Replicate 2 | | Replicate 3 | |
|---|---|---|---|---|---|---|
| FA | RT (min) | MF | RT (min) | MF | RT (min) | MF |
| 14:0 | 20.09 | 932 | 20.08 | 938 | 20.08 | 921 |
| 15:0 | 24.33 | 672 | 24.32 | 681 | 24.32 | 679 |
| 16:0 | 30.62 | 948 | 30.59 | 950 | 30.57 | 950 |
| 16:1(n-7) | 34.62 | 863 | 34.61 | 858 | 34.60 | 876 |
| 17:0 | 38.99 | 714 | 38.98 | 692 | 38.97 | 682 |
| 18:0 | 50.06 | 948 | 50.02 | 956 | 49.99 | 958 |
| 18:1(n-9) | 54.43 | 944 | 54.35 | 947 | 54.33 | 947 |
| 18:2(n-6) | 60.98 | 947 | 60.95 | 946 | 60.94 | 948 |
| 20:0 | 67.70 | 928 | 67.67 | 929 | 67.66 | 938 |
| 18:3(n-3) | 68.29 | 946 | 68.25 | 946 | 68.25 | 943 |
| 20:1(n-9) | 70.50 | 922 | 70.50 | 916 | 70.50 | 905 |
| 21:0 | 75.11 | 655 | 75.10 | 687 | 75.09 | 657 |
| 20:2(n-6) | 76.32 | 756 | 76.32 | 753 | 76.31 | 733 |
| 20:3(n-6) | 80.26 | 704 | 80.27 | 701 | 80.25 | 699 |
| 22:0 | 82.49 | 902 | 82.47 | 896 | 82.48 | 900 |
| 20:4(n-6) | 82.58 | 844 | 82.57 | 758 | 82.58 | 789 |
| 20:3(n-3) | 82.73 | 729 | 82.69 | 709 | 82.69 | 684 |
| 22:1(n-9) | 84.61 | 866 | 84.59 | 856 | 84.70 | 837 |
| 20:5(n-3) | 87.54 | 955 | 87.52 | 949 | 87.52 | 956 |
| 24:0 | 91.32 | 760 | 91.31 | 728 | 91.31 | 741 |
| 24:1(n-9) | 92.82 | 878 | 92.82 | 882 | 92.81 | 882 |
| 22:6(n-3) | 95.79 | 917 | 95.77 | 953 | 95.77 | 957 |

*Figure J.7: Data for the various FAs identified in sample nr. 58 of the calibration set by analysis with GC-MS. Information for all three replicates is included. RT = Retention time, MF = Match factor, u.i. = Unidentified isomer.*

| | Replicate 1 | | Replicate 2 | | Replicate 3 | |
|---|---|---|---|---|---|---|
| FA | RT (min) | MF | RT (min) | MF | RT (min) | MF |
| 6:0 | 8.93 | 913 | 8.93 | 882 | 8.92 | 880 |
| 8:0 | 10.54 | 934 | 10.54 | 938 | 10.54 | 931 |
| 10:0 | 12.23 | 943 | 12.23 | 947 | 12.23 | 952 |
| 12:0 | 14.97 | 956 | 14.96 | 947 | 14.96 | 952 |
| 13:0 | 17.07 | 618 | 17.07 | 619 | 17.06 | 616 |
| 14:0 | 20:12 | 946 | 20.11 | 951 | 20.11 | 950 |
| 16:0 | 30.47 | 953 | 30.44 | 952 | 30.46 | 945 |
| 16:1(n-7) | 34.61 | 807 | 34.61 | 786 | 34.58 | 818 |
| 18:0 | 49.92 | 951 | 49.89 | 956 | 49.89 | 956 |
| 18:1(n-9) | 54.07 | 940 | 54.02 | 940 | 54.03 | 939 |
| 18:2(n-6) | 60.72 | 944 | 60.68 | 945 | 60.70 | 945 |
| 20:0 | 67.59 | 882 | 67.57 | 911 | 67.58 | 906 |
| 18:3(n-3) | 68.21 | 947 | 68.16 | 946 | 68.16 | 946 |
| 20:1(n-9) | 70.48 | 892 | 70.48 | 887 | 70.46 | 920 |
| 21:0 | 75.10 | 678 | 75.10 | 681 | 75.10 | 705 |
| 20:2(n-6) | 76.29 | 757 | 76.30 | 736 | 76.28 | 766 |
| 20:3(n-6) | 80.24 | 725 | 80.24 | 717 | --[a] | --[a] |
| 22:0 | 82.50 | 892 | 82.48 | 866 | --[a] | --[a] |
| 20:4 | 82.56 | 832 | 82.59 | 838 | --[a] | --[a] |
| 22:1(n-9) | 84.62 | 828 | 84.60 | 856 | 84.62 | 819 |
| 20:5(n-3) | 87.53 | 963 | 87.52 | 953 | 87.52 | 958 |
| 24:1(n-9) | 92.83 | 904 | 92.83 | 888 | 92.82 | 896 |
| 22:6(n-3) | 95.80 | 887 | 95.79 | 956 | 95.79 | 955 |

[a] = Replicate could not be used due to poor separation of the peaks in the chromatogram.

*Figure J.8: Data for the various FAs identified in sample nr. 77 of the calibration set by analysis with GC-MS. Information for all three replicates is included. RT = Retention time, MF = Match factor, u.i. = Unidentified isomer.*

# Appendix K – PLSR based on FTIR

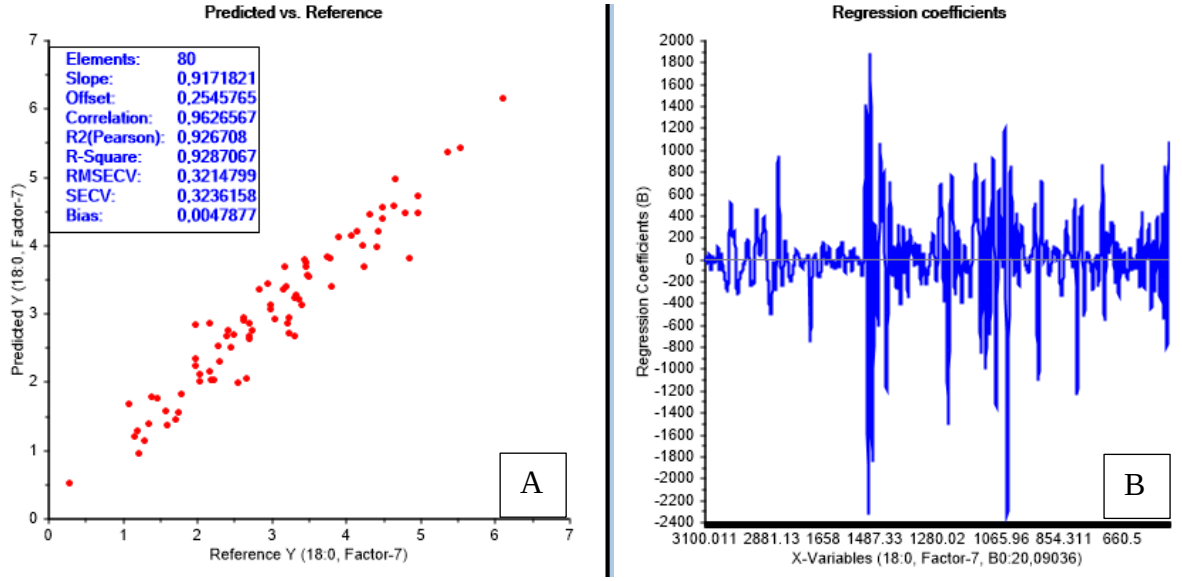


*Figure K.1: Predicted vs. reference values (A) and regression coefficients (B) for the calibration model obtained with C18:0 as response variable. The model was made using PLSR and was based on data from analysis of the calibration set with FTIR spectroscopy.*

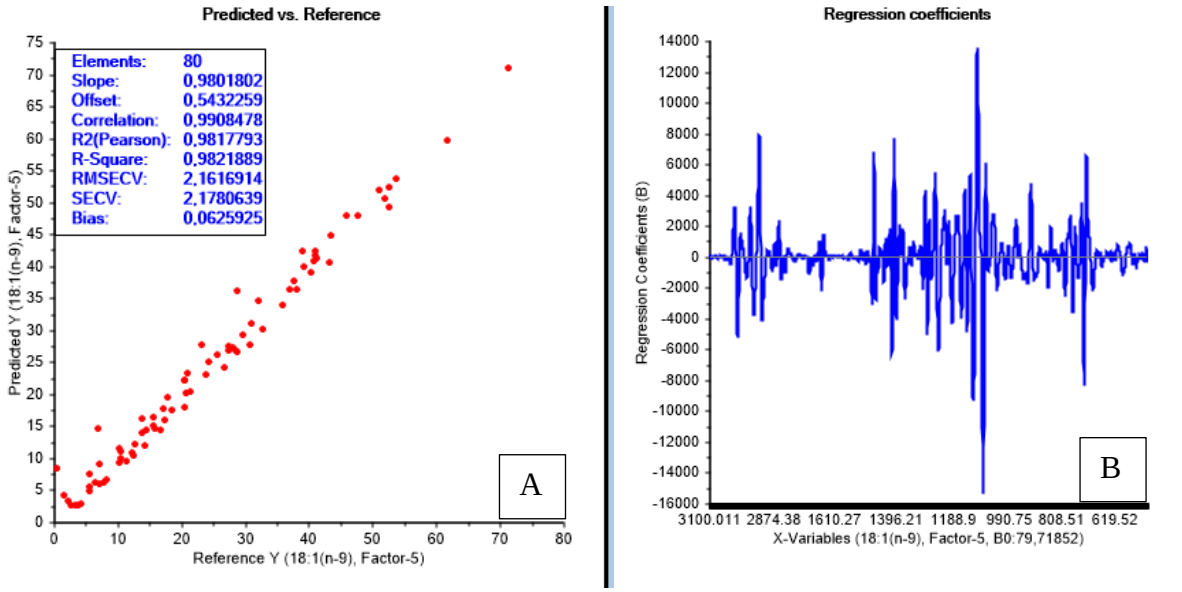


*Figure K.2: Predicted vs. reference values (A) and regression coefficients (B) for the calibration model obtained with C18:1n-9 as response variable. The model was made using PLSR and was based on data from analysis of the calibration set with FTIR spectroscopy.*

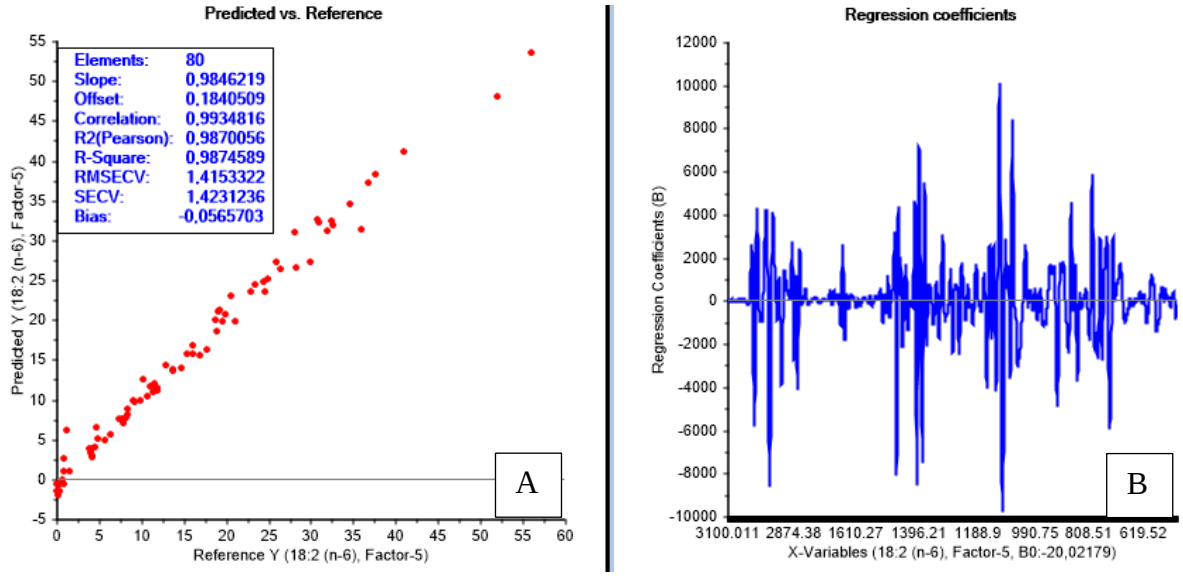


*Figure K.3: Predicted vs. reference values (A) and regression coefficients (B) for the calibration model obtained with C18:2n-6 as response variable. The model was made using PLSR and was based on data from analysis of the calibration set with FTIR spectroscopy.*

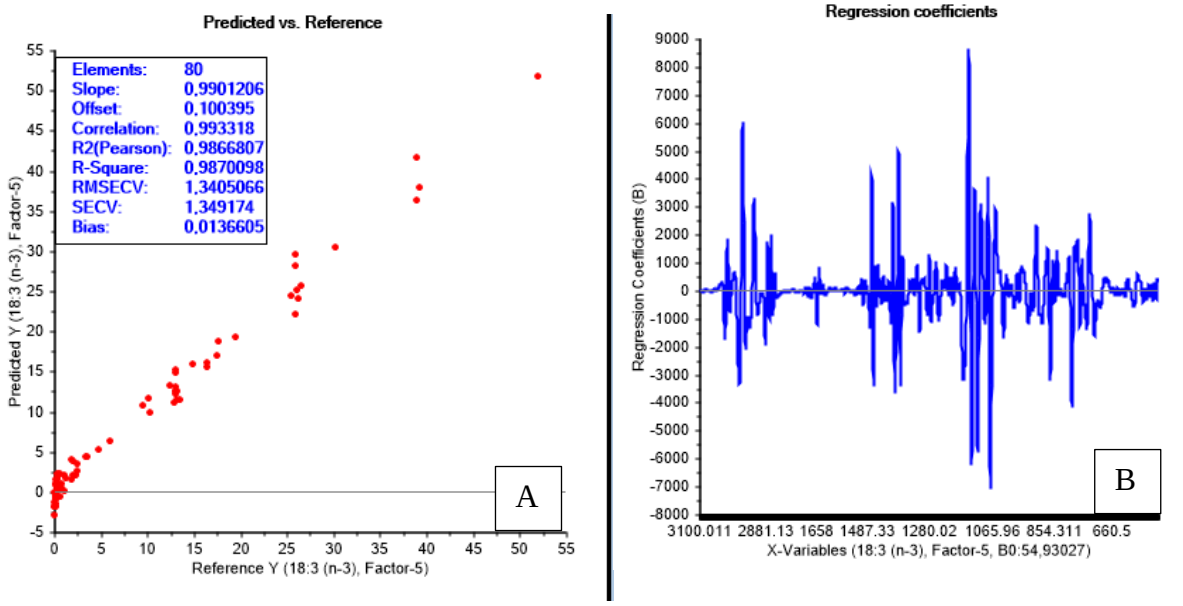


*Figure K.4: Predicted vs. reference values (A) and regression coefficients (B) for the calibration model obtained with C18:3n-3 as response variable. The model was made using PLSR and was based on data from analysis of the calibration set with FTIR spectroscopy.*

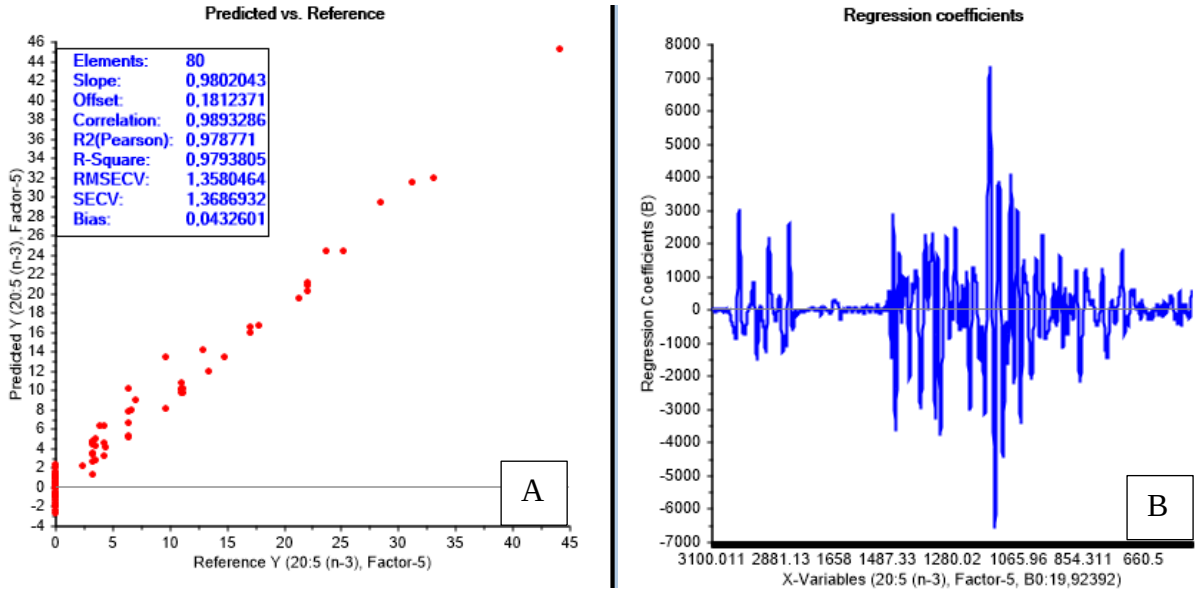


*Figure K.5: Predicted vs. reference values (A) and regression coefficients (B) for the calibration model obtained with C20:5n-3 as response variable. The model was made using PLSR and was based on data from analysis of the calibration set with FTIR spectroscopy.*

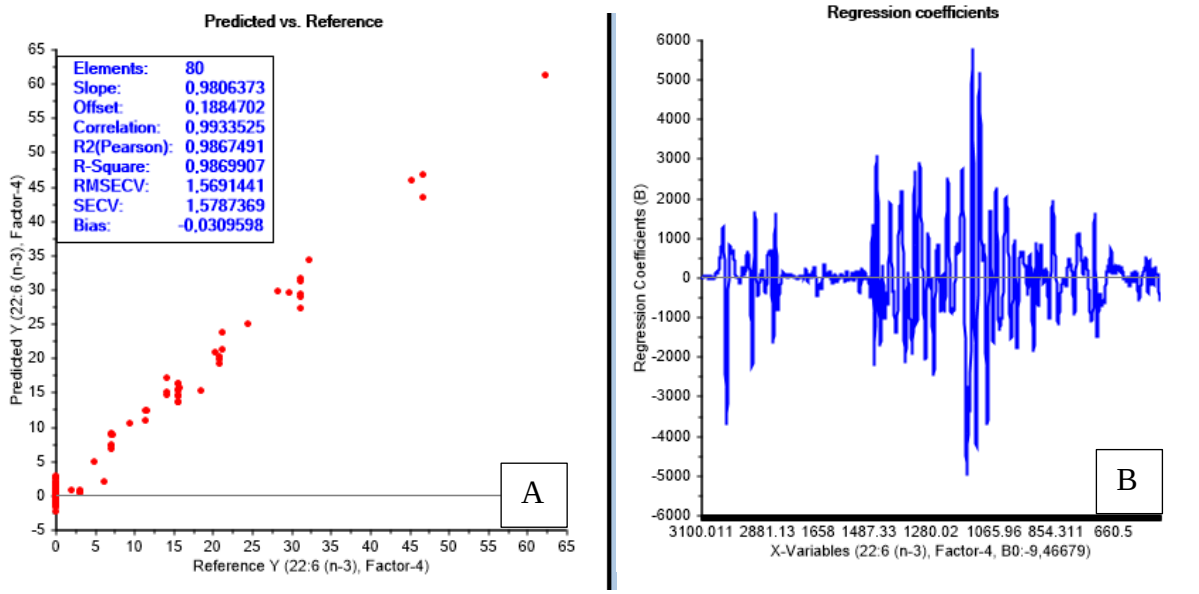


*Figure K.6: Predicted vs. reference values (A) and regression coefficients (B) for the calibration model obtained with C22:6n-3 as response variable. The model was made using PLSR and was based on data from analysis of the calibration set with FTIR spectroscopy.*

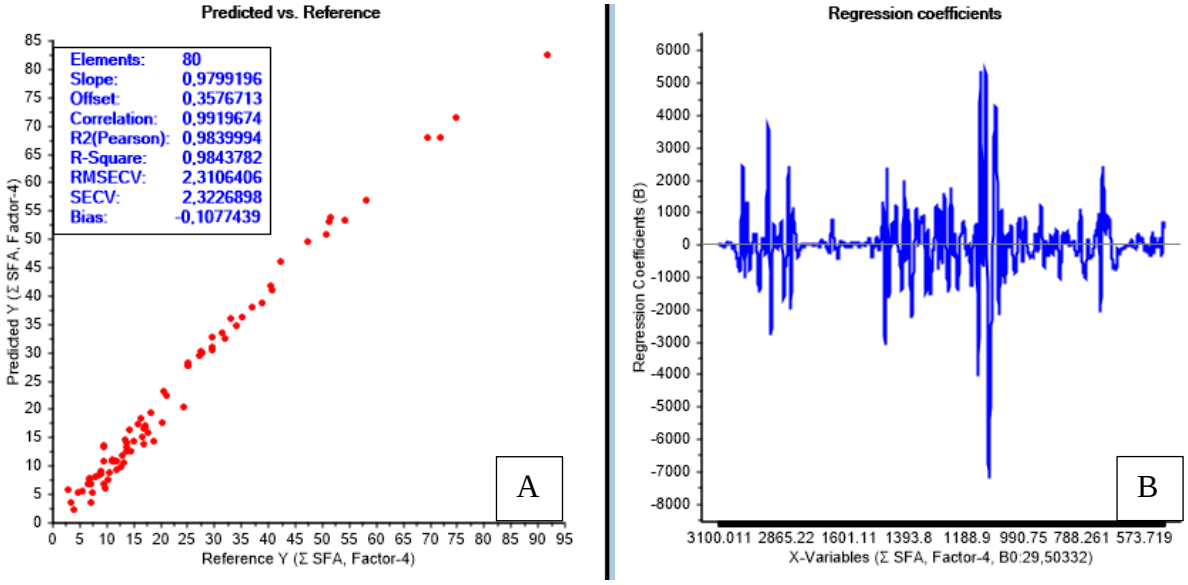


*Figure K.7: Predicted vs. reference values (A) and regression coefficients (B) for the calibration model obtained with ΣSFA as response variable. The model was made using PLSR and was based on data from analysis of the calibration set with Raman spectroscopy.*

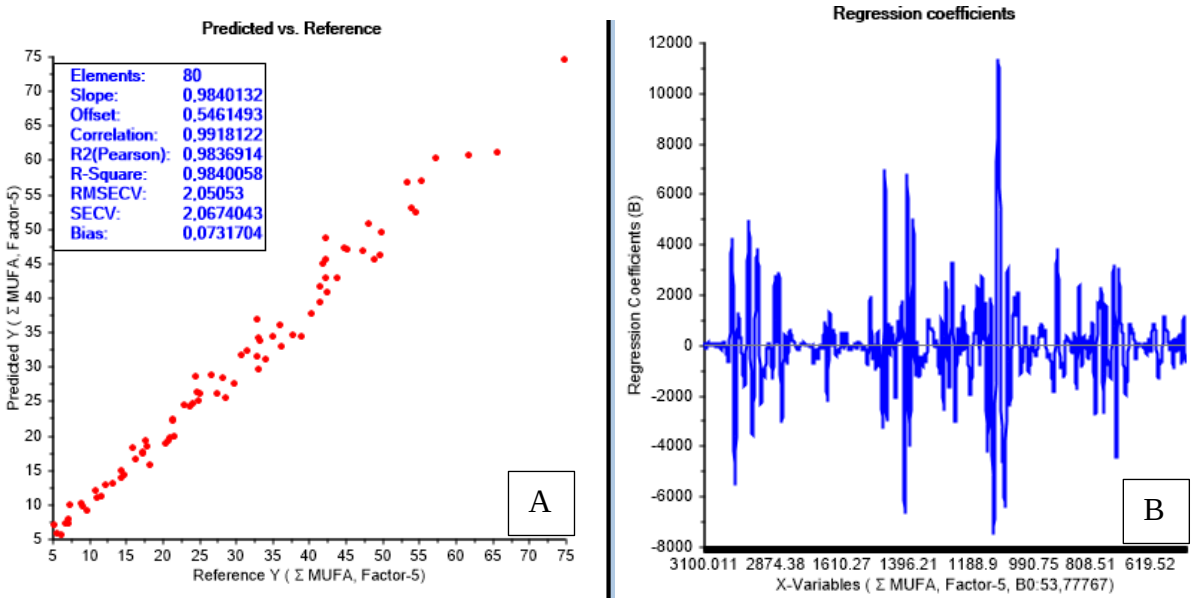


*Figure K.8: Predicted vs. reference values (A) and regression coefficients (B) for the calibration model obtained with ΣMUFA as response variable. The model was made using PLSR and was based on data from analysis of the calibration set with FTIR spectroscopy.*

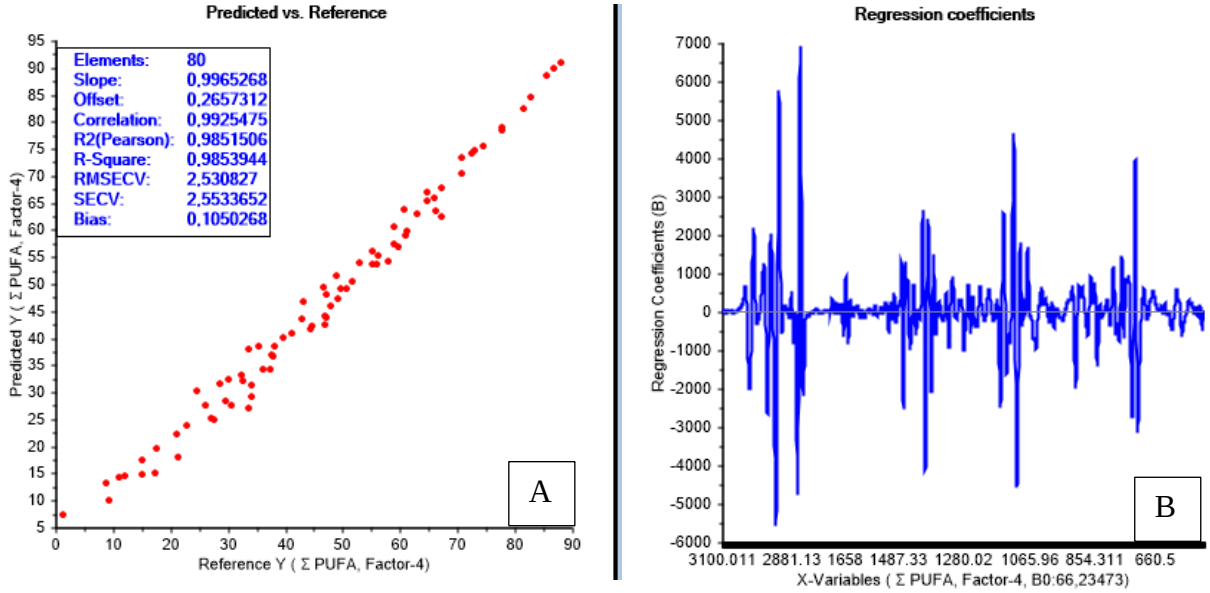


*Figure K.9: Predicted vs. reference values (A) and regression coefficients (B) for the calibration model obtained with ΣPUFA as response variable. The model was made using PLSR and was based on data from analysis of the calibration set with FTIR spectroscopy.*

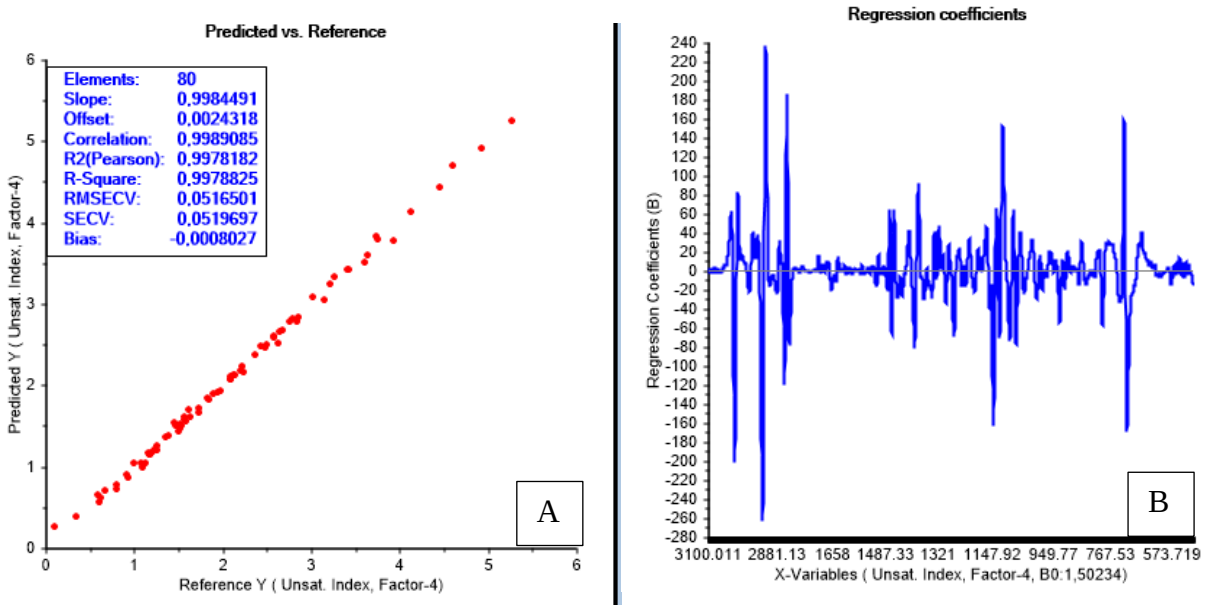


*Figure K.10: Predicted vs. reference values (A) and regression coefficients (B) for the calibration model obtained with UI 1 as response variable. The model was made using PLSR and was based on data from analysis of the calibration set with FTIR spectroscopy.*

# Appendix L – PLSR based on Raman

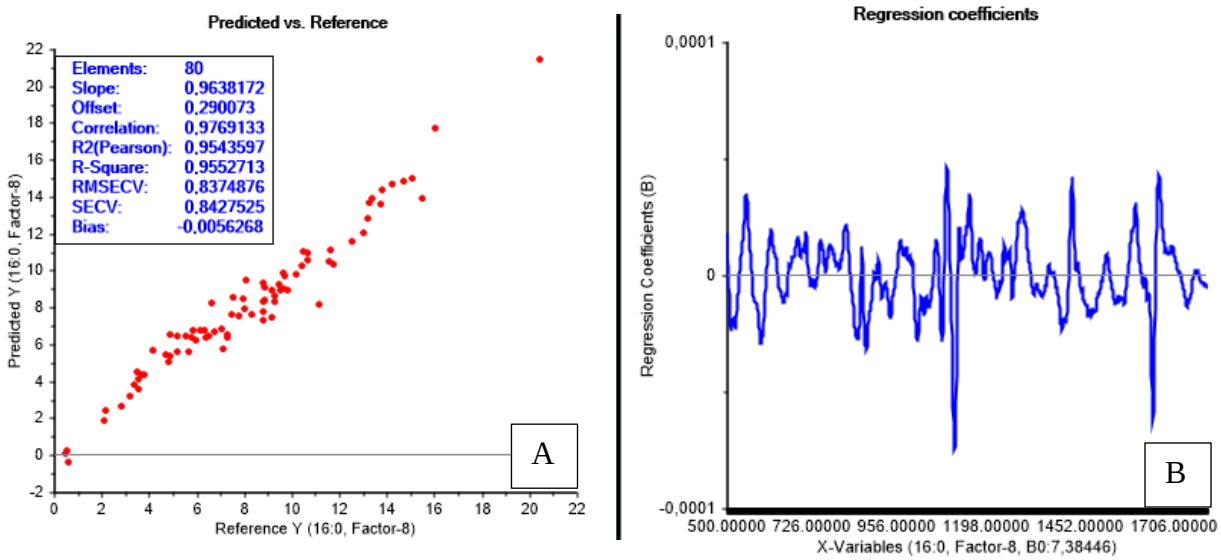


*Figure L.1: Predicted vs. reference values (A) and regression coefficients (B) for the calibration model obtained with C16:0 as response variable. The model was made using PLSR and was based on data from analysis of the calibration set with Raman spectroscopy*

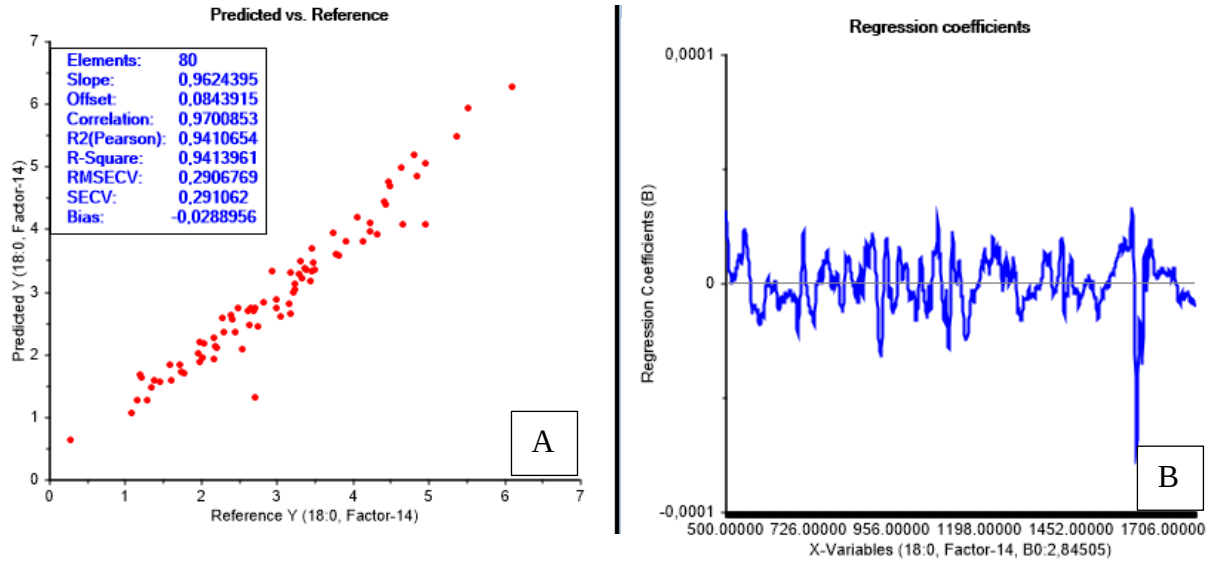


*Figure L.2: Predicted vs. reference values (A) and regression coefficients (B) for the calibration model obtained with C18:0 as response variable. The model was made using PLSR and was based on data from analysis of the calibration set with Raman spectroscopy.*

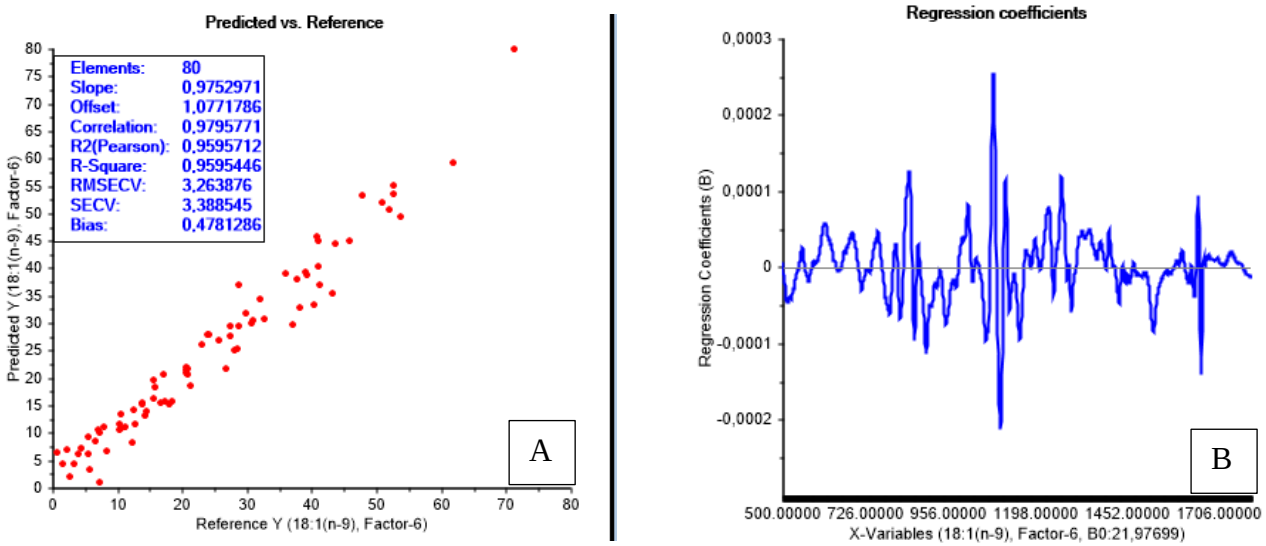


*Figure L.3: Predicted vs. reference values (A) and regression coefficients (B) for the calibration model obtained with C18:1n-9 as response variable. The model was made using PLSR and was based on data from analysis of the calibration set with Raman spectroscopy.*

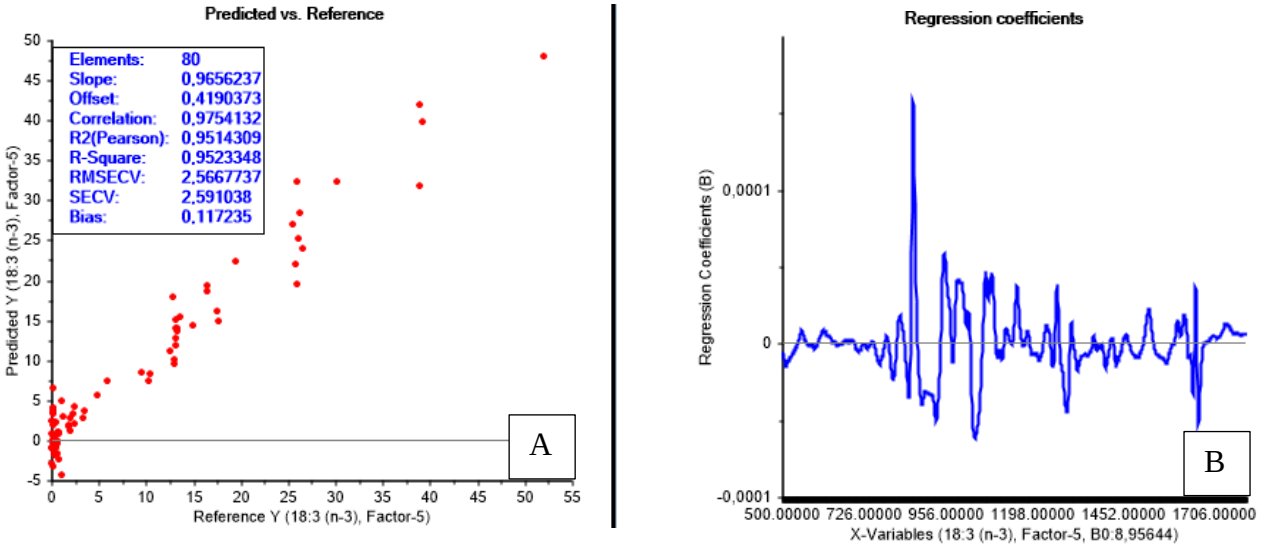


*Figure L.4: Predicted vs. reference values (A) and regression coefficients (B) for the calibration model obtained with C18:3n-3 as response variable. The model was made using PLSR and was based on data from analysis of the calibration set with Raman spectroscopy.*

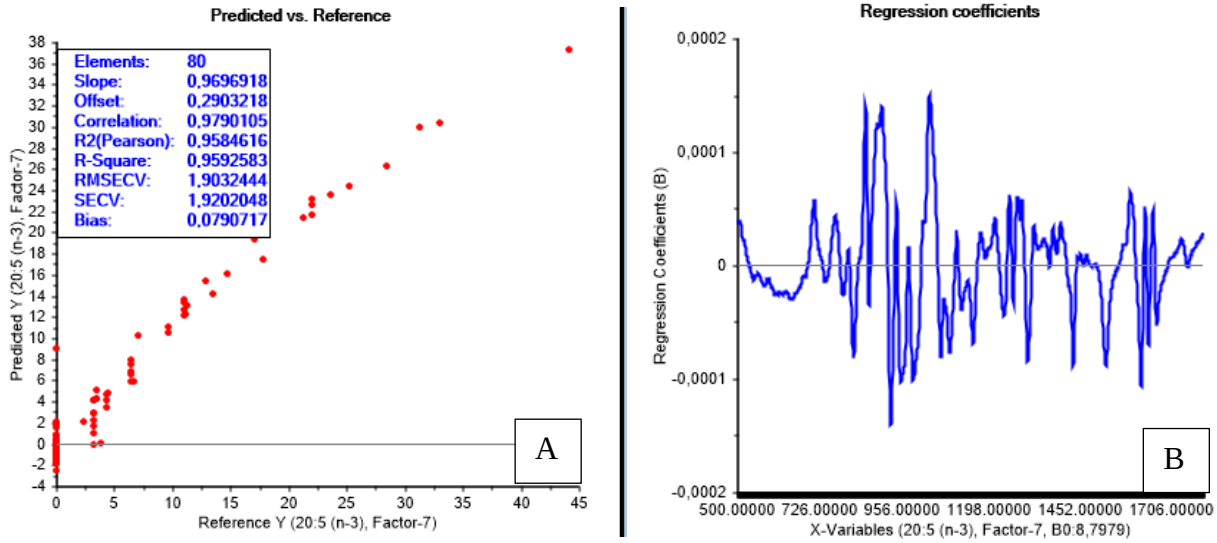


*Figure L.5: Predicted vs. reference values (A) and regression coefficients (B) for the calibration model obtained with C20:5n-3 as response variable. The model was made using PLSR and was based on data from analysis of the calibration set with Raman spectroscopy.*

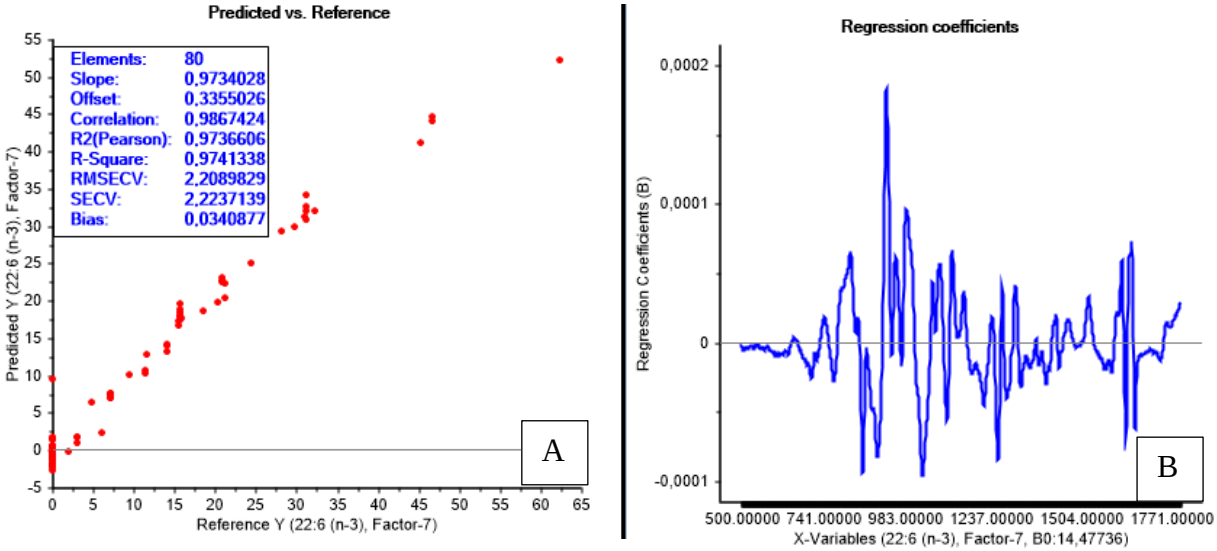


*Figure L.6: Predicted vs. reference values (A) and regression coefficients (B) for the calibration model obtained with C22:6n-3 as response variable. The model was made using PLSR and was based on data from analysis of the calibration set with Raman spectroscopy.*

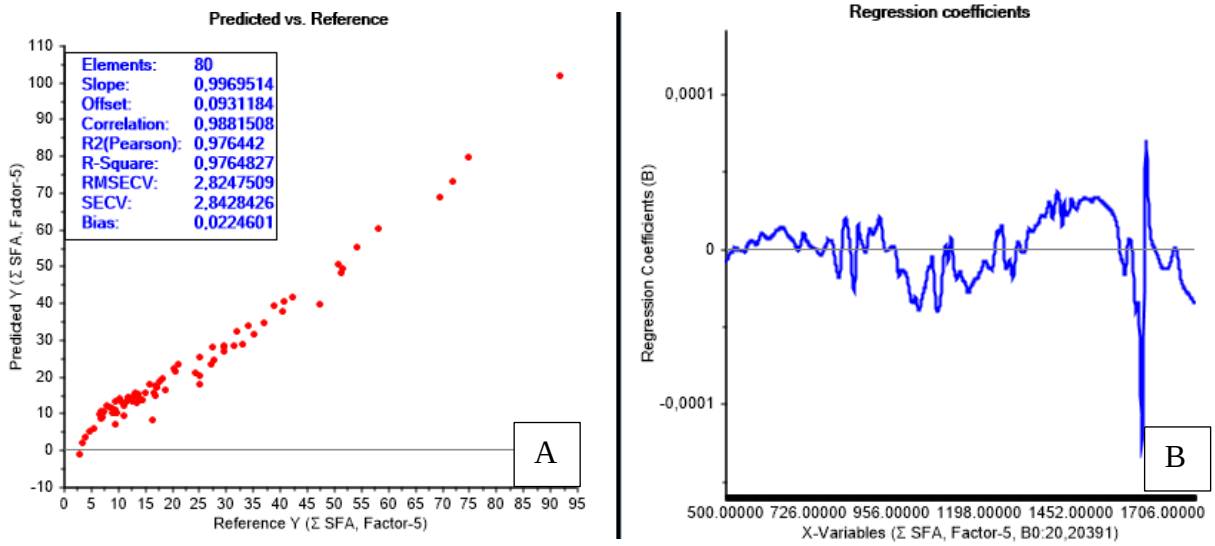


*Figure L.7: Predicted vs. reference values (A) and regression coefficients (B) for the calibration model obtained with ΣSFA as response variable. The model was made using PLSR and was based on data from analysis of the calibration set with Raman spectroscopy.*

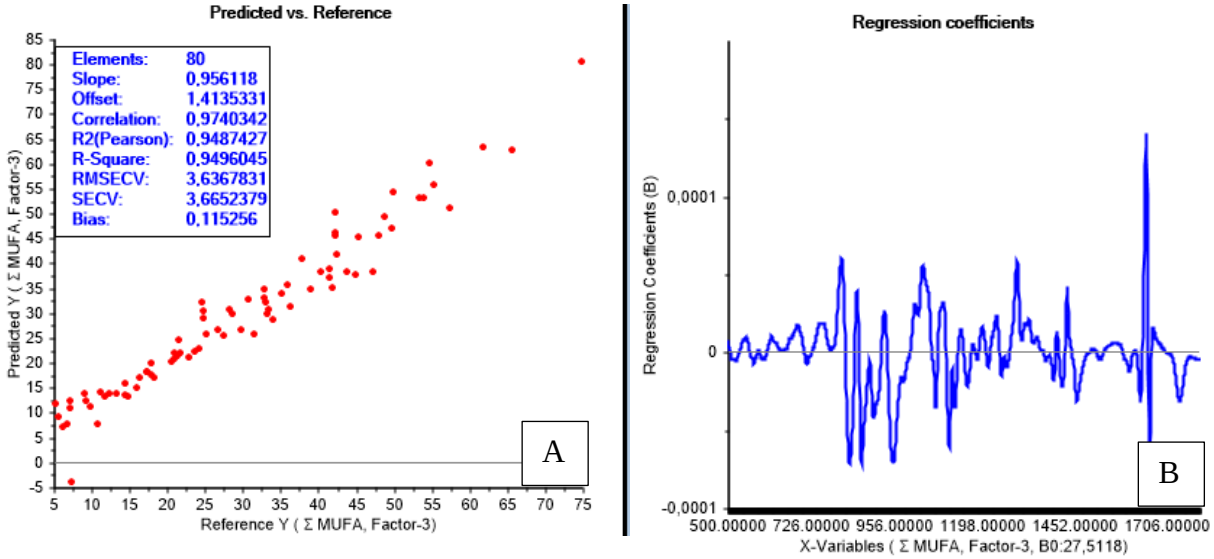


*Figure L.8: Predicted vs. reference values (A) and regression coefficients (B) for the calibration model obtained with ΣMUFA as response variable. The model was made using PLSR and was based on data from analysis of the calibration set with Raman spectroscopy.*

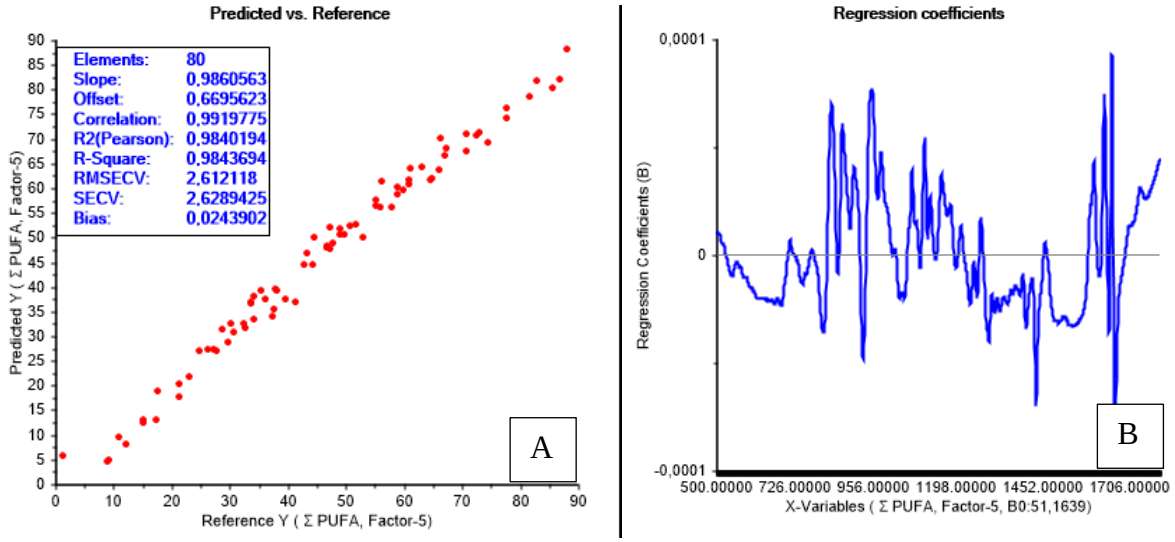


*Figure L.9: Predicted vs. reference values (A) and regression coefficients (B) for the calibration model obtained with ΣPUFA as response variable. The model was made using PLSR and was based on data from analysis of the calibration set with Raman spectroscopy.*

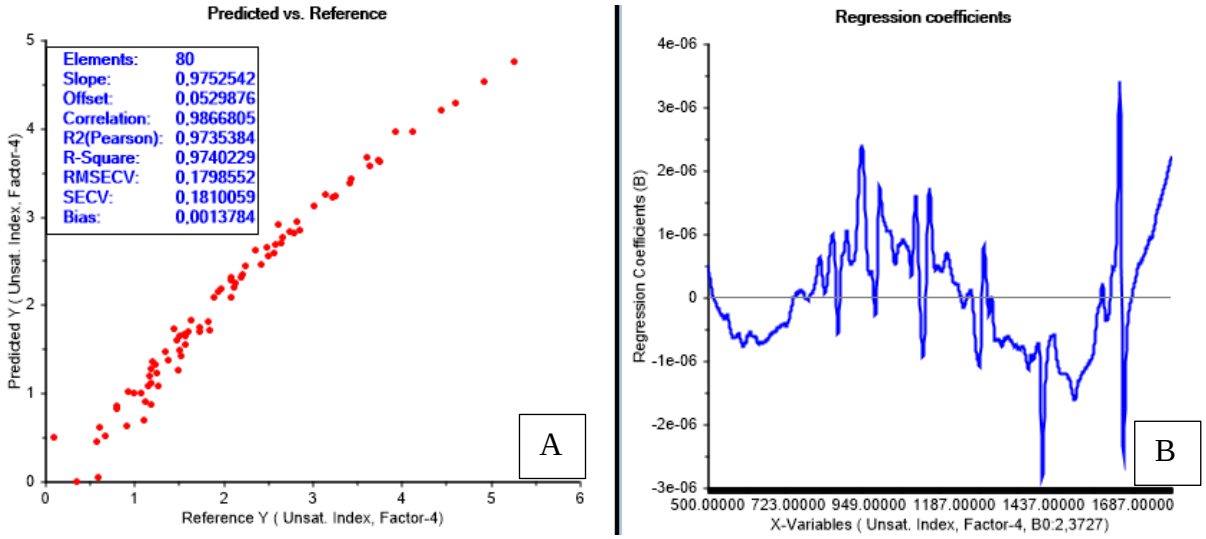


*Figure L.10: Predicted vs. reference values (A) and regression coefficients (B) for the calibration model obtained with UI as response variable. The model was made using PLSR and was based on data from analysis of the calibration set with Raman spectroscopy.*


**Norges miljø- og biovitenskapelige universitet**
Noregs miljø- og biovitskapelege universitet
Norwegian University of Life Sciences

Postboks 5003
NO-1432 Ås
Norway